RI/RD90-115

FIBEROPTIC CHARACTERISTICS FOR EXTREME OPERATING ENVIRONMENTS

FINAL REPORT
13 APRIL 1992

NASA CONTRACT NAS3-25346

NASA-CR-189189

Rockwell International
Rocketdyne Division
6633 Canoga Avenue
Canoga Park, California 91304

RI/RD90-115

FIBEROPTIC CHARACTERISTICS FOR EXTREME OPERATING ENVIRONMENTS FINAL REPORT 13 APRIL 1992

NASA CONTRACT NAS3-25346
PREPARED BY

R. DELCHER
RESPONSIBLE ENGINEER

S. BARKHOUDARIAN
MANAGER, ADVANCED MEASUREMENT CONCEPTS

A. NORMAN
PROGRAM MANAGER

1. Report No. CR189189	2. Government Accession No.	3. Recipient's Catalog No.
4. Title and Subtitle FIBEROPTIC CHARACTERISTICS FOR EXTREME OPERATING ENVIRONMENTS-FINAL REPORT		5. Report Date May 29, 1992 6. Performing Organization Code
7. Author (s) R. C. Delcher		8. Performing Organization Report No. RI/RD 90-115 10. Work Unit No.
9. Performing Organization Name and Address ROCKETDYNE DIVISION, ROCKWELL INTERNATIONAL 6633 Canoga Avenue Canoga Park, CA 91303		11. Contract or Grant No. NAS3-25346 13. Type of Report and Period Covered Final report
12. Sponsoring Agency Name and Address NATIONAL AERONAUTICS & SPACE ADMINISTRATION Washington, DC 20546		14. Sponsoring Agency Code

15. Supplementary Notes

Program Manager: A. Sovie, NASA-Lewis Research Center; Cleveland, OH

16. Abstract

Fiberoptics could offer several major benefits for cryogenic liquid-fueled rocket engines, including lightning immunity, weight reduction, and the possibility of implementing a number of new measurements for engine condition monitoring. The technical feasibility of using fiberoptics in the severe environments posed by cryogenic liquid-fueled rocket engines was determined in this contract.

The issues of importance and subsequent requirements for this use of fiberoptics were compiled These included temperature ranges, moisture embrittlement succeptability and the ability to withstand extreme shock and vibration levels.

Different types of optical fibers were evaluated and several types of optical fibers' ability to withstand use in cryogenic liquid-fueled rocket engines was demonstrated through environmental testing of samples. This testing included; Cold-Bend Testing, Moisture Embrittlement Testing , Temperature Cycling, Temperature Extremes Testing, Vibration Testing, and Shock Testing.

Three of five fiber samples withstood the tests to a level proving feasibility, and two of these remained intact in all six of the tests. A fiberoptic bundle was also tested, and completed testing without breakage. Preliminary cabling and harnessing for fiber protection was also demonstrated. According to cable manufacturers, the successful -300°F cold bend , vibration, and shock tests are the first instance of any major fiberoptic cable testing below roughly -55°F.

This program has demonstrated the basic technical feasibility of implementing optical fibers on cryogenic liquid-fueled rocket engines, and a development plan is included highlighting requirements and issues for such an implementation.

17. Key words (Suggested by author (s))	18. Distribution Statement
Fiberoptics Space Shuttle Main Engine Cryogenic Liquid Propellant Rocket Engines Condition Monitoring Sensors	

19. Security Classif. (of this report)	20. Security Classif. (of this page)	21. No. of Pages	22. Price*
Unclassified	Unclassified	133	

* For sale by the National Technical Information Service, Springfield, Virginia 22151

MANAGER, ADVANCED MEASUREMENT CONCEPTS PROGRAM MANAGER

ACKNOWLEDGEMENTS

I gratefully acknowledge the technical support and encouragement of my manager, Sarkis Barkhoudarian, and also my colleagues, Doug Dinnsen, Mike Randall, Ara Dergevorkian, Hank Thomas, Hadi Darejeh and Ed Awaya. I would also like to thank Jim Gauntner and Amy Sovie for their dedication and guidance, and Bob Baumbeck for his technical insight and suggestions. The following companies went out of their way to make this study successful: Lasergenics, Brand-REX Division of Brintec, Spectran, Hughes Aircraft, Iris, AT&T, ITT/Cannon, Fiberguide, Andrew, Infrared Fiber Systems, and Ficon Fiberoptics. The assistance of Dr. Richard Claus and Dr. Desu of the Virginia Polytechnic Institute in cladding a sapphire fiber sample is also much appreciated.

I also want to express appreciation to Ellen Segal and Lucy Sanders for their patience and diligence in preparing this report.

FIBEROPTIC CHARACTERISTICS FOR EXTREME OPERATING ENVIRONMENTS

TABLE OF CONTENTS

LIST OF FIGURES AND TABLES

I. Executive Summary

The goal of this contract has been to determine the technical feasibility of using fiberoptics in the severe environments posed by cryogenic liquid-fueled rocket engines.

Fiberoptics could offer several major benefits for such engines, including lightning immunity, weight reduction, and the possibility of implementing a number of new measurements for engine condition monitoring.

As this contract was initiated, a careful compilation had yet to be made of the issues of importance for using fiberoptics in such an engine's control system. Basic technical information was also missing. For example, little was known of the mechanical ruggedness of various fibers at temperatures of -300 degrees Fahrenheit, including their ability to withstand extreme shock and vibration levels.

During this contract, these requirements were assembled, and the feasibility of using several types of optical fibers in cryogenic liquid-fueled rocket engines was demonstrated through environmental testing of samples.

This testing included: "Cold-Bend Testing" in which the samples were flexed 10,000 times at -300 degrees Fahrenheit, "Moisture Embrittlement Testing" consisting of 30 days of water immersion to test the susceptibility of the glasses to moisture assisted breakage, "Temperature Cycling" from -300 to +257°F, "Temperature Extremes Testing" for 96 hours at -300 and +500°F, "Vibration Testing" at 40 g's for 1 hour each at both -280 and +275°F, and "Shock Testing" consisting of 48 shocks each at both -280 and +275°F.

Three of five fiber samples were deemed to have withstood the tests to a level proving feasibility, and two of these remained intact in all six of the tests. A fiberoptic bundle was also tested, and it too passed its testing without breakage.

Preliminary cabling and harnessing for fiber protection was also demonstrated. According to cable manufacturers, our successful -300 degree tests cold bend, vibration, and shock tests are the first instance of any major cable testing below roughly -55°F.

This program has demonstrated the basic technical feasibility of implementing optical fibers on cryogenic liquid-fueled rocket engines, and a development plan is included highlighting issues which now need to be addressed to do so.

The major issues for future investigation include: an evaluation of fiberoptic connectors, especially for vibration and cryogenic temperatures; development of low weight flyable cabling and harnessing, including need for increased cable stiffness at high temperatures; and the development of promising, already existing optical sensing methods into flyable technologies. Further development of sapphire optical fiber is also suggested.

Due to the failure of all the infrared transmitting fibers during environmental testing, work has been performed in an added scope extension to evaluate sapphire fiber as a possible alternative. Sapphire optical fiber is in its infancy, and was found to require more development before it can be used in rocket engine applications. However, the mechanical and optical fundamentals, as well as results of fiber development efforts to date appear quite promising. With further work, sapphire fibers can most likely be applied on rocket engines.

II. Background

Advances in high-performance propulsion systems, coupled with requirements for size and weight reduction, increased reliability, and improved fault tolerance have put new demands on sensors and control systems. Fiberoptic technologies are expected to help meet these demands.

Optical fibers possess many advantages that make them highly attractive for application to rocket-engine instrumentation and control system signal transmission. Fiberoptic cables offer EMI immunity, and excellent resistance to lightning strikes and electromagnetic pulses. They do not pose ignition source dangers due to sparks or overheating. Lack of EMI susceptibility should allow substantial weight reductions by eliminating the need for signal line shielding.

Inherent EMI-immunity can greatly benefit liquid-fueled rocket engines. At least two large U.S. rockets have been struck by lightning; Apollo 12 and Atlas centaur AC-67.

The strike to the Apollo caused the temporary shutdown of most electrical systems in the upper stages. Quick thinking by ground controllers allowed continuation of the mission by switching in a backup system. In the case of the Atlas, the lightning strike caused the controller to malfunction, resulting in the loss of the vehicle.

As few opportunities remain for engine weight reduction, the elimination of heavy signal line shielding will benefit the engines by reducing overall weight: any decrease in harness weight will increase payload capacity. The current cost of delivering payloads to orbit is approximately $5000 per pound per flight.

Development of optical fiber-based technologies would also open up new opportunities for flight measurement, which would greatly benefit engine health monitoring. Fiberoptic technologies are already being applied under the SSME Technology Test Bed program, (NAS8-40000), to provide real-time information on turbine blade temperature profiles and turbopump bearing degradation. These and other new technologies could be of great assistance in assuring engine reliability, maximizing life, and lowering overall life cycle cost.

III. Program Objectives

The general objective of this contract was to investigate the feasibility of applying fiberoptics to cryogenic-propellant rocket engines. Two specific goals were to determine the environmental requirements of sensors and transmission lines, and to devise new applications of existing materials and methods.

The overall program plan had five parts: characterization of existing fibers, materials and technology through literature searches and vendor surveys; determination of specific requirements for applying fiberoptics to rocket engines; screening of fiber candidates; selection of the most promising fibers for testing; and actual fiber testing to assess feasibility. A sixth part was added to the program to characterize a sapphire fiber.

The program philosophy was to use a generic approach, so that the resulting data could be applied to a variety of engines, and to concentrate on rocket-engine-related issues, particularly those relating to the harnesses.

The reason for the emphasis on harnesses is because of their key positions in rocket-engine control systems. To gain the benefits of an optical system, all components of a rocket-engine control system (controllers, sensors and harnesses) must be compatible with the optics to some extent. The controller can be nearly conventional with appropriate optical interfacing; however, the harnesses must be fiberoptic, and the sensors must be optical (but not necessarily fiberoptic). Optical fibers within sensors, although potentially exposed to greater environmental extremes, will typically have better mechanical support than the harnesses. Non-fiberoptic optical sensors will be required to interface with the fiberoptic harness. Therefore, since harnesses rely most on the capabilities of fiberoptics, more emphasis was given to addressing harness-related fiberoptics issues.

IV. Requirement Definition

The purpose of requirement definition was to determine the performance and configurational requirements of fiberoptic probes, non-intrusive sensors, and signal lines operating in the extreme environment of a liquid propellant rocket engine. Existing specifications for flight sensors, controller, harnesses, and wiring materials were reviewed. Although Rocketdyne has experience in Peacekeeper, Atlas and orbital transfer vehicle rocket engines, the Space Shuttle Main Engine (SSME) database was used as this was the most modern, highest-performance application database available. It is expected to be highly representative of the requirements of future liquid fueled rocket engines. In addition to this database, reference was made to various pertinent military standards.

Within this task, specifications were examined for six SSME flight sensors (See Table 1). The 7001 pressure transducer, the 7002 temperature transducer, the 7004 resistance type temperature transducer, the 7005 speed and flow sensor, the 7007 hydraulic pressure sensor, and the 7010 accelerometer specifications were reviewed, with particular attention paid to output/sensitivity (performance), operating temperature range, chemical environment, vibration level, size, weight, and pressure. Figure 1 displays the seven types of flight sensors, while the location of the sensors is shown in Figure 2 with P designating Pressure Sensors; S, Speed Sensors; T, Temperature Sensors; and F, Flow Sensors. The 1493 SSME controller specification was reviewed with emphasis on operating temperature range, chemical environment, vibration, weight, and pressure. The 40M38277 connector and the RB0150-044 cable

specifications were reviewed with emphasis on operating temperature range, chemical environment, vibration, and pressure. Figure 3 displays the harnessing on an SSME controller.

Key issues focused upon during the Requirement Definition task are discussed in detail below. For clarity, comments on these requirements derived from Tasks 2 and 3 have been incorporated into this discussion.

Size and Weight Requirements - Size and weight of existing sensors is listed in Table 1. A weight specification for the harness is not available, but a representative sample of harness has been weighed and measured, resulting in an approximate value of 10 oz/ft. The sample was a 2-1/2 foot length of stainless steel-jacketed cable which was connectorized for 3 sensors, typical of a cable used on the SSME. A harness specialist stated the total weight of harnessing on the SSME is probably in the range of 100 pounds. Fiberoptic cabling is expected to match or weigh less than this type of harness.

Vibration - The magnitude of vibration levels has been determined for various sensors and the engine controller (in Table 1). Although vibration specifications are not available for the harnesses, the vibration levels are expected to be similar, on the order of 35 g rms from 10 to 200 Hz, and up to 400 g rms transients through 20 KHz. In contrast, the E.I.A. test procedure (E.I.A. 455.11) widely used by industry only tests to 20 g rms at 2000 Hz, which points out a need for a more strenuous evaluation.

High Temperature Destruction of the Fiber's Light Guiding Ability - Maximum temperatures were determined for each area of the SSME (See Table 1). The harness specifications state that the harness in the engine area shall withstand exposure to direct localized flame or hot gas impingement between the temperature range of 816°C to 1093°C without loss of continuity in the signal line for a minimum of one minute. The construction of this harness is described as being made of a stainless steel braided outer cover, silicone rubber tape inner cover, and Teflon coated wire with all silicone molded rubber end boots. It is notable that both the heat reactive sleeving and the silicone rubber tape are not service-rated for use over 350°C.

Fiber cable construction would determine the ultimate application limitations. The limiting factors on high temperature resistance are the diffusion point of the glass fiber,

the jacket material, and any fillers which may be used for additional abrasion, vibration, or handling protection. Of these, the jackets and fillers are the more fragile components with respect to temperature. Polyimides, Teflons, and metals are materials which were investigated. Characteristics of these materials are outlined in Table 2.

Low Temperature Compatibility - The majority of the wiring harnesses will never be exposed to less than 0°C, although rated to -125°C. Certain sensors are exposed to -250°C environments (Table 1). The concern is that the fibers may lose their flexibility at these extremely low temperatures, making them extremely susceptible to breakage when flexed or vibrated. It was decided that testing under these conditions would be warranted.

Temperature Cycling - Temperature cycling should not be extreme for the engine harnesses. Sensors, however, will face rapid thermal cycling. Many must withstand rapid cooling due to the filling of the engine with cryogenic coolants. The hot gas temperature sensor must face an environmental vibration from -300°F to 2200°F which occurs almost immediately during engine ignition. Fiber testing in these areas was deemed appropriate.

LOX or GOX Compatibility - LOX compatibility is not a requirement for the wiring harness, although limited portions of the front ends of certain sensors are exposed to LOX (Table 1). Flammability limits are specified, however.

LOX compatibility is also not required for adhesives and binding materials used in their construction. The front portion of certain sensors will be subjected to LOX, and sensor design can be expected in some instances to require sealing of an optical element to a sensor housing to prevent LOX leakage.

Several adhesives have been tested at Rocketdyne to determine their LOX compatibility, and all have been found unacceptable. Other sealing methods are available which show more immediate promise for such applications. Fibers are available with gold jackets; therefore, brazing to the jacket may be an option. Larger optical elements might well be sealed using methods similar to those presently used for rocket engine joint construction.

Moisture Effects - Moisture can reduce the resistance of non-hermetic fiber to cracking. The space shuttle engine compartment is purged with dry nitrogen during chilldown, and this nitrogen is bled off during ascent. Even so, the engine compartment can be exposed to the outside air during ground maintenance work, and the specification for the harness states that it shall resist 100 percent humidity and salt spray conditions. Also, the use of a purged engine compartment should not be assumed for future vehicles.

Radiation Exposure Effects - Radiation exposure of the harnesses should only be a problem in space. Such exposure is a very strong function of orbit and any shielding provided by the rocket body. Orbits used by the shuttle, as an example, have relatively low exposure to radiation in order to protect the crew. Low orbits tend to have much less radiation than higher orbits due to Van Allen belts. The issue of radiation exposure is a complex one which will have to be addressed for each particular mission of interest. Reference 1 provides useful data for the determination of radiation levels that would be encountered.

Large levels of radiation exposure can result in increased attenuation in optical fibers due to the production of color centers. The level of attenuation depends rather strongly on the fiber itself (See Figures 4 and 5. taken from Ref. 2). While the induced attenuation due to radiation exposure is cumulative, it is also reversible for most fibers.

This recovery from radiation-induced attenuation can be due to annealing of the fiber through its own random thermal motion, or to a photochemical process in which the light traveling through the fiber that is absorbed, serves to reduce the fiber's attenuation. Because of these effects, the attenuation of a fiber due to radiation is dependent on the dose rate, the temperature of the fiber, the light intensity, the wavelength in the fiber, and the fiber material.

The effect of fiber attenuation on the reliability and accuracy of transmitted sensor data will also depend very strongly on the modulation method used by the sensor. This subject is addressed in Appendix C.

Hydrogen-Induced Opacity - A significant long-term concern in some fibers that transmit at 1300 or (particularly) 1550 nm is the possible influx of molecular hydrogen into the fiber. If a fiber is kept in an atmosphere with a large hydrogen content, the tiny

hydrogen molecules diffuse throughout the fiber, adding significantly to losses at long wavelengths. However, new materials have come into use, and heavy-duty cables intended for long-term use now are designed to avoid internal hydrogen build-up. In addition, new fibers are much less vulnerable to hydrogen-induced losses than earlier types. Because of this, and because the cable lengths will be short for rocket engine applications, hydrogen-induced opacity is not considered to be a major issue.

Jacketing and Cabling - Fibers and their buffers are not the only structural elements of cables. Many fiberoptic cables include strength members. The usual strength members are steel or Kevlar which often are at the center of the cable structure. In some cables, strands of Kevlar are wound around the bundle containing the fibers, in addition to or instead of, a central strength member. Cables apply tension along their length to them, rather than to the more vulnerable fiber. The strength member may be overcoated with a plastic or other material to make its size match cable requirements and to prevent friction between it and other parts of the cable.

The structure containing the fibers normally surrounds the strength member and, in turn, is surrounded by one or more outer jacketing layers. Rocket-engine cables will probably require one or more layers of protecting armor. Typically steel or aluminum is wound around an inner plastic sheath. An outer plastic sheath is then applied over the armor to prevent corrosion. The metal armor helps protect against crushing, abrasion, stretching, bending, chemical attach, and moisture intrusion. Research is needed to find jacket/cable combinations that can withstand the rocket engine environment.

Frictional Damage Between Fibers in a Bundle Due to Mechanical Strain/Temperature Extremes or Vibration Levels - There are three cases to be considered: 1) a bundle with adhesives joining only the ends, 2) a bundle fused only at the ends, and 3) bundles fused along their entire length. Bundles fused with adhesives are limited by the adhesive working temperature limit, which is generally around 125°C. Bundles fused at each end would not have the temperature limitation of the adhesive, but would be susceptible to abrasion between the fibers along its unfused length. Only testing based on the vibration and temperature levels listed in Table 1 can verify the extent of this hazard. Bundles fused along their entire length, usually referred to as fused rods, are less susceptible to interval abrasion, but still might suffer from

differential expansion strain due to thermal gradients. Again, testing would be required to determine the exact extent.

The requirements for proving out the capability of fiberoptics in a liquid propellant rocket-engine environment have been presented. These requirements which were qualified by calling for research or testing are the basis for the testing conducted within the practical limits of this contract.

V. Fiber Candidates Selection

When this contract was granted, little information was available to establish that optical fibers were sufficiently robust for application to cryogenic liquid-fueled rocket engines. During this effort, experts and relevant documents were consulted to determine and set requirements for demonstrating fiber feasibility. An extensive literature search and vendor survey, encompassing over 200 literature citations and 50 fiberoptic vendors and distributors, was then conducted to identify suitable candidate fibers and technologies, and identify major weak points.

Most of the information available from these sources dealt with the following issues: moisture effects, radiation-induced opacity, hydrogen-induced opacity, fiber transmission wavelengths, jacketing and cabling, cryogenic cabling and fiber bundles. The information obtained from the literature search and the vendor survey is presented in the Fiber Material Characteristics table. (Table 3)

In this table, the candidate optical fibers have been divided according to their core material. For each candidate, properties such as operating temperature range, tensile strength, optical transmission band, minimum bend radius, attenuation, buffer material, fiber type, chemical and radiation resistance, index of refraction, and approximately price are included. The four major core materials are:

1. Silica - Silica fibers are the most commonly used and widely available fibers in the industry. These fibers, traditionally used for communications, can be produced to transmit in the ultraviolet region of the spectrum. This ultraviolet transmission capability is useful for fluorescent temperature sensors. Major advantages of silica fibers

include their high tensile strength, low attenuation levels, wide temperature range, ease of handling, and commercial availability.

2. Sapphire - Sapphire fibers are currently manufactured by a single vendor on an experimental basis. Sapphire has excellent mechanical and optical properties. The drawbacks, however, are the lack of development in cladding the fiber, high attenuation levels, and lack of quality control which are at least partially the result of the low maturity level of this technology. Sapphire fiber is also difficult and expensive to manufacture as it cannot be pulled as a glass, as are other standard fibers, but must be grown as a crystal.

- Infrared fibers - In the late seventies, optical fibers made from silica glasses reached their theoretical limits of transparency. A second generation of materials are now emerging that transmit infrared light at longer wavelengths. Theoretically, the infrared fibers promise much greater transparency than is feasible with silica fibers, but the relatively young technology has not been able to reach these transparency limits. (Reference 5). The two major classes of infrared fiber materials are the fluoride glasses and the chalcogenide glasses. Sapphire also can be used in the infrared.

3. Fluoride - The fluoride family of fibers has the capability of transmitting in the infrared region. The theoretical intrinsic attenuation of 0.01 decibels per kilometer has not yet been achieved or even approached with the heavy-metal fluoride glasses, but even at current levels of transparency, these glasses offer technological opportunities. The most important application is in temperature sensors.

4. Chalcogenide - The chalcogenide glasses are also capable of transmitting in the infrared region. Further interest stems from their ability to transmit in the six to twelve micron region which enables them, in the bundle form, to transmit simple infrared images or information on the object temperature. These fibers suffer from their very low tensile strengths, unacceptable losses, and in general, the relatively experimental stage of their new technology.

The jacket materials have also been incorporated into Table 3. The standard jacket materials (Acrylate, Nylon, and Teflon) offer no exceptional protection against harsh environments. Polyimide and Tefzel jackets offer some high-temperature capabilities. Titanium carbide jackets are of interest because of their hermeticity. Metal jackets (Gold, Aluminum, Indium) offer both hermeticity and flexibility. Gold and aluminum also offer the ability to withstand temperature extremes. The data in this table was obtained from the manufacturers.

The Fiber Materials Characteristics table, however, is missing key information such as cold flexibility, vibration/shock, temperature extremes, thermal shock and LOX compatibility which are not of great concern for many fiber users.

Additional information on individual core, cladding, and jacket materials has been provided in Table 4. This includes melting point, modulus of rupture, thermal shock resistance, index of refraction, and optical transmission band. For metal jackets, the tensile-strength is used instead of the modulus of rupture, the latter being more applicable to brittle materials.

It is important to understand that the mechanical values for glasses presented in Tables 3 and 4 correspond to bulk materials and that some mechanical properties vary when the material is in fiber form. As an example, the tensile strength of bulk fused silica, as obtained from OCLI and Elgin Optical, is 7.1 and 8.5 KPSI respectively, but AT&T presents fused silica fiber as having a tensile strength of 800 KPSI when unprotected in room atmosphere. (Reference 6). The material, in a pristine crack and defect free fiber form, is much stronger than in bulk form, since the cracks act as stress concentration centers. This data was collected by contacting the manufacturers and through consultations with Rocketdyne materials engineers.

Selection of Test Samples - The first task completed was the setting of criteria for the selection of test samples.

From the total of 20 fiber types identified in Table 3, it was decided, in a tradeoff between technical and budget constraints, to submit six to testing . To this end, a set of screens were identified. They are the following:

- Maximum and minimum operating temperatures were established for screening. The temperatures extremes were determined based on the maximum capability of commercial fibers.

- For the purposes of fiber candidate selection, a power attenuation level of 0.5dB/m was judged to be the limit below which transmitted signals would not be suitable for processing. (4 meter harnesses on a large liquid-propellent engine such as the SSME would attenuate the signal about 63 percent at this level.)

- Hermeticity - It was determined, that for long-term usage, the fibers must be hermetic to avoid moisture penetration which can increase attenuation and decrease tensile strength to undesirable levels.

The above criteria are summarized in table 5 in which all 20 candidate fibers from Table 3 are examined with respect to the screening criteria. With the aid of Table 4, four of the six types of fiber to be tested have been chosen. They are:

1&2 Gold-jacketed silica single fibers and bundles - These were chosen because of their large temperature range, excellent hermeticity, low attenuation, and long-term resistance to embrittlement. Such bundles could be useful for spatially modulated sensors in which light position in the bundle carries the information. The sensors of this type, presently seen as showing great promise for liquid propellant rocket engine applications are diffraction-grating pressure sensors, deflectometers, and optical encoders.

3. Aluminum Jacketed Quartz Multimode Fiber - Aluminum jackets are an inexpensive alternative to gold jackets, and they have similar properties to those mentioned above for gold except for extreme high temperature applications. They are rated only to 450°C.

4. Fluoride (Far Infrared) Fiber - This fiber was chosen for its ability to operate in the far-infrared region of the spectrum which could be useful in infrared temperature sensor applications. The specific choice for this sample will be made from the results of cold-bend tests.

The additional two samples for testing were chosen from candidates mentioned in Table 6. Standard commercially available samples of the fibers listed in Table 5 were submitted to cold bend testing before the final two selections were made. The major considerations were:

- The single mode and polarization maintaining Aluminum coated fibers were under consideration because an interferometric sensor requiring such fibers like a bearing deflectometer or an accelerometer may be implemented.

- The Indium-coated polarization maintaining fiber was of interest because of its hermeticity and polarization maintaining ability. However, Indium does not offer the strength and high-temperature capabilities of Aluminum and Gold

- The new carbon-coating technology, representing the final candidates, offers another choice for hermetic fibers. The thin (500 Angstroms) layer of Titanium Carbide on the cladding provides hermeticity. However, such present fibers lack the resistance to high temperatures exhibited by Aluminum and Gold.

After the "preliminary cold-bend" testing of the candidate fibers, the two additional fibers chosen for continued testing were:

- Titanium Carbide-Coated Silica (Spectran)

- Amorphous Carbon-Coated Silica (AT&T)

The results of the fiber selection effort are shown in Table 7. The complete results of the "cold-bend" testing are covered in the Fiber Severe Environment testing section. Tests conducted on a sapphire fiber sample are discussed in a separate Sapphire Fiber Results section.

VI. Test Selection

Testing Optical Fibers - There are presently no optical fiber test requirements/ specifications specifically for liquid-propellant rocket engine applications. However, there are industry standard fiberoptic testing requirements and procedures for qualifying fiberoptics in areas where the environmental conditions are much less severe. Due to the great variety of tests, an effort has been made to select our own tests based upon Task I requirements (with an emphasis on harness requirements), present related test methods such as EIA and MIL Standards 1678, and compatibility with the contract budget.

Qualifying fiberoptics for rocket engine applications is beyond the scope and budget of this contract. The contract purpose lies in establishing the feasibility of using fiberoptics on rocket engines. This is approached through the development of a package of tests which closely simulate rocket engine environments.

Optical sensors require fiberoptic cables and harnesses for communication with the engine controller. Although optical sensors can utilize bulk optics, fiberoptics are the only viable means of communication between the sensors and the controller. For this reason, proving the feasibility of optical fibers for harness implementation is judged the highest priority and emphasis is being placed on the testing of fiberoptics for harness applications rather than sensor applications.

Test selection is based upon contract requirements, the likelihood of fiber failure due to the prevalent fiberoptic failure modes in severe environments, and the lack of reliable fiber data for the test parameter in question. The tests specifically identified in the contract, namely temperature cycling, hot and cold temperature extremes, fatigue due to vibration, and embrittlement due to moisture, have been included in the listing of tests to be performed as displayed in Table 8. Additionally, shock and cold bend tests have been selected which will be similar to those stated in the SSME harness and cable requirements. These six tests listed in Table 8 are also similar to those recommended by the EIA (Electronic Industries Association) fiberoptic standards document.

Selected tests will provide pertinent information on fiber degradation and failure mechanisms such as fatigue, embrittlement, mechanical stress, moisture exposure,

and frictional damage of fibers in a bundle which address key issues stated in Task I and contract requirements. Issues such as fiber melting when subjected to flame and attenuation due to exposure to radiation have been evaluated but will not be tested.

A brief description of all six tests is given below.

COLD BEND - The purpose of this test is to determine the ability of optical fibers to withstand specified bending at low temperatures. Fibers will be inspected for breakage during and upon completion of the test.

SHOCK - This test is conducted to investigate the ability of the fibers to withstand the shock associated with engine firing, take off, and landing. Fibers will be examined for breakage, discontinuity, and signal attenuation after the test.

MOISTURE EMBRITTLEMENT - This test is performed to determine the moisture resistance of fiber, addressing the hermeticity of the fiber jacket, and the effect of moisture on embrittlement. Fibers will be examined for damage to this jacket or the glass as well as breakage due to embrittlement.

TEMPERATURES EXTREMES - This test is conducted to determine the ability of fibers to withstand high and low temperatures for predetermined periods of time. The fibers will be examined for signal attenuation during and breakage after each test.

THERMAL CYCLING - This test is performed to determine the ability of the fiber to withstand a specified number of cycles between high and low temperatures. Fibers will be examined for attenuation and breakage.

CRYOGENIC VIBRATION - This test is performed to determine the ability of the fiber to withstand vibration related to engine firing and flight. Fibers will be checked for breakage and attenuation before and after this test.

VII. Fiber Severe Environment Testing

A test plan was derived from requirements and procedures outlined in Table 1. With the aid of this test plan, six tests were conducted during this effort: a "cold-bend" test consisting of 10,000 $\pm 45°$ flexure cycles at -300°F; a moisture embrittlement test in

which stressed fibers were immersed for 30 days in water; temperature cycling from -300°F to ±257°F; extreme temperature exposures for 96 hours at -300°F and +500°F; and 40 g vibration and shock testing at -280°F and 235°F.

COLD BENDING TESTING

This test repeatedly flexed fibers ±45° around 1/2" mandrels 10,000 times while at -320°F (see figures 7,8).

Although 10,000 bend cycles represent much more bending than harnesses would normally be expected to withstand, during standard engine gimbaling, the fibers were submitted to testing and periodic examinations up to this level to establish the relative resistance to bending between each of them, and to observe failure modes. The ability to leave the automated test apparatus unattended during long bend test runs made this economically feasible.

Ten fibers were tested including a gold-jacketed imaging bundle. Microscope photographs were taken before and after testing to record any mechanical deterioration. They appear as Figures 9 through 19.

Overall, the test results were very promising. Most of the fibers remained intact for the entire 10,000 cycle duration.

For the first fibers tested, separate samples were submitted to cold bend testing at dry ice and liquid nitrogen temperatures. This was done mainly due to the uncertainty of whether a sufficient number of fibers could withstand the liquid nitrogen test. After several tests, it became clear that many fibers could indeed withstand the liquid nitrogen test, and that the dry ice test was difficult to perform due to ice and dry ice crystals being jostled into the bend area where they created stress concentrations on the fiber. At this realization, the dry ice tests were discontinued.

As stated in test selection, the cold bend tests were stopped for sample observation under a microscope at 500, 1000, 5000, and 10,000 cycles. Due to the large number of photographs involved, the figures displayed in this report and this discussion itself are both limited to points during the tests when alterations in fiber condition were observed.

Individual fiber test results are outlined below.

Gold Jacketed Silica Fiber (Superguide G size 200/220/250) from Fiberguide - In the dry ice test series, this fiber showed moderate scuffing of the gold jacket at 1000 cycles. At 5000 cycles, 2 small cracks appeared in the gold jacket through which the silica could be observed. The silica showed no apparent damage. Testing was continued to 10,000 cycles without breakage or a major shift in the fiber's condition.

During the liquid nitrogen cold bend test, depicted in Figures 9a-c, this fiber displayed some scuffing and wrinkling of the jacket material at 5000 cycles. At 10,000 cycles, 2 small circumferential cracks were observed in the fiber jacket.

Aluminum Jacketed Fiber (Hughes Aircraft Co.) - The results, depicted in Figures 10a-b, show considerable wrinkling of the aluminum jacket was observed at 10,000 cycles.

Titanium Carbide coated silica fiber (Spectran 100/140/162.5) - The liquid nitrogen test, depicted in Figures 11a-b, yielded excellent results. The only signs of degradation after 10,000 cycles of bending were minor surface scratches in the fiber's outer coating.

Fluoride glass fiber (Infrared Fiber Systems) - This brand of Infrared fiber presently appears to be mechanically inadequate for the requirements of a rocket engine.

This fiber broke at the actuator contact point just before 500 bend cycles in the dry ice test.

The fiber also broke during the liquid nitrogen test depicted in Figures 12a-b. The break occurred after 192 flexure cycles. The resulting pieces were very brittle, breaking again when touched, as displayed in Figure 12b. Microscopic examination revealed fine spirals running the length of the immersed portion of the fiber. The fiber tested in dry ice did not display these spirals. A subsequent experiment showed that simple immersion to liquid nitrogen did not generate the spirals, but immersion and flexing a specimen did.

The manufacturer, when contacted, stated that this fiber is presently still under development in their facility. They expect to produce this fiber with much greater tensile strength in the future; however, at the present time it is unsuitable for rocket engine use.

Indium Jacketed Single Mode Polarization Preserving Fiber (Andrew 1.25X2.5/80) - Upon examination of both the dry ice and liquid nitrogen tested samples of this fiber after 500 cycles, both samples displayed holes in the jacket material. An untested sample was then carefully inspected, and it had a similar appearance (see Figure 13). Upon rolling the fiber on a sheet of paper, the jacket material rubbed off onto the paper. The supplier was contacted, and he confirmed these problems to be normal for this fiber. The fiber was deemed unsuitable for rocket engine use, and testing of this fiber was discontinued.

Zirconium Fluoride Infrared Fiber (Iris 100/140/230) - In the dry ice test, depicted upon examination of the fiber after 500 cycles of vibration, the jacket material was seen to be badly cracked. The fiber itself within the jacket was intact. At this point, dry ice testing of the fiber was discontinued. It is believed that an ice crystal may have acted as a stress concentrator on the bend mandrel.

The liquid nitrogen test conducted on this fiber, depicted in Figures 14a-b, was carried out to 10,000 cycles with little apparent degradation of the fiber. The only signs of degradation were minor wear spots on the surface of the jacket material.

Deflectometer Fiber (MTI glass either 80/90 or 50/64) - This is a sample of the fiber presently used in an optical deflectometer manufactured by MTI. This deflectometer is a multiple fiber sensor which detects the amount of light that is transmitted from one fiber, reflected off of a surface, and coupled into an adjacent fiber, in this manner measuring surface deflection. The exact specifications of the fiber used in the MTI unit are proprietary to MTI; however, it is known that this fiber has a much larger numerical aperture than standard fibers, allowing light to be coupled into this fiber from larger angles.

A sample of the fiber was cold bend tested in liquid nitrogen to 10,000 cycles without visible signs of damage. The results of testing are depicted in Figures 15a-b.

Aluminum Jacketed Silica Fiber (Fiberguide 200/240/300) - This fiber was cold bend tested to 10,000 cycles in liquid nitrogen (results depicted in Figures 16a-b). After 10,000 cycles, the fiber displayed only minor wear spots on the surface of the aluminum jacket. It should be noted that this fiber had a roughened appearance prior to testing, making a direct comparison to the final roughened appearance of the Hughes aluminum jacketed fiber difficult. The Hughes fiber was smooth prior to testing.

19-Fiber Imaging Bundle (Fiberguide Gold-Jacketed 100/110/140 Silica Fiber) - The cold test bundle (and bundles for shock and vibration testing) were purchased in a customized cable package. The custom jacketing was requested for the bundle because, although Fiberguide's gold jacketed silica fibers are available inserted loosely into metal gooseneck tubing, this cabling method would allow excessive movement, and therefore abrasion between the fibers themselves and the fibers and the metal gooseneck.

As no other vendor was found with a better cabling method for bundles to be placed in a mechanically taxing liquid nitrogen temperature environment, a method was devised to provide some mechanical support for the fibers using materials which maintain their mechanical properties well at liquid nitrogen temperatures.

It was decided to pack the fiber bundle inside of braided Kevlar (brand name) fibers, in order to provide some mechanical support, and in an attempt to reduce rubbing between the fibers and abrasion of the gold jackets. To provide overall protection against outside tensile loads and abrasion, the packed fiber bundle assembly was then inserted in a braided tube of Silverflex brand fluorocarbon coated fiberglass material.

The fiber bundle ends were then soldered inside of a stainless steel ferrule to produce sturdy terminations. Fiberguide has a well-developed capability to perform this particular operation of soldering the gold jacketed bundle inside of a metal ferrule. As this is the case, it was deemed most efficient to request Fiberguide to perform the entire cabling operation described above and deliver a completed bundle.

A picture of the completed fiber bundle, ready for testing in the cold bend tester, appears in Figure 17. Figure 18a shows one end of the fiber bundle, observed under

a microscope, while the other end of the bundle was placed under strong illumination. Light can be seen emanating from the individual fibers in the bundle, indicating that all fibers are intact.

The bundle was placed in the tester and submitted to 10,000 flexure cycles as specified in the test plan. It was removed at intervals and checked per the test plan in order to allow identification of individual fiber breakage during testing.

No optical degradation was observed in the bundle at any time during testing, or after 10,000 cycles. Figures 18a, 18b, and 18c show one end of the fiber bundle after 10,000 cold-bend cycles, illuminated on the other end to produce an image analogous to that shown in Figure 18a, taken before testing.

Amorphous Carbon-Coated Silica Fiber (ATT 50/125/187) - The signal amorphous carbon-jacketed fiber sample, manufactured by AT&T also was successfully submitted to 10,000 cycles in the cold-bend tester. A microscopic picture of a portion of the fiber which underwent bending over the mandrels of the cold bend tester is displayed in Figure 19a.

Although there were no signs of breakage or mechanical or optical degradation of the fiber, upon removal of the fiber, water was observed between the plastic protective jacket and the fiber itself (see Figure 19b). It appears to have been constrained to the lower half inch of the fiber, which sat in the bottom of the liquid nitrogen Dewar flask after testing. Water does not appear to have impregnated the portion of the fiber which underwent flexure around the mandrels during testing.

This is the first fiber specimen in which this effect was observed. Although the method of water entry can not be proven with certainty, it is believed that the water entered at the end of the fiber (see Figure 19c). The end of this fiber, as well as all the other fibers tested, is cut and not sealed. Therefore it is surmised that the water was able to enter between the plastic jacket and the fiber itself at the fiber's end. The fiber was left in the cold bend tester after testing, during which time the liquid nitrogen boiled off and some condensation accumulated.

It should be noted that the hermetic amorphous carbon jacket appears as the outer layer of the fiber underneath the plastic jacket. It is meant mainly to seal the fiber,

while the plastic jacket is meant to provide mechanical protection against nicks. All the other fibers tested, except for the metal jacketed ones, employ a similar outer plastic jacketing.

Although the amorphous carbon jacketed fiber appears to have suffered no damage from the water intrusion, the observation of this occurrence does raise some concern. At low temperatures, ice between the fiber and plastic jacket could possibly abrade the fiber when it is bent. Abrasion to the fiber itself can greatly reduce the fiber's tensile strength due to the stress concentration created at the bottom of the nick when the fiber is placed under tension. Such a nick could also damage the fiber's hermetic coating, allowing water exposure to the silica itself, again further reducing the fiber's tensile strength.

Moisture Embrittlement Test

Moisture embrittlement testing was performed according to the test plan. All of the fibers except the fluoride fiber from Iris and the amorphous carbon fiber from AT&T showed no signs of degradation whatsoever.

Hermeticity was an important issue in the selection process of the fibers. Fused silica fiber tested in room atmosphere, has its strength reduced to 800 KPSI (from 2 MPSI in an inert environment), because of the presence of moisture. This mechanism, termed static fatigue, indicates that only 1/3 of the initial proof test strength can be applied continuously for a survival life of 25-40 years. (Reference 6) The moisture attacks the surface of the glass fiber under tension. This results in growth of microflaws at the glass surface and a gradual reduction in fiber strength.

The moisture embrittlement tester consists of a 3 inch diameter mandrel immersed in a plastic tube filled with 7.6 cm distilled water. The fibers were not cabled to ensure water contact with the fiber jackets.

They were tightly wound around the mandrel and held in place with small dabs of paraffin wax at quarter revolution intervals around the spool. The wax ensures that the fiber remains tight throughout the test, while it covers only an insignificant fraction of the fiber. A picture of the test setup is shown in Figure 20.

The fibers were measured for attenuation at intervals during the testing and also visually inspected at the same time. After the conclusion of testing, they were examined under a microscope as a further method of detecting and identifying failure modes.

Handling uncabled connectorized fibers is rather difficult due to their fragility and small size. However, it was decided for moisture embrittlement testing to test the fibers in their bare, uncabled, state in order to ensure that water contact actually took place.

Difficulties arose in handling the fibers while inspecting them at the intervals specified in the test plan. The titanium carbide fiber broke twice, once due to the spool being pulled too far away from the power meter during removal from the water bath, and the other time due to the spool being dropped accidentally during removal from the bath for fiber inspection. The fiber was reconnectorized after the breakages which occurred right at the connector and at the spool.

It does not appear that either case of fiber breakage had any correlation to moisture embrittlement. In both cases a piece of thin copper wire of the same diameter as the fiber would almost certainly also have broken. As previously stated, in the first case of fiber breakage, the break occurred at a connector that was well away from the water. In the second case, the break occurred roughly where the fiber first made contact with the spool, which was under water.

In short, it is believed that the major significance of the fiber breaks from a program point of view is to again point out the fact that fiberoptic cables should be designed to ensure that the cable and not the fiber is responsible for withstanding large tensile loads. The fibers in the moisture embrittlement test were not cabled at all.

After these breakages, a new method of examining the fibers was successfully implemented: the water was syphoned out of the tub leaving the spool untouched.

A good deal of variation was found to take place in attenuation measurements due to variation in connector losses as the connectors were repeatedly connected and disconnected. Table 9 shows the attenuation measurements taken during this test. Once this problem was fully realized, several attenuation measurements were made,

repeatedly connecting and disconnecting a connector, in order to average the loss values for a more accurate fiber loss measurement.

Except for the fluoride fiber, which broke during testing, there were no signs of attenuation in the fibers during the moisture embrittlement test. The variations in attenuation shown in Table 9 appear to have taken place in the connectors.

Microscopic observations of the gold-jacketed fiber from Fiberguide (Figure 21), the aluminum-jacketed fiber from Hughes (Figure 12), and the titanium-carbide-coated fiber from Spectran (Figure 13) all showed no signs of degradation.

The fluoride fiber did show severe degradation, both under the microscope and as breakage during water immersion. It was first broken early in the test, during the inspection which took place on the third day. Unlike the previous fiber breakages, due to handling errors, the breakage of the fluoride fiber took place with little force being exerted. It also appears likely from the attenuation values taken before breakage that the fluoride fiber suffered some attenuation beyond connector attenuation before breakage.

This break during handling of the fiber was followed later during the test with several more breaks which took place with no outside disturbance.

The fluoride fiber was examined under a microscope both before and after the moisture embrittlement test. Figure 24a shows a portion of the fiber before testing, and Figure 24b displays a piece of the fiber after water immersion. The fluoride fiber pieces examined after testing, revealed that the fiber itself within the acrylate plastic jacket had a mottled whitened appearance, whereas it had appeared perfectly clear during the pretest observations.

IRIS FLUORIDE FIBER - Iris, the manufacturer of the fluoride infrared fiber, was consulted on the issue of moisture embrittlement, and stated that they had run their own test indicating that moisture embrittlement could be a problem. They stated that for this test they used a fluoride fiber with no acrylate plastic jacket. The fiber we tested was protected by an acrylate jacket.

Iris stated that during their test, the fiber attenuation started to increase greatly after only a few minutes, and the fiber broke. They have suggested encapsulating the fiber in a small stainless steel tube the size of a hypodermic needle in order to seal the fiber against moisture. A sample of the fluoride fiber inside such a protective 0.010"/.018" stainless steel tube is shown in Figure 25.

Iris also led us to an article on the moisture embrittlement of fluoride glass (Ref. 5). This article describes the probable mechanisms for moisture embrittlement failure in fluoride glasses, and also states that "water attack on zirconium fluoride based glasses has been observed at or slightly above room temperature under medium to high humidity conditions (>35% relative humidity)".

The information discussed above indicates that if fluoride fibers are to ever be used on rocket engines, the fibers would have to be hermetically sealed against moisture. Iris' suggestion of encapsulating the fiber in stainless steel tubing would seem appropriate.

Fluoride fibers are necessary only for transmission of infrared radiation for such applications as low temperature turbine blade pyrometry. Performing such a measurement without an optical fiber is difficult, as mounting the detector directly in an environment such as that on the preburner of a rocket engine is undesirable. For such specialized applications, the use of a fluoride fiber encapsulated inside small stainless steel hypodermic type tubing could be a viable solution to the problem of moisture embrittlement. Sapphire fibers, although not yet well developed, show great promise for such applications, due to their high strength, ability to withstand high temperatures, and infrared transmission properties.

AT&T AMORPHOUS CARBON-COATED FIBER - The amorphous carbon-coated fiber from AT&T also showed signs of degradation due to moisture embrittlement. The "bubbles", observed when the first amorphous carbon-coated fiber subjected to moisture embrittlement testing was examined under a microscope appear to be water trapped between the fiber's outer acrylate plastic jacket and the amorphous carbon layer underneath.

It should be noted that the hermetic amorphous carbon jacket appears as the outer layer of the fiber itself underneath the plastic jacket. It is meant mainly to seal the fiber, while the plastic jacket is meant to provide mechanical protection against nicks. All

other fibers tested, except for the metal jacketed ones, employ a similar outer plastic jacket. The fluoride fiber is also jacketed in acrylate while the Spectran titanium carbide-coated fiber is jacketed in polyimide.

Although the amorphous carbon-jacketed fiber appears to have suffered no decrease in transparency from the water intrusion, the observation of this occurrence does raise some concern. At low temperatures, ice between the fiber and plastic jacket could possibly abrade the fiber when it is bent. Abrasion to the fiber itself can greatly reduce the fiber's tensile strength due to the stress concentration created at the bottom of the nick when the fiber is placed under tension. Such a nick would also damage the fiber's amorphous carbon hermetic coating, allowing water exposure to the silica itself, again further reducing the fiber's tensile strength through moisture embrittlement.

These issues were raised with the intrusion of water underneath the plastic jacket of the amorphous carbon-coated fiber in the cold bend tester. In that case, water intruded about half an inch up the fiber from the bottom of the tester. It appeared to have gained access at the end of the fiber and simply wicked its way up between the amorphous carbon coating and its overlying jacket. It was stated that proper connectorization of the fiber end could probably seal off such a route for water intrusion.

The results of the moisture embrittlement test show that water can gain access through the protective plastic jacket of the AT&T amorphous carbon-coated fiber and form observable "bubbles" underneath it. Solution of this problem would require alteration of the fiber's plastic jacket. It is not necessary that the plastic jacket be impermeable to water, that task is addressed by the amorphous carbon coating on the fiber. However, the jacket would now allow visible quantities of water to collect underneath it.

AT&T has been contacted concerning the results of the moisture embrittlement tests of its fiber. The first fiber subjected to moisture embrittlement testing, which displayed "bubbles" afterward, and the second fiber tested which showed no signs of degradation were from two different numbered spools. Both spools were from the same run. However, AT&T mentioned that future runs will incorporate an improved acrylate coating material.

AT&T has offered to examine the degraded fiber from the moisture embrittlement test to assist in determining the cause of the problem, and we have accepted their invitation. However, they were not able to conclusively determine what happened.

One last important point, not directly related to the fibers themselves is the variation observed in connector attenuation, or more precisely coupling efficiency, during the moisture embrittlement test. The connectors did not seat in the same positions each time they were connected, and could be made to vary coupling efficiency by pushing on them with moderate amounts of pressure. On a rocket engine, such properties could allow large amounts of vibration induced noise.

Use of the ruggedized connectors, such as the ones obtained for the vibration and shock tests should reduce or eliminate this problem. Even so, the connectors will have to be tested to ensure vibration induced noise is not a problem.

Temperature Cycling Tests

The temperature cycling was performed in a temperature cycler in the Rocketdyne Instrumentation Laboratory according to the test plan. The cycler was designed to allow retrofitting for use down to liquid nitrogen temperatures. Liquid nitrogen temperatures are required for this temperature cycling test, and therefore the temperature controller for the chamber was altered to allow operation down to those temperatures. Figure 27 displays a photograph of the temperature cycling test setup.

The bare fibers were fed through a port in the cycling oven and coiled with a 300 mm diameter. The fibers were then shielded from splashing nitrogen with aluminum foil. A type J thermocouple, calibrated at both water and nitrogen boiling temperatures provided reference temperatures of the fibers. Both temperature and fiber attenuation data were logged automatically. The temperature data was logged every five minutes, and the fiber attenuation every two minutes throughout the test.

Fiber attenuation results are displayed in Figures 29 through 32. The fibers were tested two at a time, allowing the attenuation monitoring of each fiber using available fiberoptic power meters without the need to disconnect and reconnect fiber connectors. Not disturbing the connectors avoided the variations in attenuation seen in the previous moisture embrittlement test.

Discontinuities in the temperature curves are due either to opening the oven door for inspection or pausing the test to refill the liquid nitrogen dewer.

The attenuation results show very little variation for the gold jacketed, aluminum jacketed, and titanium carbide jacketed fibers as can be seen from the results displayed in Figures 28, 29 and 30, respectively. In all cases, the variation in attenuation is roughly a quarter of a decibel. The power meters used are specified with an uncertainty of .22 decibels, or about 5 percent.

The fluoride fiber which failed the moisture embrittlement test also failed during the temperature cycling test. Several facts taken together tend to strongly point to moisture embrittlement as the cause. These facts are the following: fiber transmission was quite steady through several temperature cycles until it dropped precipitously, after the point where it entered the temperature cycler, and this point had been observed to be covered with condensation during portions of the test.

It should be noted that the attenuation measurements taken before the fluoride fiber failed, appear to show that operation throughout the cycling temperature range did not alone produce any major variation in fiber attenuation.

Under microscope examination, the fluoride fiber did not show any signs of the severe white spotting observed during the moisture embrittlement test. If moisture embrittlement contributed to the breakage, it must weaken the fiber before it becomes visible under 70x magnification.

A sample of the AT&T amorphous carbon-coated fiber also yielded what may be questionable results in the temperature cycling test. The total variation in attenuation for the fiber was about 3.5% throughout the duration of the test. It should be noted that the data for this fiber is presented in microwatts instead of decibels, and that a different power meter was used from that used with the other fibers.

Although this level of variation is not expected to be a problem in and of itself, the observations that the increases in attenuation coincide with the beginning of the chilldown portion the temperature cycles one and four, and that this attenuation is far from repeatable from cycle to cycle, together indicate the possibility of a more serious

problem for this fiber. This attenuation could be taking place due to fiber microbending losses. This kind of loss is caused by a number of bends in the fiber which each have a small radius of curvature but occur for only a short distance.

Considering the results of the first moisture embrittlement test of the amorphous carbon-coated fiber, and the condensation formed during the temperature cycling tests, microbending of the fiber could well be caused by the freezing of water caught between the fiber's jacket and the fiber itself. This type of microbending would tend to confirm the concern that the water under the fiber jacket could abrade the fiber or its amorphous carbon hermetic coating. Such a failure mode would be of great concern on a rocket engine due to the temperature variations and high vibration levels inherent in the environment.

Careful examination under a 70x microscope did not reveal any bubbles or anomalies in the fiber. However, the long length of the fiber (5 meters) made it impractical to manually check the entire surface area.

Temperature Extremes Testing

The five-meter long fibers were coiled with a 300 mm diameter and fed through a port in the oven. The oven was set to maintain 260 $\pm$ 10°C (500 $\pm$ 18°F) for 96 hours. A calibrated thermocouple provided the fiber's temperature, which was logged by a Fluke datalogger every 45 minutes. The fiber's attenuation was measured every day at 8 am and 5 pm. Each fiber was connected five times to average out random connector mismatches.

Figure 33 shows the test results. There was no significant change for the titanium carbide and amorphous carbon coated fibers and only a 5% drop for the gold and aluminum coated fibers. For all the fibers, no change was noticed during the first 48 hours of testing, so that even if the 5% variation of the metal-coated fibers were a problem, it would not show up until after many hours of hot firing.

The fluoride fiber, which was not measured because it broke in the last test, burned during this test. Figure 34 shows the burned fiber.

The cold temperature extreme testing was done by floating fibers on liquid nitrogen in a large Dewar. The fibers were coiled into 140 mm diameter circles and floated on a thin piece of Styrofoam. The fibers were fed through a hole in the Dewar's lid to a power meter where the light transmitted from an 850 mm diode was monitored every 30 minutes. A thermocouple was mounted on the Styrofoam to record the temperature and it was logged every 45 minutes. The results were plotted, and appear as figures 35 through 37 and 39. The fibers did very well except the amorphous carbon-coated fiber whose transmission dropped to zero shortly after the test began. Microscopic analysis revealed the cause as a smashed fiber (Figure 38). The smash occurred outside of the Dewar. Someone probably bumped into it, and not seeing any damage let it go unreported.

The aluminum and titanium carbide-coated fibers showed less than 0.1 dBm change over the full 120 hours. The gold fiber had a slight attenuation increase which remained constant throughout the test. The fluoride fiber was not tested because it was burned in the hot temperature extreme testing. In short, the gold, aluminum and titanium carbide-coated fibers showed little or no change in attenuation due to long term exposure to liquid nitrogen temperatures. The amorphous carbon-coated fiber performed well until it broke independent of this test.

Shock and Vibration Testing

Shock and vibration tests were performed simulating the mechanical environment of a typical rocket engine. For the tests, an oven equipped for electric heating and liquid nitrogen cooling was mounted above a shaker to provide the required thermal environment. Fixtures were designed to extend the shaker armature into the oven (see Figure 41). An accelerometer was mounted on the fixture to control and monitor the vibration and shock levels. Air temperature measurement in the oven was provided by a suspended thermocouple.

Before each test, the oven was precooled (or pre-heated) so that a constant temperature could be maintained during the test. After each test, the system was given one hour to return to room temperature. The fibers were then removed for monitoring. Attenuation was measured before and after testing using a standard fiberoptic LED source and a fiberoptic powermeter, mating each connector 5 times to average out misalignment losses. In order to isolate the shock and vibration effects, separate

harnesses were used for the shock and vibration tests. Figure 42 depicts the vibration harness.

Each harness contained five 2-meter long single fibers and a 1-meter long gold bundle. Each single fiber was cabled in Brand-REX OC-1170 loose-tube cabling for mechanical protection. The cable jacket was made of a high-temperature fluorocarbon with braided Teflon-coated Kevlar as a strength member. The 0.89 mm I.D. inner tube which loosely held the fiber was a fluoropolymer. Each of the single fibers was terminated with an ST connector at one end. At the other end pin contacts were mounted for use in an ITT Cannon 38999 Series III multifiber connector. This type of connector is being strongly considered at Rocketdyne for use as a standard electric control system connector. It has a positive locking action and no torquing or lockwire requirements. The vibration harness used an 11-channel connector with male pins and the shock harness used an 8-channel version with female pins or sockets. Each connector had a strain relief clamp and silicon tape was wrapped around the five cables until the diameter was large enough for the clamp to grip firmly. Half inch diameter Silverflex (a Teflon-coated fiberglass braid) was used to harness the cabled fibers and was fastened onto the multi-pin connectors with the backshell.

Separate test receptacles were made with connectors that mated with the multifiber connectors of the test harnesses, Seicor 100/140 fibers, and ST connectors on the other end allowing connection to a fiberoptic source or powermeter.

The gold bundles were of the same construction as the bundle that was cold-bend tested, except that they had ST connectors mounted at each end.

Vibration Testing

All vibration tests used a random noise generator filtered to give a flat random signal from 20-2000 Hz. This was compared against several vibration curves from SSME, RS-27, and Delta engines. The flat-random spectrum was chosen because it has equally large g^2/Hz valves across the spectrum and hence effectively encompasses all possible engines.

Hot and cold vibration tests were performed for one hour each on two axes at a level of 40 g's. The hot tests were at +275°F. The cold tests were at -280°F.

Two preliminary room-temperature tests, not specified in the test plan were performed to provide a better understanding of the fiber's vibration tolerance. These room-temperature tests and the 20g axial tests were performed on an Unholtz-Dickey 300-lb. force shaker. Samples of the vibration spectra readings from the tests are included in Appendix D.

During the 20g cold testing, the vibration levels fell off at low frequencies due to freezing of the armature (see Appendix D). The remainder of the testing, including all 40 g testing, was moved to a LING 30,000 lb. force shaker with a 400 lb. armature, that could not freeze up during testing (see Figure 40). As the vibration plots of Appendix D show, this shaker was able to maintain a 40 g rms flat spectrum even after an hour of cryogenic shaking.

The test results are shown in Figure 43. The amorphous-carbon coated fiber broke during the first hot test at 20 g's. It broke right at the back of the pin in the multi-channel connector indicating a need for greater strain relief. A significant transmission drop is noticeable after the first 40g test for both the aluminum and titanium-carbide coated fibers. This may be due to pin misalignment. The 11-channel connector has .0625" diameter pins which stick out about a quarter of an inch. Because these were free to move during the test, their alignment may have changed slightly, reducing light coupling. If this is the case, the gold fibers larger 200 micron core (as opposed to 100 micron for the aluminum and titanium carbide coated fibers) would be less susceptible to alignment changes. On a rocket engine, connectors would always be used as mated pairs so the pins would be fixed in sockets and would not be free to move.

The fluoride fiber does not appear in Figure 43 because it broke during the preliminary room temperature tests. The loose-tube cabling came loose from the contact pin, so that the fiber was free to slide out, indicating a completely severed fiber. The break occurred somewhere in the middle of the fiber, and the added fiber stress due to lack of strain relief from the cable may have contributed to or caused it. It is not known which of the room temperature tests caused the break since the fluoride fiber was measured only after the second test. The reason for this was to preserve the mating reference of the aluminum fiber which shared the same test-receptacle channel in powermeter testing. The gold, aluminum and titanium-carbide coated fibers, as well as the gold bundle, passed all the vibration tests.

Shock Testing

All of the shock tests were performed on the 30,000 lb-force shaker in a manner similar to the vibration tests. Four shock tests were performed: hot (+275 °F) and cold (-280°F) tests were conducted for both the radial and axial directions. Each test had 48 shock pulses. The spectrum used for the tests is shown in Table 10.

All of the fibers did well in the shock tests: only the gold fiber broke and it did so during the final test.

The fluoride fiber was included in the test, but does not appear in these graphs. The softness of zirconium fluoride glass makes it hard to connectorize. It came out of its socket before the tests began and therefore could not be measured. After testing, the fluoride fiber was removed from the harness. Visible light was coupled into one end of the fluoride fiber and observed at the other, indicating that it did not break. The same test on the gold fiber confirmed that it was broken.

The sudden increase in the transmission of the titanium carbide fiber after the last test is believed to be the result of human error in data recording.

Although the fluoride fiber could not be measured, it did not break. It should be noted, that since the fluoride fiber could not be held in its socket during shock testing, it did not experience the same loading forces at the connector pin as the other fibers. Thus the fluoride fiber receives a qualified passing grade for this test. The gold-coated fiber did very well, holding out till the last test and the other three fibers and the gold bundle did exceptionally well, suffering no breakage at all. The breakage of the gold fiber was probably due to excessive flexibility in the cable during its final high temperature test. The high temperature reduces the cable stiffness.

It is interesting to note that the vibration harness was also used to film a video in which it was subjected to an additional 15 minutes of 40 g rms vibration and 48 full-level shock pulses at room temperature. There was no measurable change in transmission after these additional tests demonstrating that the same fibers can withstand both shock and vibration.

IR&D: Vibration - Induced Loss Testing

Although this work was not funded by this contract, interesting results are included here.

The purpose of this test was to study in situ vibration effects on an optical fiber. Light was transmitted through the fiber while it was vibrating at 20 g's up to 2500 Hz. The fiber chosen was amorphous carbon-coated 50/125 silica fiber from AT&T. The fiber was cabled in brand-REX OC-1170 loose-tube cabling and attached to a B&K shaker. The shaker was driven with filtered pink noise for the flatest possible random spectrum from 20-2500 Hz. A calibrated accelerometer monitored the vibration. The light transmitted through the fiber was received with a fast photodiode and monitored with an oscilloscope and processed by a spectrum analyzer.

Figures 45 and 46 show a schematic and photo respectively. No change was observed in the D.C. optical component, and as the plot in Figure 47 shows, at the higher frequencies the induced modulation in light transmission was less than .05%. The vibration signal was recorded first, then the no-vibration signal. The large peak at 2 KHz in the no-vibration signal came from the accelerometer signal conditioning electronics.

This test showed that the optical fiber transmission was not substantially affected by vibration at 20 g rms.

VIII. Sapphire Fiber Results

INTRODUCTION

Sapphire fiber was studied due to the lack of promise shown by the fluoride infrared fibers in environmental testing. Further development appeared unlikely to compensate for both the extreme susceptibility to moisture damage and low tensile strength of fluoride fibers. Sapphire appears capable of providing high tensile strength and resistance to moisture similar to that of silica glass. It also can provide other advantages such as high temperature capability and ultraviolet transmission which would be of great interest for engine applications.

Ultraviolet transmission would be useful for combustion diagnostics techniques such as laser-induced fluorescence and oxygen absorption. The high temperature capability could be used to simplify the monitoring of high temperature combustion environments. It could also be used for health monitoring of crucial high temperature components such as hydrogen cooled leading edge sections of the National Aerospace Plane. Sapphire fiber is already being studied for use in composite materials to provide strength at high temperatures.

Information was gathered on sapphire optical fiber through a literature search and also through discussions with researchers in the field. Data was gathered on the present status of sapphire fiber, and areas in which improvement appears necessary were identified. This information is discussed in the section below. Test results we obtained for a cold bend test and an ultraviolet transmission test on a sapphire fiber sample clad with amorphous silica are discussed in a separate testing section following the overall technical discussion.

SAPPHIRE FIBER TECHNICAL DISCUSSION

Sapphire optical fiber shows great promise, although it is not fully developed and is commercially available only on an experimental basis. Tensile strengths of 200,000 psi have been reported by several sources at room temperature. Room temperature tensile strengths up to 400,000 psi and nominal tensile strengths to 75,000 psi at 1400 C were quoted by Saphikon. A bend radius as small as 4 mm for a 125 micron fiber was reported by G.A. Magel of Stanford University. Good transmission appears possible from less than 200 nanometers in the hard ultraviolet to somewhat beyond 4 microns in the mid-infrared.

Although the fibers appear capable of providing exceptional performance for the parameters described above, they are not fully developed. Only one commercial source of the fiber (Lasergenics) was found, and they provide fiber only on an experimental basis. One other previous commercial source of sapphire optical fiber (Saphikon) now will only sell structural fiber. A Saphikon representative indicated however that they are considering reentering the optical fiber business.

Two major factors inhibit the commercialization of sapphire fiber. One is the fact that sapphire optical fiber must be grown as a single crystal. Standard silica based optical

fibers are grown as a glass. Growth of a single crystal fiber is slower than glass fiber growth, and requires completely different drawing techniques. The other major factor inhibiting the commercialization of sapphire optical fiber is the lack of a suitable cladding material. The cladding layer, surrounding the fiber core is necessary to keep the light inside the fiber.

Sapphire fiber has generally been produced unclad. Air can serve as a cladding material, but this leaves the fiber susceptible to surface contamination, which will result in loss. Optical fibers, even those as hard as sapphire, also need a protective jacket layer to prevent surface scratches, which otherwise result in a major loss in tensile strength. This jacket is usually applied over the cladding in glass fibers.

Two techniques have been identified by which sapphire optical fibers have been made. The first, used by Lasergenics, and originally developed at Stanford University, slowly draws a fiber from a larger crystal while remotely applying controlled heat with a beam from a carbon dioxide laser. The second technique, used by Saphikon, is Edge-Defined Film Fed Growth. In this technique, the crystal fiber is slowly drawn from a melt through a die.

Several advantages and disadvantages appear inherent to each technique. Edge Defined Film Fed Growth is now being used to produce large amounts of structural fiber for aerospace applications, drawing multiple fibers from one melt. Economies of scale already exist, and it is assumed that many lessons from production of structural fiber will be applicable to optical fiber.

The process appears more subject to contamination, however, which could result in attenuation in an optical fiber, especially in the ultraviolet. A Saphikon representative stated that fiber attenuation levels on the order of 2 dB per meter in the infrared are achievable with the present level of the technology.

The laser drawing technique was developed specifically for the production of optical fibers. The possibility of contamination is reduced, as the fiber touches nothing, except surrounding gas, during the growth process. However cost most likely will be higher, due to the drawing of only one fiber at a time and the expenses of the laser. It should be noted that carbon dioxide laser costs have recently been dropping dramatically.

ATTENUATION: In conversations with researchers at Stanford University, Saphikon, Lasergenics, and Rutgers University, all agreed that attenuation in the blue and ultraviolet is still quite high. All also agreed that this attenuation can most likely be reduced significantly. Attenuation in the infrared in the 3 micron range is much lower, on the order of 1 or 2 dB per meter. Most of the research in sapphire optical fibers evidently is being aimed at this wavelength region. The main incentive for development appears to be the use of fibers for transmission of infrared energy for various medical applications such as tissue ablation.

Jundt, Fejer, and Byer at Stanford reported their results for ultraviolet and infrared attenuation tests on sapphire fiber at the 1989 SPIE Proceeding on Infrared Fiber Optics. The sample tested was an unclad fiber produced by the laser drawing process in an air environment.

Scattering was measured by collecting light scattered out of the fiber with an integrating sphere. Their scattering measurements varied moderately from .13 to .18 dB/m in the 457 to 1064 nm range. Absorption was determined by monitoring the heat flux from the fiber. Absorption losses varied from 1.7 dB/m at 2.936 microns to 17.4 dB/m at 457nm. A single absorption measurement taken with a fiber grown in an oxygen atmosphere found a 0.88 dB/m loss at 2.936 microns.

The absorption, at 17.4 dB/m was very high in the blue, but not high in the red, with a reading of 1.3 dB per meter at 632.8 nm. This roughly correlates with the results we obtained for absorption, discussed in the next section. Attenuation readings reported at 488 nm and 514 nm were respectively 6.3 and 4.6 dB/ meter.

The high absorption in the blue is apparently due to impurities (probably including hydrogen or effectively hydroxide) and color centers. Possible ways to reduce this attenuation would include procedures to reduce the introduction of impurities, and annealing the fiber at high temperatures. Some further effort to clearly identify the causes of the absorption may still be useful. Only the researchers at Stanford indicated that they were pursuing ultraviolet attenuation reduction.

CLADDING: As stated earlier, sapphire fiber is usually produced unclad. Such fiber does not appear suitable for rocket engine applications. The only work found relating

to the cladding of sapphire fiber was that performed at the Virginia Polytechnic Institute and Rutgers University. Both apply the cladding after the fiber is drawn.

The cladding at Rutgers was limited to a plastic, which could be used in the infrared. Such a plastic can also serve as a jacket, protecting the fiber against scratches, and could conceivably serve quite well for short fiber lengths operating at moderate temperatures. No other information was found indicating that anyone has investigated the jacketing of sapphire fiber.

Discussions with, and papers by Dr. Desu at the Virginia Polytechnic Institute indicate that a number of other promising candidate cladding materials have been identified. Only a few have been deposited on a sapphire fiber at this date.

Properties of interest in a fiber cladding include the wavelength range of transparency, index of refraction as a function of wavelength over this range, solubility level in water, mechanical strength, melting point, and coefficient of thermal expansion.

Information was gathered on a number of candidate optical materials, and evaluated on the basis of these properties. The results are presented in Table 11.

Candidate cladding materials were rejected if they were found to be water soluble or to have an index of refraction higher than that of sapphire. A number of better known infrared materials such as germanium, salt, and silicon are excluded from the chart on this basis.

A coefficient of thermal expansion close to that of sapphire is desirable to avoid excessive stress and possible delamination of the cladding material. Materials were not excluded, however, for this reason.

The most promising candidates on the basis of the data collected are listed at the top of the table. Some information exists to help narrow the field. MgO appears to be at least very slightly soluble in water. Materials with an index of refraction very close to that of sapphire (including BeO, MgO, and to a lesser extent $MgAl_2O_4$) will allow light to leak from the fiber at a much larger bending radius, and are thus of less interest.

The top candidates remaining are $Al_6Si_2O_{13}$, Mg_2SiO_4, $MgSiO_3$, SiO_2, SiO_xN_y, $Ti_xSi_yO_2$, and chemical exchange of oxygen in the outside layer of the sapphire fiber with fluorine. Plastic claddings as that used at Rutgers, were excluded from Table 11, but could be quite useful in the infrared for short runs at moderate temperatures. Absorption may be a problem in the ultraviolet.

SAPPHIRE FIBER TESTING

As part of this program, a 209 micron diameter 6 inch long sapphire fiber sample was acquired from Lasergenics and clad with a 1 micron layer of amorphous silica by Dr. Desu of the Virginia Polytechnic Institute. Cold-Bend and transmission tests were conducted on this sample.

Amorphous silica was chosen for the cladding material because it is relatively easy to apply, has a high melting temperature, is relatively transparent from the ultraviolet to the infrared, and is reasonably moisture resistant. One disadvantage of silica is that it has a much lower coefficient of thermal expansion than sapphire. It was hoped that the thinness of the layer would help avoid delamination.

Although silica is the basis for most optical fibers, a number of advantages can be obtained by limiting it to the cladding layer. Although the melting point of amorphous silica is roughly 1700 degrees C, its strength is reduced markedly at such high temperatures. The use of sapphire as the core of the fiber provides the advantage of its much higher strength at high temperatures for mechanical support.

The transparency range of sapphire exceeds that of silica in both the infrared and ultraviolet. Silica is transparent from well into the vacuum ultraviolet to well beyond 3 microns in the infrared from the standpoint of window applications. Attenuation is high however for fiber lengths toward either end of these wavelength regions, especially in the infrared. The silica fiber requires the addition of an impurity to achieve different indices of refraction in the core and cladding, which causes another attenuation problem.

A marked increase in wavelength range should be achievable over standard silica fibers by a sapphire fiber clad with a layer of pure silica. The light will travel the great majority of its path through the sapphire, thus greatly reducing attenuation in the silica.

Also, as no impurities are necessary in the silica, the full wavelength range of amorphous silica is available.

Cold bend testing at liquid nitrogen temperatures was performed on the fiber sample using the same device and method described for the earlier fiber tests. No jacket was applied to the fiber, and it was placed in a tight weave fiberglass tube during the testing. The fiber broke after slightly more than 3000 flexure cycles.

These results are actually quite promising for a fiber under these circumstances, but a jacket material is obviously necessary. Scratches to the fiber during testing almost certainly caused the breakage. Keeping the fiber to a smaller diameter, on the order of 125 microns would also be advisable as sapphire is very stiff (Young's modulus about 9 times that of glass) increasing the stress on the fiber as it is bent. The force on a fiber varies as the forth power of its diameter.

A four inch section of the fiber, remaining from the cold bend test, was tested to determine its absorption profile versus wavelength. Due to the short length of the fiber, and other test parameters discussed below, the results should be used for indication purposes and not as precise values.

Tests were conducted with two different optical sources, an Optonic Labs Radiometric Photometric Calibration Standard Lamp driven by a dedicated precision current supply and a Hamamatsu L879 deuterium lamp. Light was coupled into the fiber via an amorphous silica lens for both of the sources. A Tracor TN6600 spectrometer system, including an intensifier was used as the detector.

Attenuation readings were determined by first taking a spectrum with the fiber, and then placing an aperture in the system in place of the fiber to produce roughly the same throughput. The spectrometer integration time was then adjusted to attain the same number of counts at a particular wavelength as was seen with the fiber. The two transmission level files with the fiber and aperture were then processed to determine the transmission of the fiber relative to the aperture as a function of wavelength. The result is normalized to 100% transmission at the wavelength for which the aperture count level was made to match the fiber count level.

The results obtained with the Optonic Labs Radiometric Photometric Calibration Standard Lamp are displayed in Figure 48. They are believed to be reasonably accurate beyond the inability to account for coupling variations into the fiber versus wavelength and some random noise on the order of a few percent, which can be observed in the curve.

Fiber transmission appears rather steady from about 440 to 580 nm and then starts dropping rapidly as the wavelength decreases. About 50% of the level seen in the visible is passed by the fiber at 360 nm. The curve was cut off at 360 nm due to the low number of counts obtained below this wavelength. The source intensity drops very quickly in this region.

Transmission for this fiber does not appear to drop starting at as long a wavelength as the fiber tested at Stanford, discussed in the proceeding section. The precipitous drop, though a bit further out, is still there. The wavelength readings of the spectrometer were calibrated with a mercury lamp and are accurate.

Transmission data taken further in the ultraviolet with the deuterium lamp was more difficult to take and is less accurate. It should be used for indication purposes only. The same basic method was used, however the deuterium lamp source provided a spectrum which varied quite considerably with spatial position within the focal spot. Data appears to be useful from about 330 nm to 240 nm with increasing error at either end. Beyond that range the error quickly becomes very large. A curve displaying transmission data within this region is displayed in Figure 49.

Although the data can not be meaningfully quantified below 240 nm, some transmission is taking place through the fiber down to 180 nm, the lowest wavelength collected.

Unfortunately, the useful data range taken with the deuterium lamp does not quite overlap with the data taken from the other source. The deuterium lamp data shows that the transmission is relatively flat across the 330 to 240 nm range. Apparently, the rapid increase in attenuation seen from roughly 440 nm to the last data taken with the other source at 360 nm stops somewhere in the 360 to 330nm region.

IX. Conclusions

Single Fiber

Fused silica fibers were demonstrated to withstand rocket-engine environments. Fibers coated with gold, aluminum and titanium carbide withstood moisture-embrittlement for 30 days, temperature cycling between -184°F and +257°F and, 96 hours of temperature extreme testing at -299°F and +500°F. They also survived 40 g's vibration (20-2000 Hz) at both -280°F and +275°F and all but the gold-coated fiber withstood shock tests peaking at 340 g's rms at both -280°F and +275°F (the gold-coated fiber survived all except the last shock test).

The performance of these robust fibers demonstrates that they are viable for rocket-engine applications. Properly cabled, they could provide lighter weight, EMI and lightning-immune sensing and data transmission in otherwise inaccessible environments, and at higher date rates.

This program also demonstrated that acrylate-coated zirconium fluoride fibers are not suitable in their present state for rocket engines. However, if they were coated with one of the above hermetic coatings or encased in metal capillary tubing, they might survive in lower vibration ground test applications.

The results from the amorphous carbon-coated fiber suggest that is susceptible to water damage.

Bundles

The non-mechanical conclusions from single fibers would apply to bundles made of those single fibers because fiberoptic imaging bundles are single fibers packaged together. Thus we can conclude that bundles made of gold, aluminum or titanium carbide-coated silica fibers can withstand 30 days of moisture embrittlement, temperature cycling between -299°F and +257°F, 96 hours of temperature extremes at both -299°F and +500°F. Also, the testing has shown that bundles made from gold-coated fibers can withstand vibration up to 40 g rms (20-2000 Hz) at both -280°F and +275°F as well as shock pulses up to 340 g's at these same temperatures. Bundles therefore appear quite capable of withstanding liquid-fueled rocket engine environments.

Sapphire Fiber

Sapphire fibers were found to still be in their infancy. Little development work has been done on fiber cladding. Attenuation is very high in the ultraviolet and 1 to 2 dB/m in the infrared. Even so, a plastic clad sapphire optical fiber would most likely be suitable for ground test applications at the present level of development. The fundamentals are strong and the technology appears quite promising.

IX. Development Plan

Several items were identified during this program that warrant further investigation. Three areas of continued development are recommended at this time: fiberoptic connectors, flyable cabling and harnessing, and optical flight sensors. Another suggestion, not discussed further below, is that data from optical fibers flown on the long duration exposure satellite, and possibly the fibers themselves, be examined for relevant and important information.

Fiberoptic Connectors - Several major issues have been identified for fiberoptic connectors. Vendors surveyed typically rate their connectors to minimum temperatures of -55°F and maximum vibration level of 20 g's; however, rocket-engine environments demand performance to temperatures as low as -300°F, and to vibration levels as high as 40 g's. Also, connector manufacturers appear to have little experience attaching pins to the new hermetic metal-jacketed, or otherwise coated, fibers of interest for rocket engine applications.

Another survey should be performed to establish a comprehensive list of vendors dealing with mil-spec or aerospace-rated connectors. Once candidate connectors are selected, their ability to couple with the new fibers should be tested.

Couplers proven to be compatible with the selected fibers should then be dynamically tested (shock and vibration) over the rocket-engine temperature range. At least three specific signal degradation mechanisms should be explored: change in intensity coupling (attenuation), variable Fabry-Perot color filtering (wavelength-dependent attenuation), and fresnel zeroing (diffraction). This investigation should also address

the impact of these three degradation mechanisms on various sensor modulation schemes (see Appendix B).

Finally, methods to relieve any excessive strain on the cable where it exits the connector backshell, and also the fiber where it exits the connector pin itself should be explored.

Flyable Cabling and Harnessing - During some of the high-temperature environmental testing, it was noted that the cabling surrounding the fiber tended to soften. Softening of the cabling may crimp the fiber or allow the harness to be bent beyond its allowed minimum radius, causing fiber breakage or signal attenuation (due to loss of total internal reflection between the of the core and cladding of the fiber). A comprehensive search of available cabling materials as well as material studies and testing should be performed to find suitable cabling that can maintain necessary stiffness over the full temperature range expected.

In addition to high temperature stiffness, flyable cabling and harnesses will need to be lightweight, and will have to provide adequate tensile support, flame resistance, and strain relief at termination.

Finally, the minimum bend radius that a given fiber can withstand over a long period-with and without moisture present-can greatly affect the harness design. Therefore, long-term (one year or more) variable-radius moisture embrittlement tests should be performed on fibers envisioned for application to rocket engines.

Bundle Application - An application of a bundle on a rocket is presently in early planning. A window has recently been developed at Rocketdyne for use in high pressure (5600 psi), high temperature (tested to hardware temperatures of 1000 F) environments. It presently appears likely that a window of this design will be installed for ground testing purposes on a Space Shuttle Main Engine fuel preburner, and that images will be transmitted from the window through a fiberoptic bundle.

Flight Sensors - Optical or fiberoptic sensors should be used to fully take advantage of the benefits of optical fiber signal transmission. Many commercially-available technologies use optical, single-fiber or fiber bundle sensors for detecting parameters such as temperature, pressure, strain, refractive index, vibration, acceleration, etc.

While many of these sensors are designed only to survive industrial or laboratory environments, it is possible to adapt them for use in rocket engines. Two examples of this already exist: the fiberoptic turbine blade pyrometer and the fiberoptic deflectometer are commercial instruments that are being adapted for use on SSME turbopumps. Evaluation of both modified instruments is underway prior to their installation on an SSME Technology Test Bed engine.

Some of the optical sensor measurements that are of particular interest (along with appropriate sensor candidates) are: turbine blade temperature profile (fiberoptic pyrometer), cryogenic temperature (phosphorescent decay), combustion gas temperature (hot gas pyrometer), valve position (differential deflectometer or bundle coupled encoder), radial and axial shaft motion (fiberoptic bundle deflectometer), shaft speed (optical pulse sensor), vibration/acceleration (bundle deflectometer or fiberoptic interferometer), fuel flow (optically-encoded turbine), gas or propellant pressure (Fabry-Perot wavelength filtering), and combustion diagnostics (optical spectrometer).

Non-intrusive fiberoptic sensors needed for air mass flow and combustion diagnostics measurements in the hypersonic flowstream of a NASP engine are also of interest.

A new vendor survey and specification analysis should be performed to identify candidate optical sensing technologies, assess their applicability to rocket engines, and estimate the level of effort required to adapt them for rocket engine use. The robustness of promising sensor candidates should then be tested. Generic research can be performed to find ways of strengthening the sensors that do not survive.

Sapphire Fibers

Sapphire fibers could be promising for high temperature applications, applications requiring infrared transmission capability, and apparently with much more development ultraviolet transmission. The fibers could conceivably be incorporated into critical hydrogen cooled structures in the National Aerospace Plane to monitor structural integrity. They also would be useful to perform combustion diagnostics and pyrometry measurements for both standard rocket and supersonic Ramjet engines.

Ground test-bed and low temperature flight applications requiring infrared transmission could probably be accomplished with plastic clad and jacketed sapphire

at little development cost. High temperature applications will require development of claddings just being investigated and jacketing yet to be investigated.

Attenuation of present fibers in the ultraviolet is very high. It appears this attenuation could be substantially reduced, and that sapphire fiber should be capable of transmitting reasonably well to about 200 nm. Research into the causes of this attenuation, as well as an attempt to reduce it would appear justified.

Space Exploration Initiative - Another area to consider is sensor development for space-based nuclear reactors. Due to the high achievable specific impulse of a nuclear powered engine system, it appears interest is increasing in the use of such engines for Space Exploration Initiative applications including a mission to Mars. The extremely high neutron flux levels of an engine system similar to the NERVA would present major problems for either optical or conventional instrumentation.

One area in which optical sensing might be of major benefit is profiling of radiation flux (and thus power level) throughout the reactor core through the use of Cerenkov radiation. Sapphire or liquid core fibers might be candidates for extremely high radiation environments.

Appendix A.

BIBLIOGRAPHY OF FIBEROPTIC REFERENCES

1. Lacy, E. A. - "Fiber Optics".

2. Murata, H. - "Handbook of Optical Fibers Corp. ' "Fiber Optics".

3. Technical Memorandum - Galileo Electro-Optics Corp. - "Fiber Optics: Theory and Applications".

4. Application Notes - Hewlett Packard - "Fiber Optics SMA Connector Technology.

5. Application Notes - Hewlett Packard - "Fiber/Cable Selection for LED Based Local Communications Systems".

6. Application Notes - Hewlett Packard - "High-Speed Optocouplers vs. Pulse Transformers".

7. Application Notes - Hewlett Packard - "Baseband video Transmission with low cost Fiber Optic Components".

8. Application Notes - Hewlett Packard - "Connector/Cable Guide".

9. Department of Economics University of Colorado - "Economic Analysis of the National Measurement System".

10. Schneider W. E. - "Standards for Calibration of Optical Radiation Measurement Systems".

11. Military Standard - 30 November 1977 - "Fiber Optics Test Methods and Instrumentation".

12. Tomasi, G. P. - "Fiber Optic for Military Service".

13. Tomasi, G. P. - "Fiber Optic Cables for Aircraft Deployment".

14. Chester, A. N. - "Optical Fiber Sensors".

15. Harmer, A. L. - "Spectroscopic and Fibre-Optic Transducers".

16. Jacobs, G. L. - "Parts and Components Evaluation Report".

17. Skutnik, B. J. - "Fiber Optic Trends".

18. Gulati, S. T. - "Strength Measurement of Optical Fibers by Bending".

19. Carr, J. J. _ "Changing Attitudes on the Fragility of Optical Fibers".

20. Gulati, S. T. - "Fracture Stress and Mirror Size for Optical Fibers".

21. Quan, F. - "The ABC's of Glass Fiber Strength".

22. Love, R. E. - "The Strength of Optical Waveguide Fibers".

23. Nevins, R. C. - "Testing for a Long Service Life".

24. Vandewoestine, R. V. - "Developments in Optical Waveguide Fabrication by the Outside Vapor Deposition Process".

25. Crow, J. D. - "Power Handling Capability of Glass Fiber Lightguides".

26. Network World - Murphy, K. W. - "Fiber Myths Debunked".

27. Reitz P. R. - "Optical Fiber Test Standards Ensure Efficient Manufacturing and Effective Products".

28. Keck, D. B. - "Fundamentals of Optical Waveguide Fibers".

29. Mattewson, M. J. -"Strength Measurement of Optical Fibers by Bending".

30. Gulati, S. T. - "Strength and Static Fatigue of Optical Fibers".

31. Keck, D. B. - "Single-mode Fibers Outperform Multimode Cables".

32. Friebele, E. J. - "Temperature and Dose Rate Dependence of Radiation Damage in Single Mode and Multimode Optical Fiber Waveguides".

33. Gulati, S. T. - "Water Integrity of Optical Fibers".

34. Holmes, G. T. - "Propagation Parameter Measurements of Optical Waveguides".

35. Friebele, E. J. - "Radiation Damage in Single Mode Optical Fiber Waveguides".

Appendix B

GLOSSARY OF FIBEROPTIC TERMS

Acceptance Angle: The angle over which the core of an optical fiber accepts incoming light; usually measured from the fiber axis.

Bandwidth: The highest frequency that can be transmitted in analog systems.

Birefringent: Having refractive index that differs for light of different polarizations.

Bundle: A group of fibers packaged together, with end points in a common plane. The bundle may be rigid or flexible. In coherent fiber bundles, the fibers retain a fixed position relative to each other and are used as image transmitters.

Cladding: The layer surrounding the light-carrying core of an optical fiber. It has a lower refractive index than the core.

Coating: The protective layer applied to the outside of the cladding. The coating may be designed to handle extreme temperatures, or other environmental effects such as humidity.

Core: The central part of the optical fiber that carries light.

Critical Angle: The angle at which light undergoes total internal reflection.

Fluoride Glasses: Amorphous materials made of fluoride compounds. Fibers made of fluoride glasses can transmit infrared radiation to roughly 5 microns.

Gradient-Index Fiber: A fiber in which the index of refraction changes gradually from the fiber axis.

Hard-Clad Silica Fiber: A fiber with a hard plastic cladding surrounding a step-index silica core.

Hydrogen Losses: Increase in fiber attenuation due to diffused hydrogen into the glass.

Index of Refraction: The ratio of the speed of light in the vacuum to the speed of light in the material.

Kevlar: A strong synthetic material used in cable strength members. (Kevlar is trademark of the DuPont Company.)

Large-Core Fiber: A fiber with core 200 mm or more.

Loose Tube: A protective tube loosely surrounding a cabled fiber, often filled with a gel.

Microbending: Tiny bends in a fiber that allow light to leak out and increase loss.

Mode: An electromagnetic field distribution that satisfies theoretical requirements for propagation in a waveguide or oscillation in a cavity (e.g., a laser). Light has modes in a fiber or laser.

Multimode: Transmits or emits multiple modes of light.

Numerical Aperture: NA, the size of half the angle over which a fiber can accept light. This is multiplied by the refractive index of the medium containing the light, which equals 1 for air, the normal medium from which NA is measured.

Packing Fraction: The fraction of the surface area of a fiberoptic bundle that is fiber core.

Plastic-Clad Silica (PCS) Fiber: A step-index multimode fiber in which a silica core is surrounded by a lower-index plastic cladding.

Plenum Cable: Cable made of fire-retardant material that generates little smoke, for installation in air ducts.

Polarization: Alignment of the electric and magnetic fields that make up an electromagnetic wave; normally refers to the electric field. If all light waves have the same alignment, the light is polarized.

Polarization-Maintaining Fiber: Fiber that maintains the polarization of light that enters it.

Preform: Cables in which many fibers are embedded in a plastic material in parallel, forming a flat ribbon-like structure.

Ribbon Cables: Cables in which many fibers are embedded in a plastic material in parallel, forming a flat ribbon-like structure.

Silica glass: Glass made mostly of silicon dioxide, SiO_2, used in conventional optical fibers.

Single Mode: Containing only one mode. Beware of ambiguities because of the difference between transverse and longitudinal modes. A laser operating in a single transverse mode typically does not operate in a single longitudinal mode.

Single-Polarization Fibers: Optical fibers able to carry light in only one polarization.

Splice: A permanent junction between two fiber ends.

Step-Index Multimode Fiber: A step-index fiber with a core large enough to carry light in multiple modes.

Step-Index Single-Mode Fiber: - A step-index fiber with a small core able to carry light in only one mode.

Tight Buffer: A material tightly surrounding a fiber in a cable, holding it rigidly in place.

Total Internal Reflection: Total reflection of light back into a material when it strikes the interface with a material having a lower refractive index at an angle below a critical value.

Appendix C

CANDIDATE SENSOR INFORMATION MODULATING SCHEMES

Requirements for Referencing Systems and Modulation Schemes

Some referencing and modulation schemes implemented in fiber sensing systems can have an effect on the accuracy and robustness of the system as a whole. Environmentally induced alternations to the sensing system, such as variable microbending losses or path length alternations due to vibration, attenuation due to radiation or partially uncharacterized connector losses, and polarization shifts due to stress-induced birefringence will all have markedly different ramifications for different modulation and referencing methods. The choice of modulation schemes that are relatively insensitive to the rocket engines harsh environment could be of great benefit in implementing a fiberoptic based sensing system.

Furthermore, some referencing and modulation methods may introduce undesirable artifacts, such as non-monotonic response or loss of ability to establish the specific value of the measurand after a power system anomaly. Both of these limitations would be undesirable for a rocket engine sensing system and should be remedied by proper design. Choice of referencing and modulation methods affects such issues as engine controller cost, complexity, weight, and even controller radiation resistance.

Many of the methods examined did not suffer such difficulties and in addition could provide substantial assistance in increasing noise immunity. For implementation purposes, a fiber-based sensing system will be evaluated as a system, not as individual components.

Obviously, each of the sensors must be capable of meeting or exceeding the environmental condition specifications of the present sensors listed in Table 1. The discussion below points out major issues which can be expected in meeting these requirements.

Interferometric (phase-sensitive) Sensors: This modulation method and the sensors that use it tend to be capable of providing great sensitivity with the sacrifice; however,

of vibration susceptibility. Such vibration susceptibility is an issue for rocket engine applications.

Fringe processing methods used for this class of sensors can include direct fringe counting, heterodyning, and multi-wavelength interpretation schemes. These firing counting methods tend to be weak in assuring accurate resumption of measurement output after a power glitch and can also require unacceptable assumptions about knowledge of initial values of measurements during initial power-up of the system. Non-fringe counting techniques used for measurement of acceleration and ultrasonics are more immune to these power interruptions and can be more readily integrated into rocket engine instrumentation. Multi-wavelength methods may overcome some of these problems with some expense of extra cost, complexity, and weight. These sensors should be expected to require polarization preserving fiber; thus, to make use of this modulation method, such fiber and its related connectors must be proven capable of operating in the rocket engine environment reliably.

Intensity Based Sensors - There are several sub-categories of intensity based sensors:

a. Intensity attenuation sensors - These sensors include their data as light attenuation, using such processes as microbending losses. Other losses in the system may be expected due to such effects as connector losses, fiber bending due to stress and vibration, and radiation-induced opacity. All of these loss mechanism will be difficult to account for, and the sensor will have to meet specifications in their presence. Variations in intensity of the source could be monitored. However, variations of efficiency of the detectors maybe more difficult to ascertain.

b. Fluorescence decay sensors - This type of sensor, usually used for temperature measurement or chemical sensing, relies on the alteration of the decay time of a phosphor to send its data as a temporarily modulated signal. In this way it greatly reduces attenuation problems. A pulse of light of one wavelength enters the sensor, and light of a longer wavelength leaves with a delay time that is a function of the measurand. This simple system appears promising for rocket engine application. Vibration may be less of a problem for this method and the choice of phosphor and decay time

may be useful here. Another possible issue is that non-monotonic response may be exhibited by the phosphor for very low or very high temperatures. The recent invention of an ultraviolet light-emitting diode in Japan may provide future new opportunities for this class of sensor.

c. Differential beam-splitting sensors - A sensor can be devised to split light intensity between two return fibers as a function of the measurand. This would virtually eliminate the effect of loss in the sensor's light path, and close routing of the return lines may well keep stress and radiation-induced losses similar. This could not be expected for the couplers in the return lines, however.

d. Time-domain reflectometer - The time-domain reflectometer allows distributed measurement along a fiber by sending an ultra-fast light pulse and monitoring radiation returned back down the line as a function of time. This method appears to be overkill for the present rocket engine applications due to the complexity of such as system and the lack of any immediate need for such distributed measurements. This method is, however, under consideration at the University of Alabama, Huntsville, as a method of determining if a sensor is operating within a desired bandwidth.

Polarization-Based Sensors - These sensors modulate the signal by varying the polarization of light passing through them. This can be accomplished using such methods as the photoelastic effect, Faraday effect, and Pockels effect. They require polarization maintaining fiber.

Wavelength-Varying Sensors - There are two obvious subcategories of wavelength varying sensors.

a. Passband varying wavelength sensors - these sensors relay on the variation of optical wavelength passband to encode their signal. Examples of such sensors include interference filter-based sensors that vary wavelength with temperature and chemical sensors that monitor chemical absorption bands. This modulation scheme avoids the problems of unknown and varying fiber and connector losses and could offer great benefits in a rocket engine environment. However, radiation-

induced fiber losses can be a function of wavelength, and may be a problem for some applications involving high radiation exposure orbits.

b. Emission-based wavelength-varying sensors - Emission based sensors, such as some pyrometers and fluorescence-based temperature sensors, rely on the wavelength distribution of the light they emit encode their signal. Like passband varying wavelength sensors, their modulation method offers distinct advantages, and for the same reasons.

Ribbon, or Bundle-Based Sensors - This sensor designation includes such sensors as:

a. Optical encoder - The optical encoder senses position and conveys this position information by spatially modulating light through a fiberoptic ribbon, or bundle, in a digital code. Absolute, as opposed to relative, position measurement is readily obtained with this method, as is a monotonic output. This encoding scheme's only this method, as is a monotonic output. This encoding scheme's only weaknesses for rocket-engine application appear to be the requirement for the use of bundles, and the limited sensing applications to which it can be applied.

b. Reflection position sensing sensors - Similar to the above, this category relies on sweeping a beam of light along a ribbon, or bundle, as a method of encoding information. This is accomplished by such as method as reflecting a beam of light off a diaphragm. The advantages and disadvantages from a rocket-engine implementation point of view are the same as above.

c. Bundle-based cone-aperature - This sensing method operates by placing a bifurcated bundle tip in close proximity to a reflective surface. The light emitted by half the fibers in the bundle is reflected off the surface and coupled into the other fibers with an efficiency that is proportional to the distance of the bundle type from the surface. Such a sensor is presently being viewed with interest for the application of turbopump bearing condition monitoring. Requirement specifications for this application have not yet been established. Although this method can be expected to suffer the same difficulties as both the intensity

attenuation sensors and the above bundle based sensors, the application mentioned is not expected to require the high precision levels set for many of the presently used sensors.

Pulse Rate - Pulse rate sensors can be used to convey information on such quantities as rotating shaft velocity. Due to their simple, direct, digital nature, they appear quite promising for rocket-engine applications which could make use of them.

Fuller consideration would have to be given to the sensors themselves to go beyond the generalizations that can be made from modulation method suitability alone. From the above discussions, modulation methods of greatest interest would include: fluorescence decay for temperature measurement; wavelength-varying sensors for temperature, pressure and strain; ribbon/bundle-based sensors for position, displacement and vibration (e.g., fiberoptic deflectometer); pulse rate sensors for shaft speed; intensity for high-speed noncontacting temperature (e.g., turbine blade pyrometer); and interferometric for displacement and acceleration.

Appendix D

Acceleration level plots from vibration tests.

All plots were taken from the reference accelerometer. The vibration plots were taken at 19 minute intervals and all pertinent test information was included on each plot. One sample plot is included for each test.

+275° 20g 1 Hour Run

DATE 11-29-89 | Control
RUN NO. 60 min | Radial | Radial
FILTER BW | OVERALL LEVEL 19.84
NO. OF AVERAGES 128 | 10
2000

Fiberoptic Cables

64

+275 20g 1 Hour Run

DATE 11-28 89 Control

RUN NO. 1 60MIN Axial Axial

FILTER BW 19.96

NO. OF AVERAGES 128 10

2000

Fiberoptic Cables

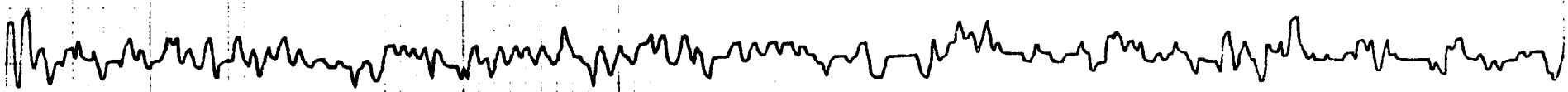

ORIGINAL PAGE IS
OF POOR QUALITY

2 6 8

5 15 20

-300° 20g 1 Hour Run

DATE 11-29 89 Control

RUN NO. 50 min Axial Axial

FILTER BW 11.86

NO. OF AVERAGES 128 1C

2000

Fiberoptic Cables

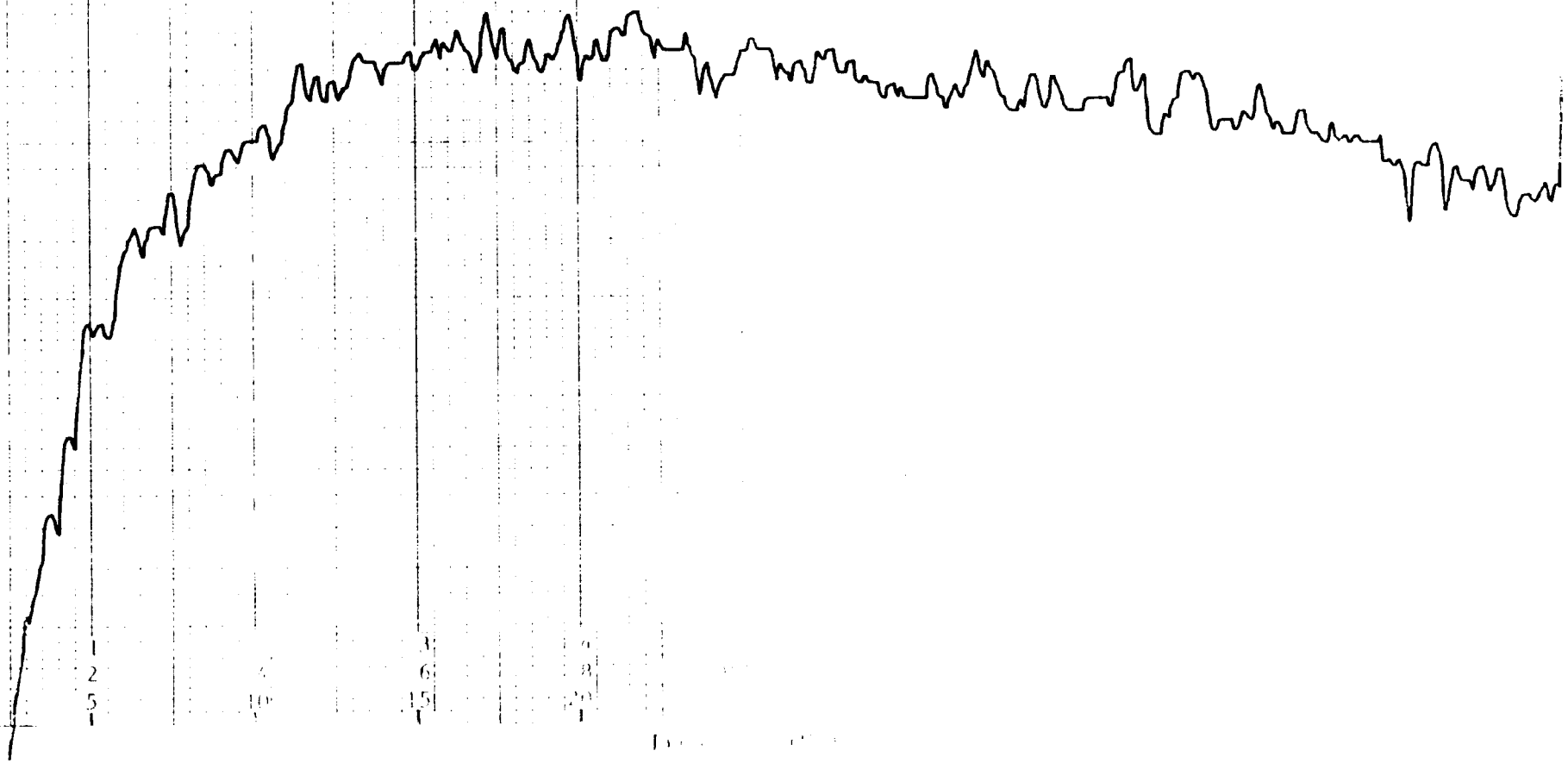

Fiberoptic Cable

DATE 12/6 89 Control Advanced Programs

RUN NO. 1 60 min. Rad. Rad.

FILTER [illegible] 7.5 39.95

NO. OF [illegible] 128 100

2000 Hot (275 °C)

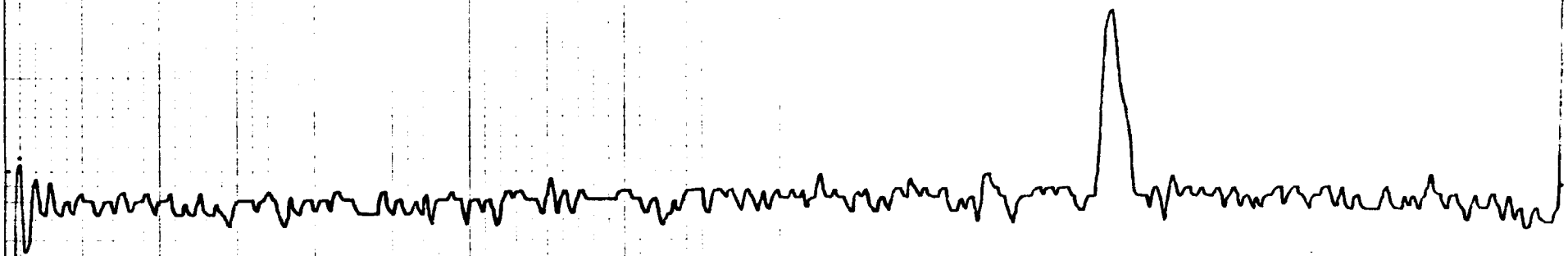

Fiberoptic Cable

DATE 12/6 89 Control
RUN NO. 2 60 min Rad. Rad.
FILTER BW 7.5 40.20
NO. OF AVG 128 100
2000

Advanced Programs

Cold (-280 °F)

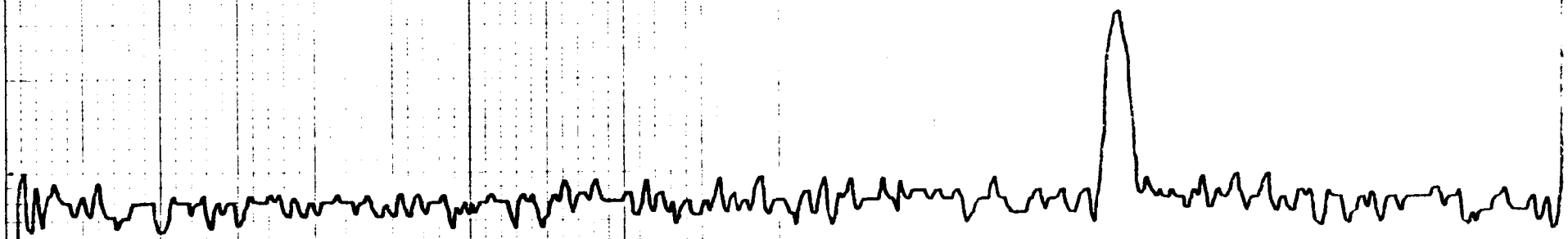

ORIGINAL PAGE IS
OF POOR QUALITY

Fiberoptic Cab.

DATE 12/7 89 Control

RUN NO. 1 60 min. Axial Axial

FILTER 7.5 40.20

NO. OF AVE 128 100

2000

Advanced Programs

Cold (~ -290°F)

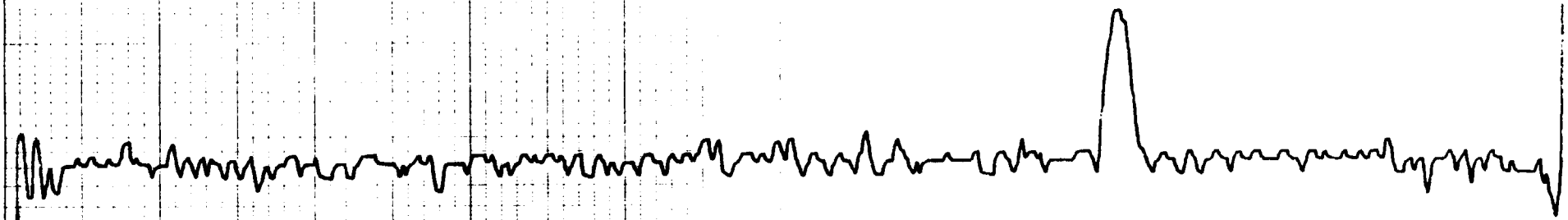

SSME SENSORS

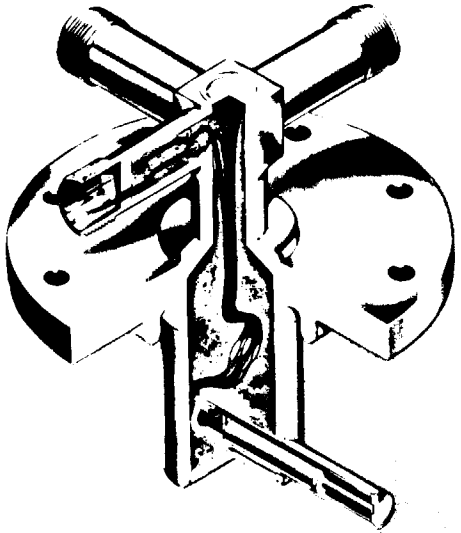

LPOTP SPEED SENSOR

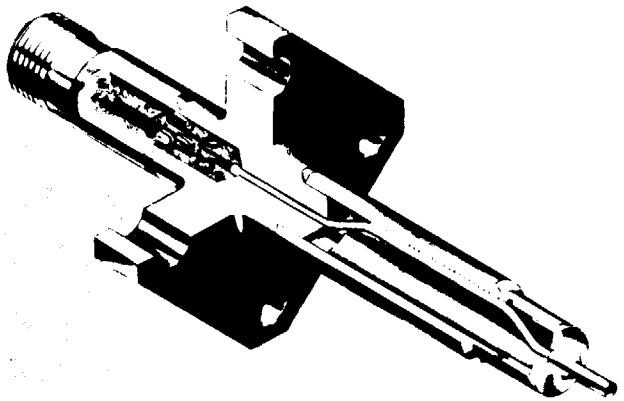

HOT GAS TEMPERATURE SENSOR

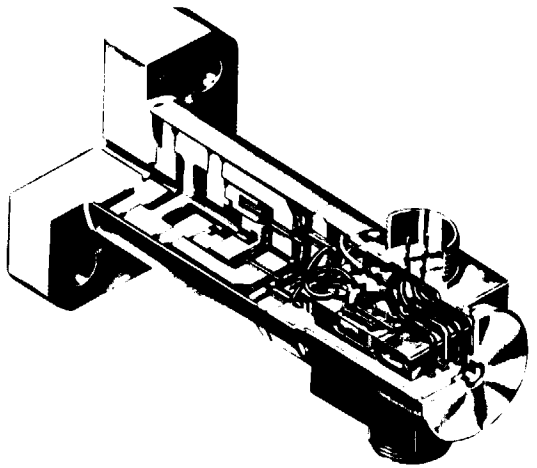

SSME PRESSURE TRANSDUCER

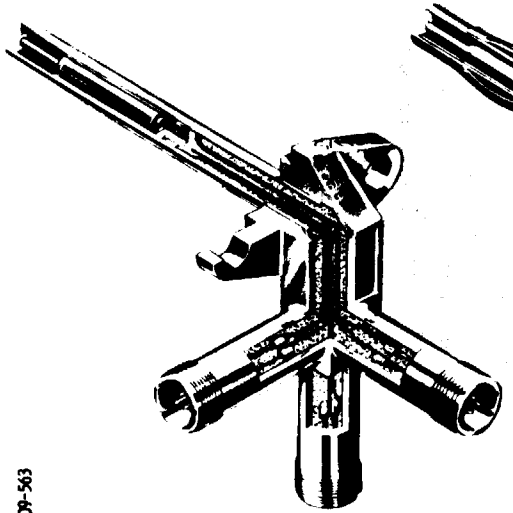

HPFTP SPEED SENSOR

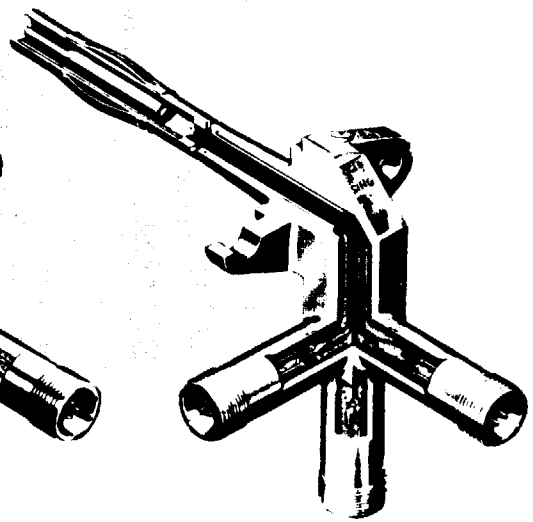

LPFTP SPEED SENSOR

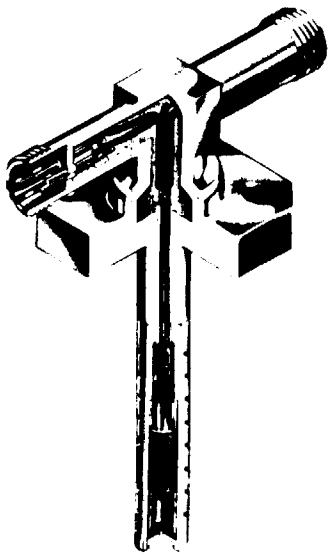

CRYOGENIC TEMPERATURE SENSOR

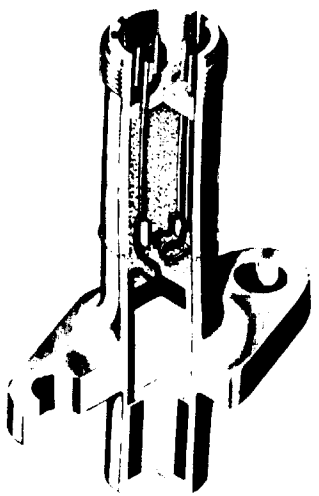

FLOW SENSOR

LC309-563

Rockwell International

Fig. 1. SSME Flight Sensors

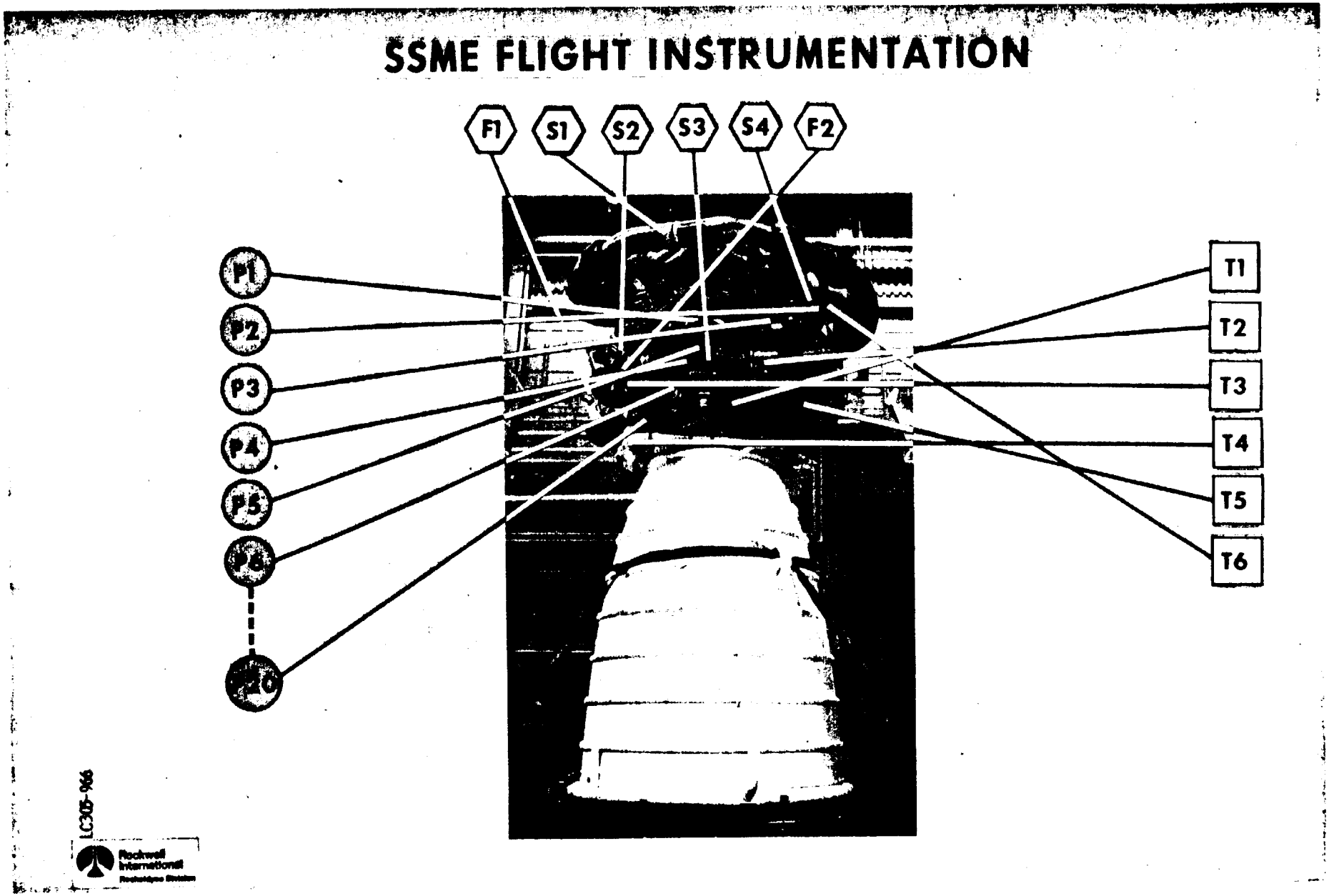

Figure 2. SSME Instrumentation Locations

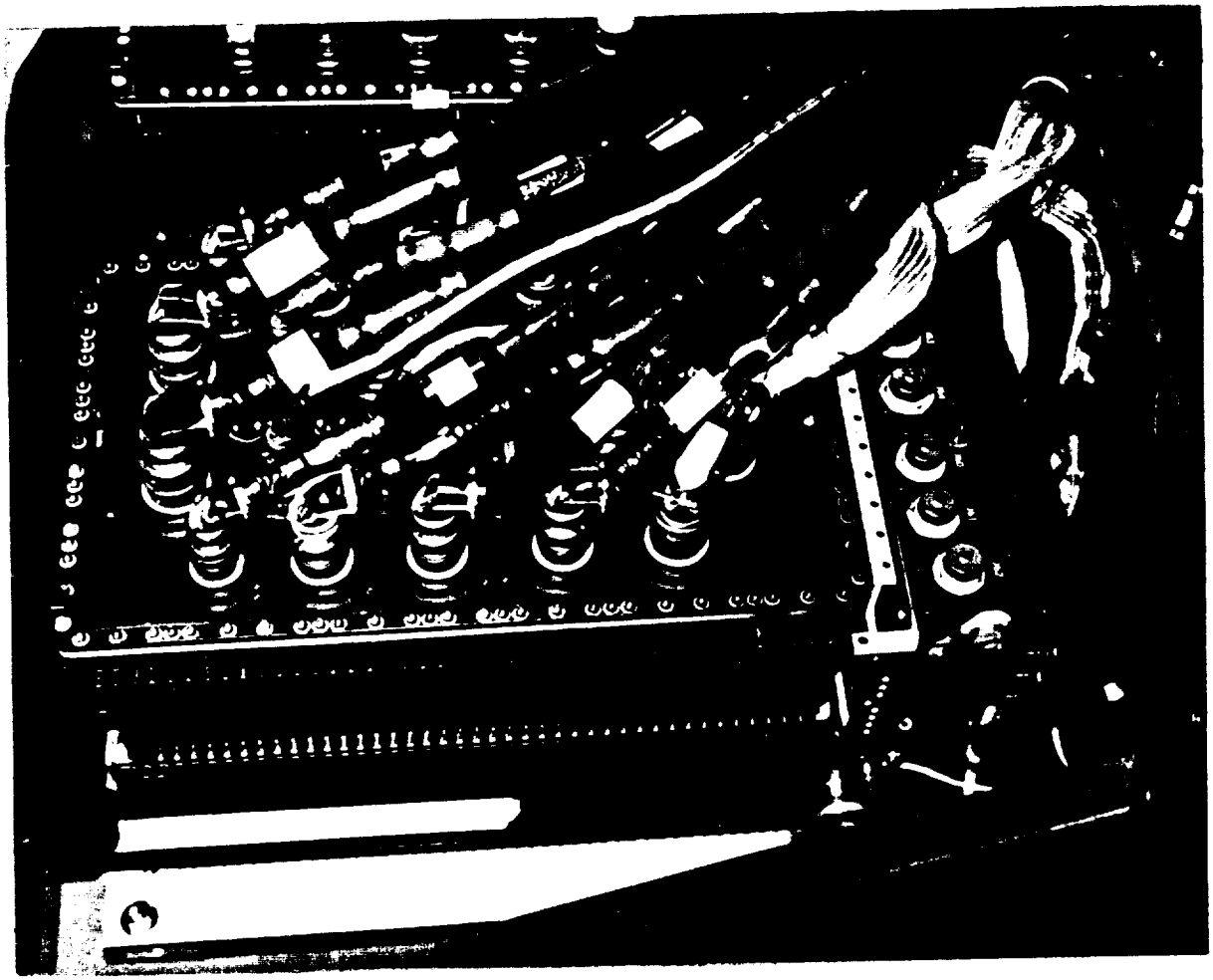

Fig. 3. SSME Harnessing

LC308-937

Rockwell International
Rocketdyne Division

Figure 4 Fiber Attenuation vs Radiation

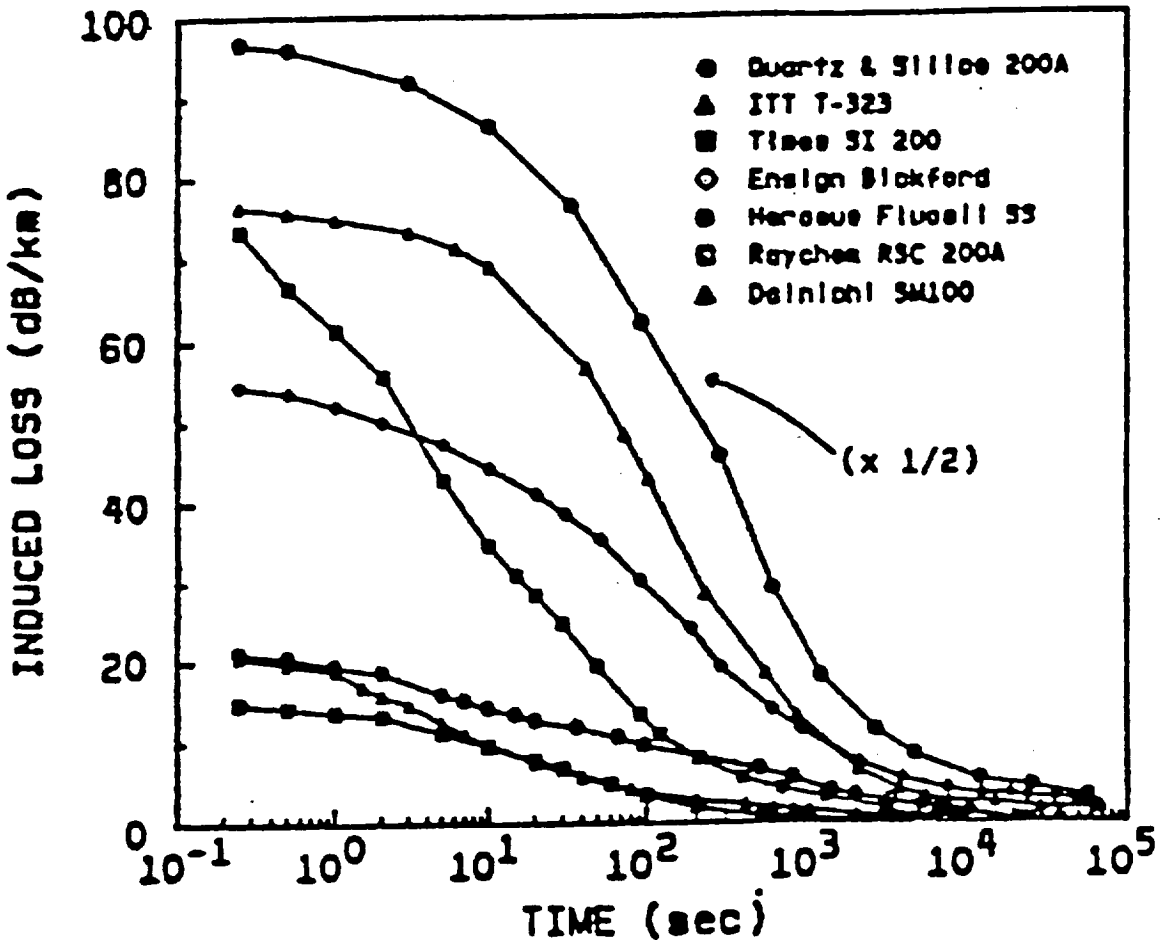

Recovery of the radiation-induced attenuation at 0.85 μm in various pure silica core fibers following an exposure of 3700 rad at 23°C. The Quartz & Silice, ITT, Ensign Bickford and Raychem fibers had polymer claddings; the others had glass claddings. The Quartz & Silice and Dainichi fiber cores had low OH contents (3–10 ppm), whereas the others had 1200 ppm. Light power guided in the fiber during recovery was < 300 nW.

Figure 5. Doped Fiber Attenuation vs Radiation

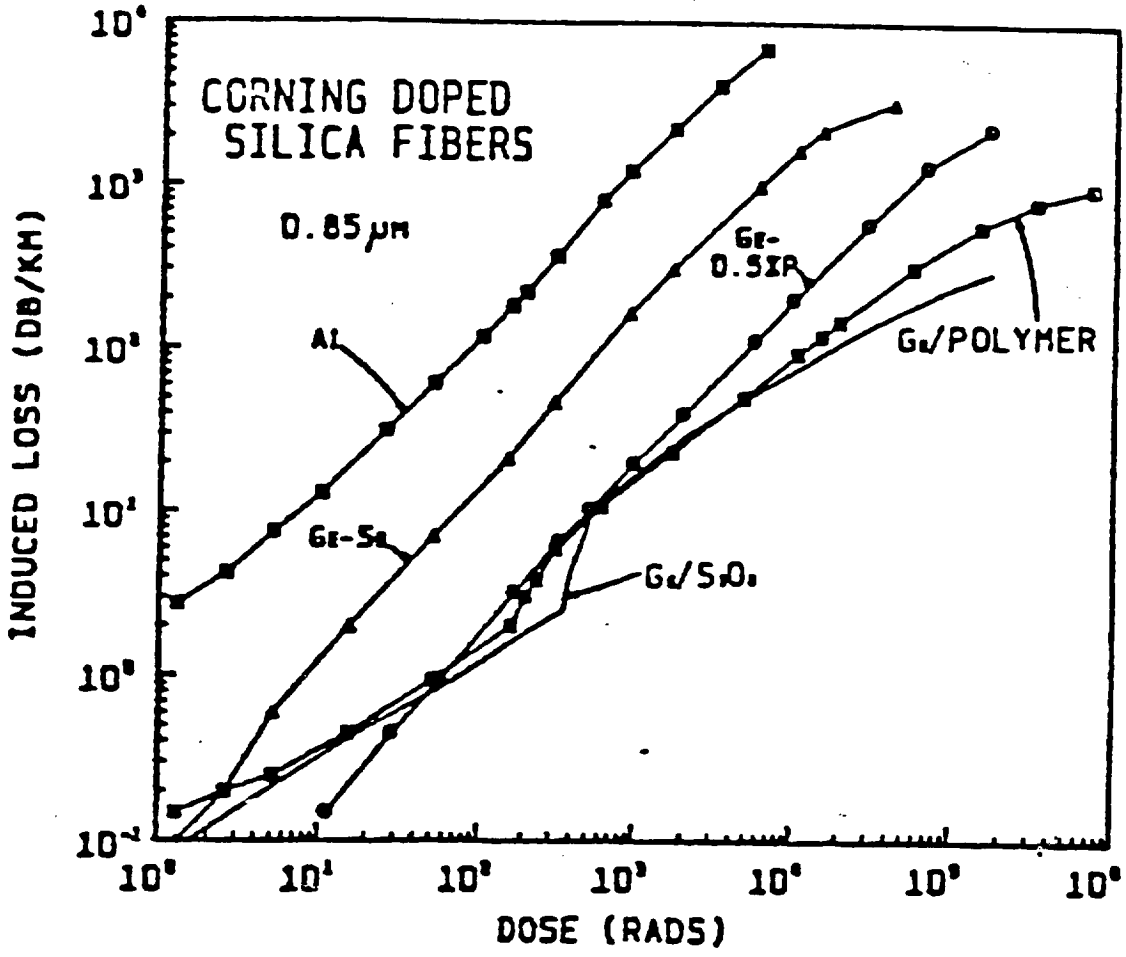

Growth of the radiation-induced attenuation at 0.85 μm in several fibers measured in situ during steady state ^{60}Co irradiation. The dose rates used were ~ 300 rad/min for doses less than 200–350 rad and $\sim 10^4$ rad/min for higher doses. The discontinuities evident in the Ge-doped silica core fibers clad with silica or polymer (Ge/SiO_2 and Ge/Polymer) fibers near 200–350 rad arise because the fiber is moved from the lower to higher dose rate positions in the source (see text). $T = 23°C$.

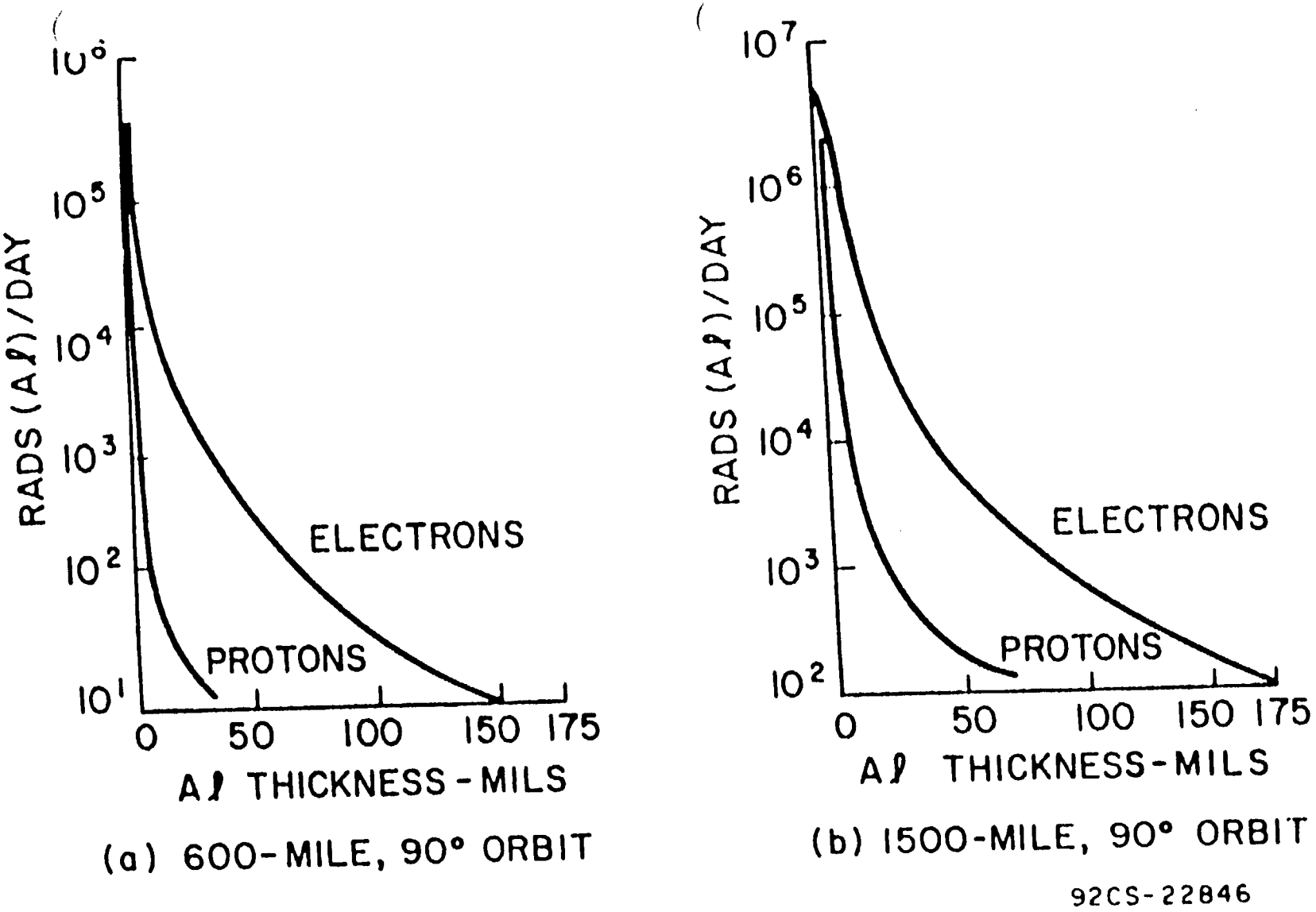

Figure 6 Van-Allen Belt Radiation Levels

Dose-depth curves for trapped electrons and protons in space-craft in orbit.

Fig. 7. Cold Bend Test Apparatus

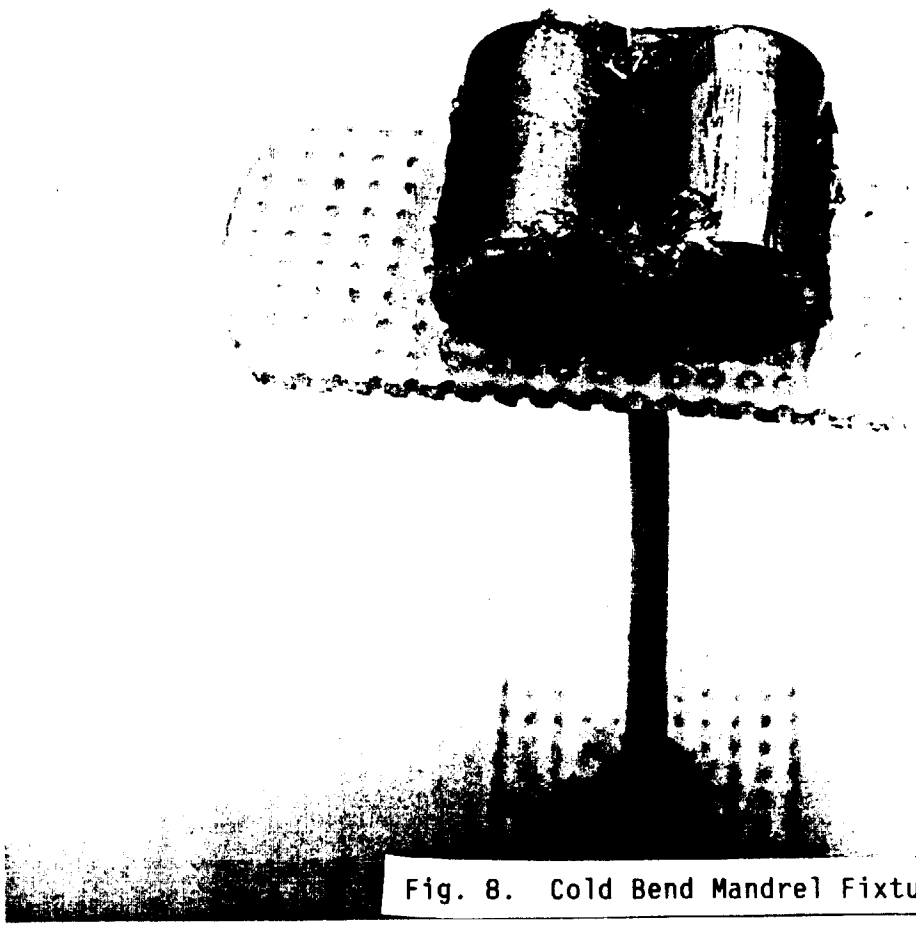

Fig. 8. Cold Bend Mandrel Fixture

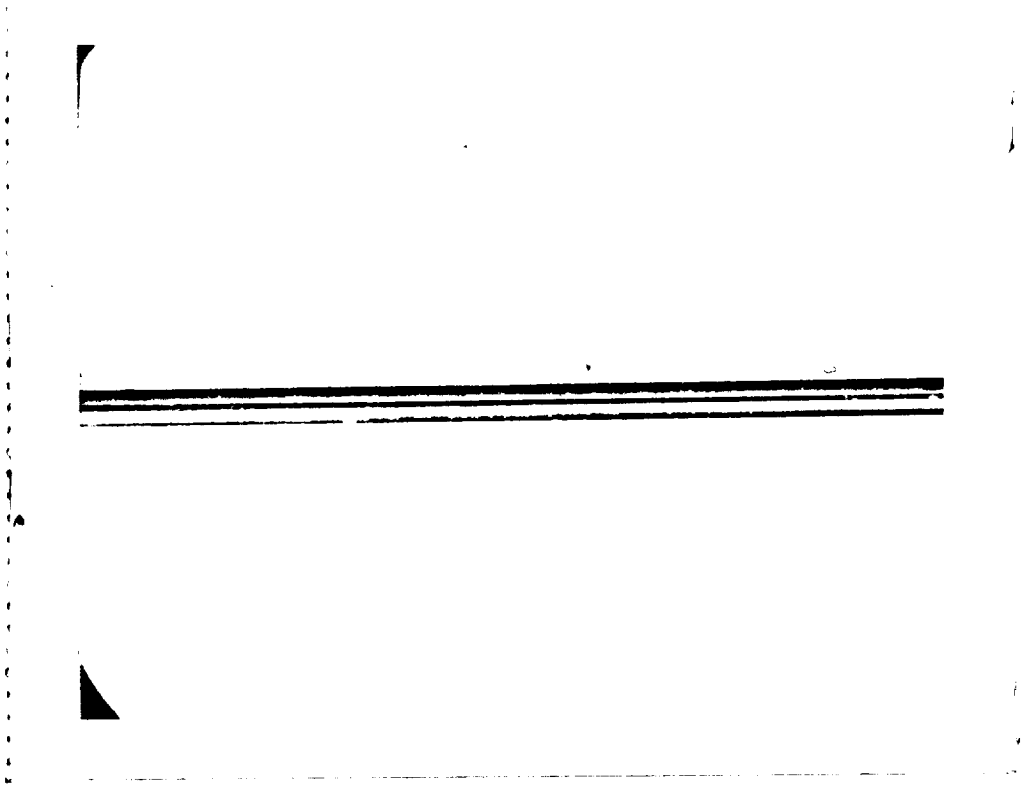

Fig. 9a. Gold Jacketed (Fiberguide) - Pretest

Fig. 9b. Gold Jacketed (Fiberguide) - after 5000 cycles

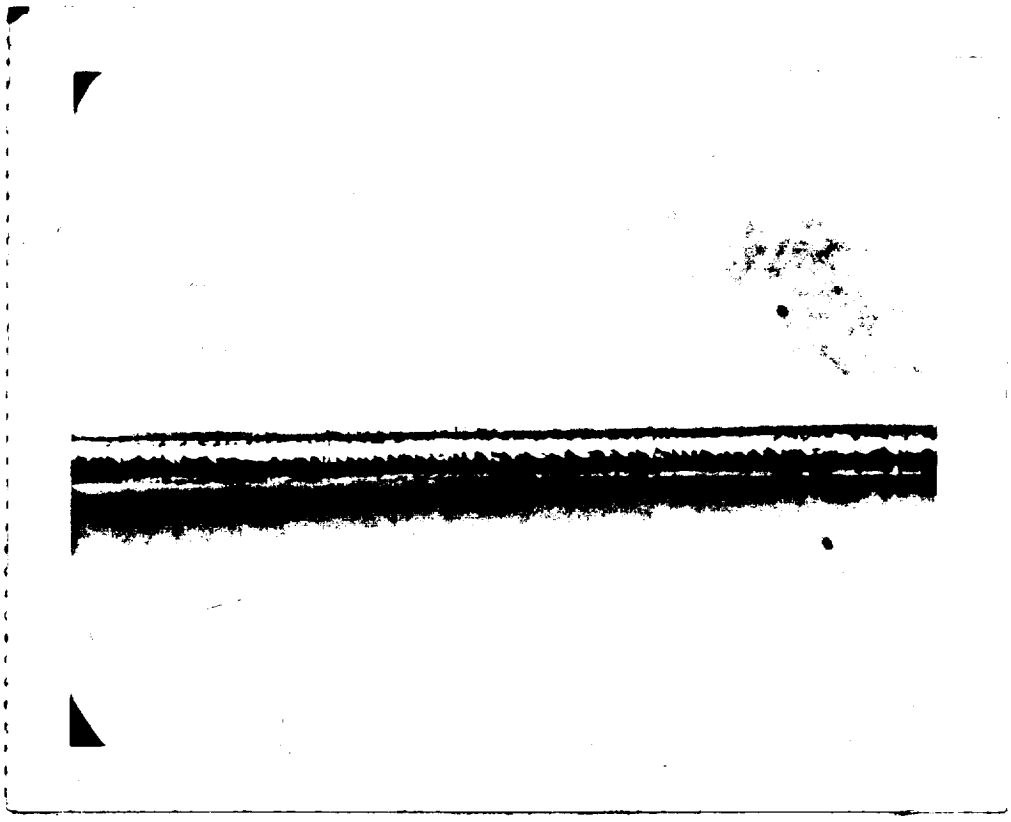

Fig. 9c. Gold Jacketed (Fiberguide) - after 10,000 cycles

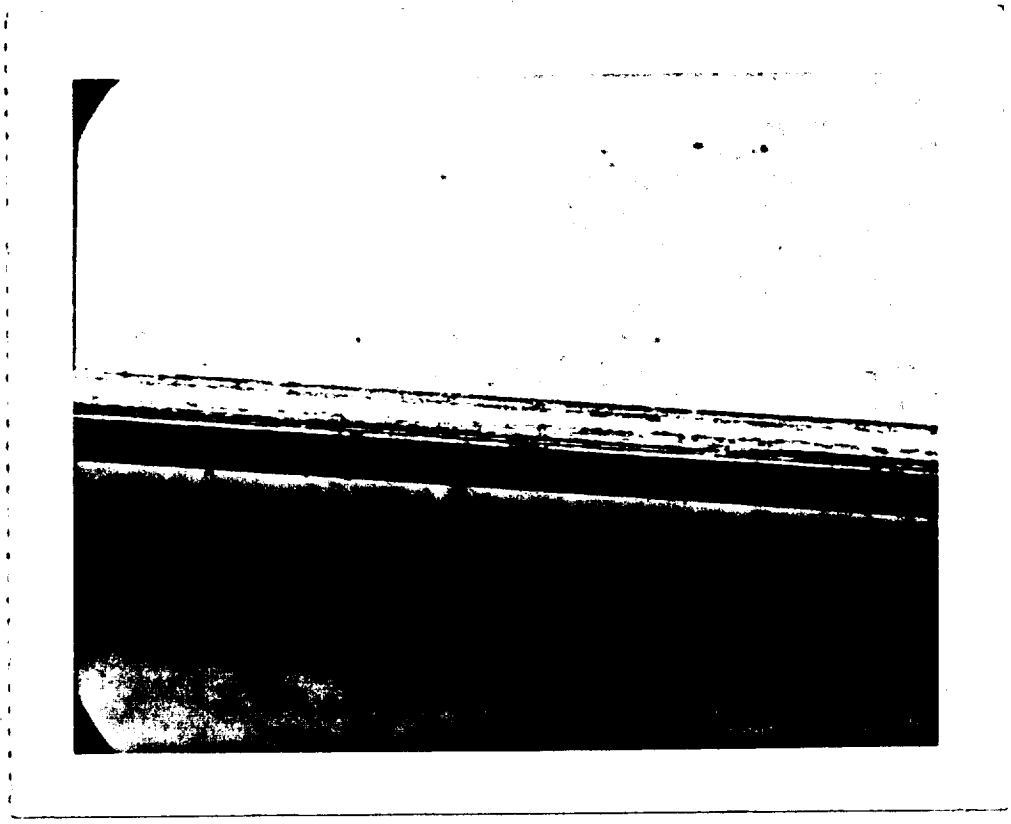

Fig. 10a. Aluminum Jacketed (Hughes) - Pretest

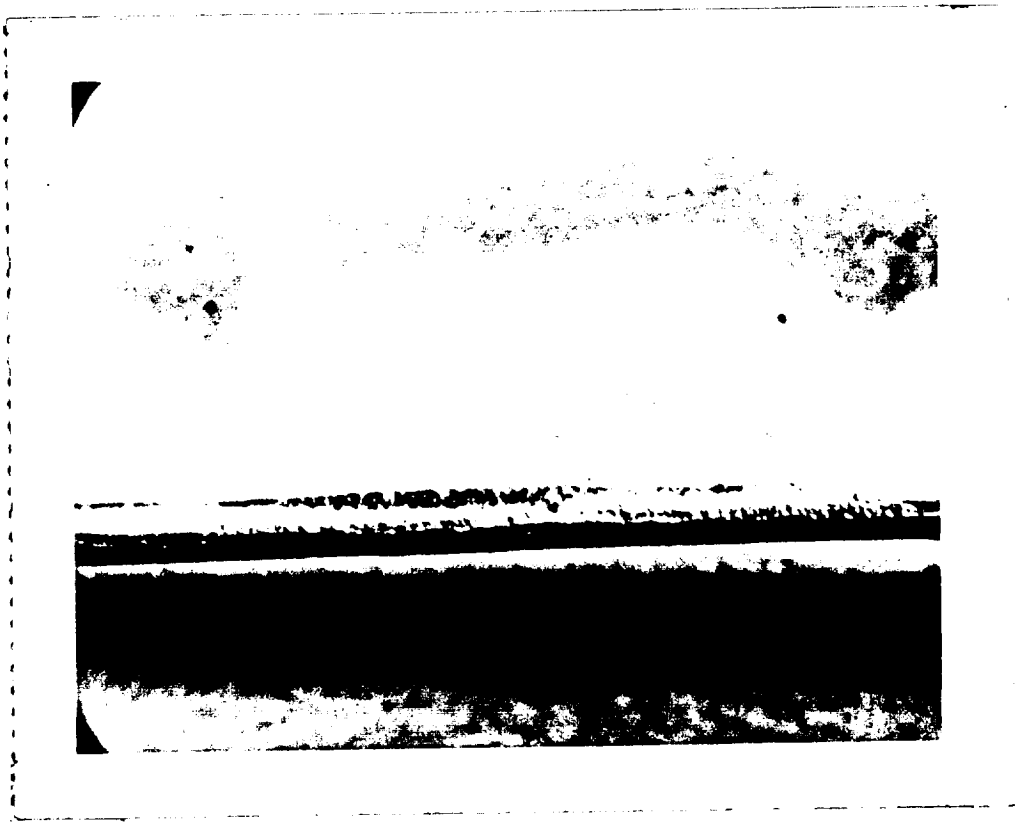

Fig. 10b. Aluminum Jacketed (Hughes) - after 10,000 cycles

Fig. 11a. Titanium Carbide (Spectran) - Pretest

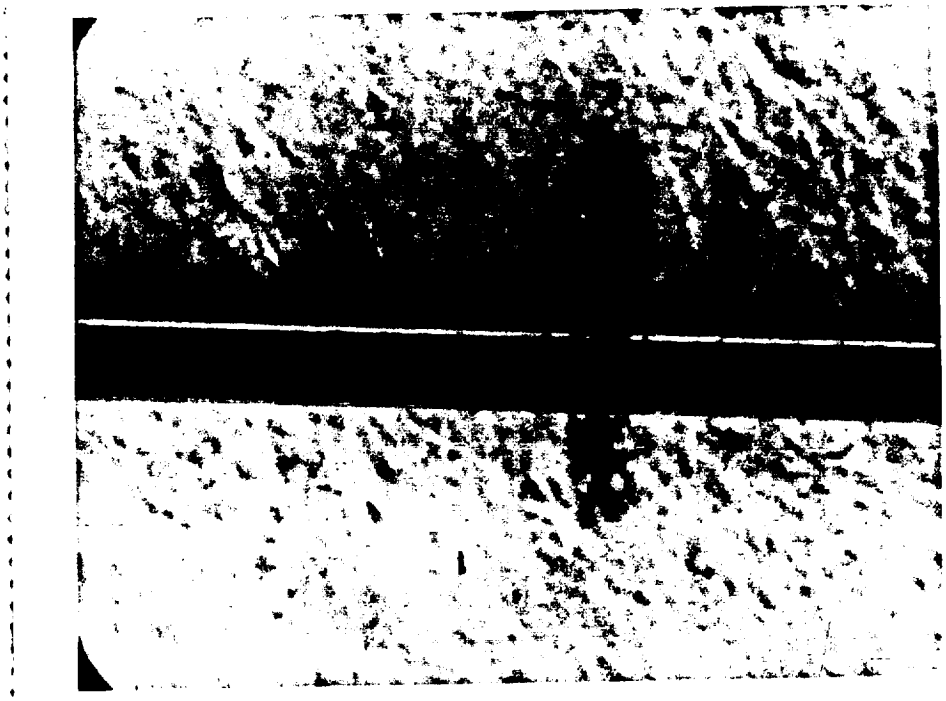

Fig. 11b. Titanium Carbide (Spectran) - after 10,000 cycles

Fig. 12a. Fluoride (Infrared Fiber Systems) - Pretest

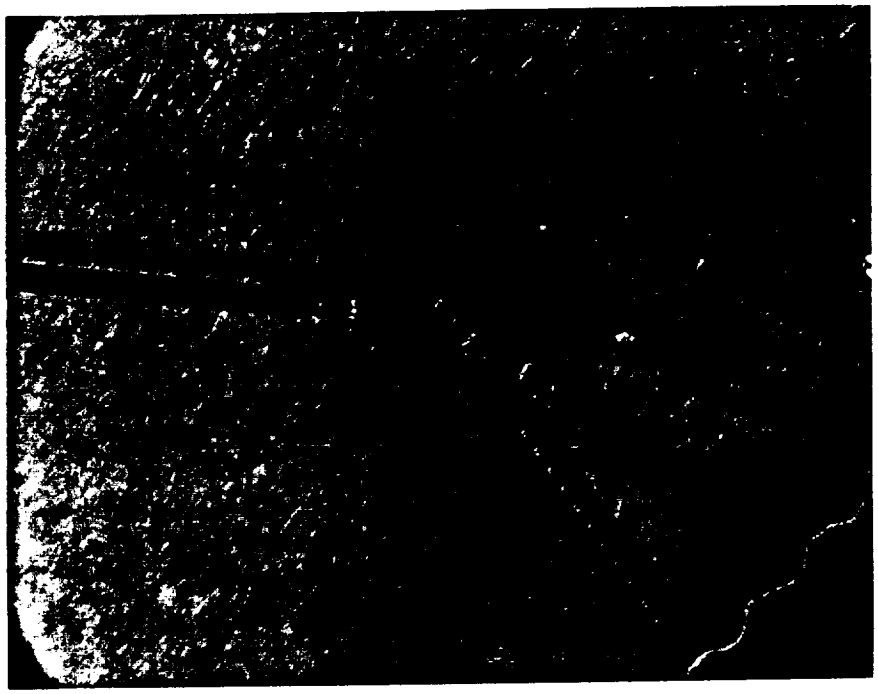

Fig. 12b. Fluoride (Infrared Fiber Systems) - Fiber Broken

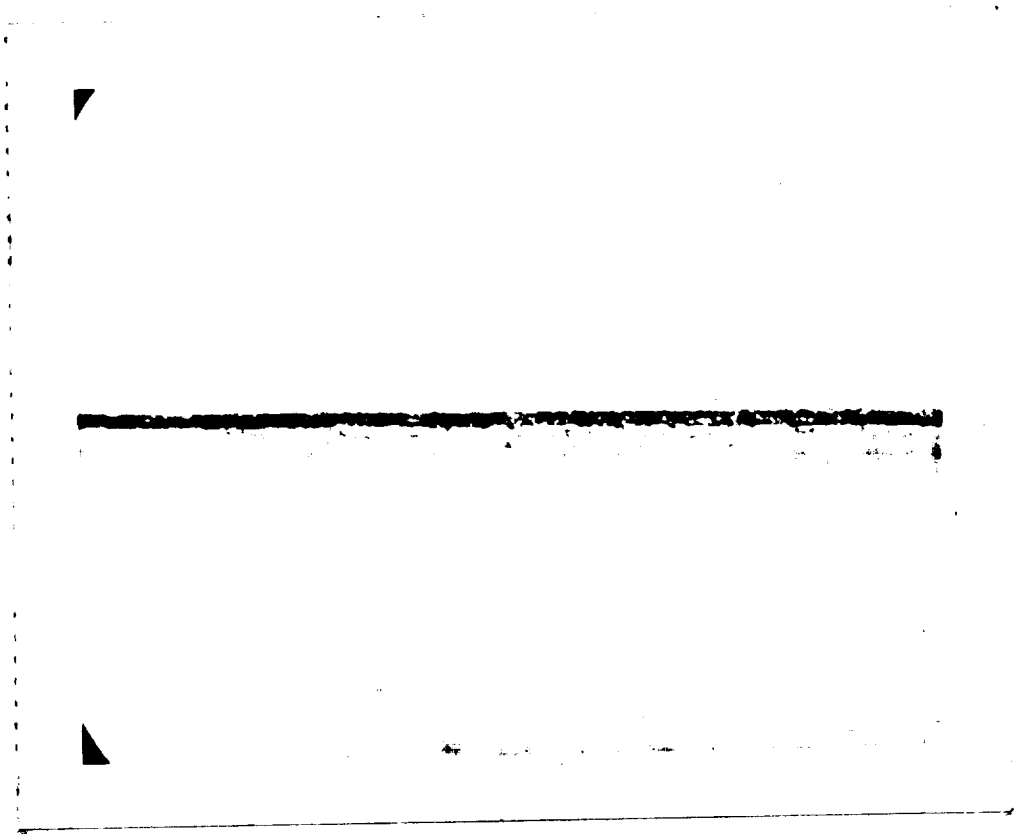

Fig. 13. Indium Single Mode Polarization Preserving - Pretest

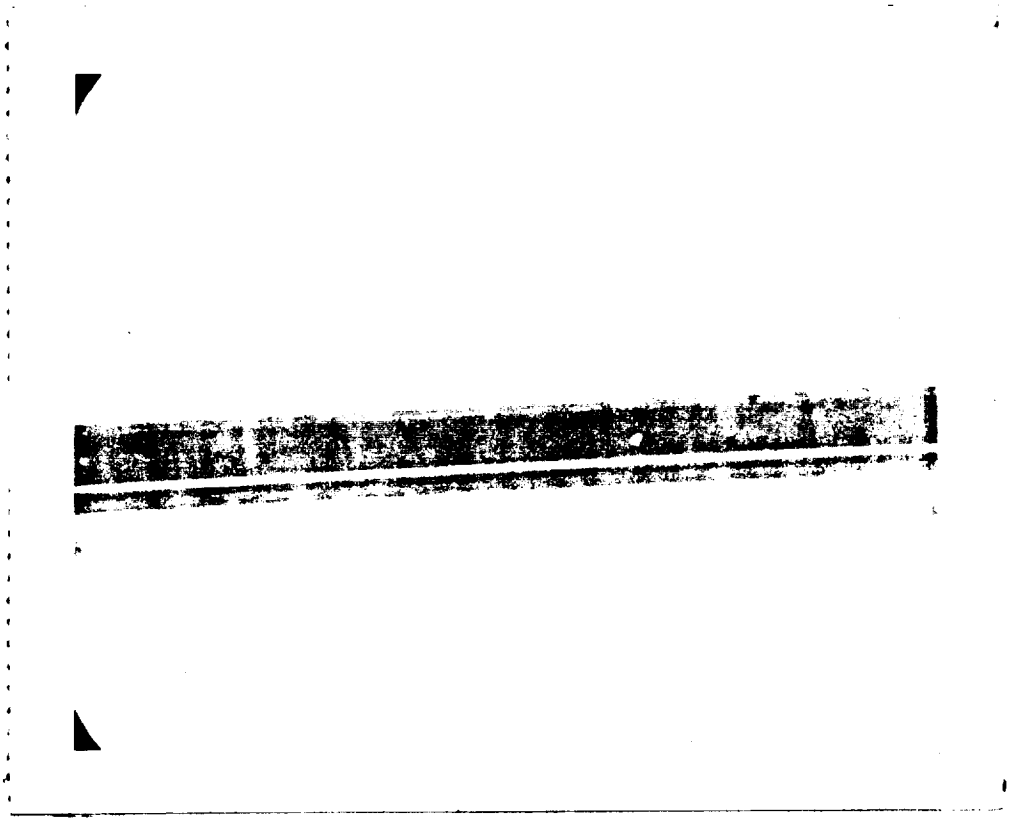

Fig. 14a. Fluoride (Iris) - Pretest

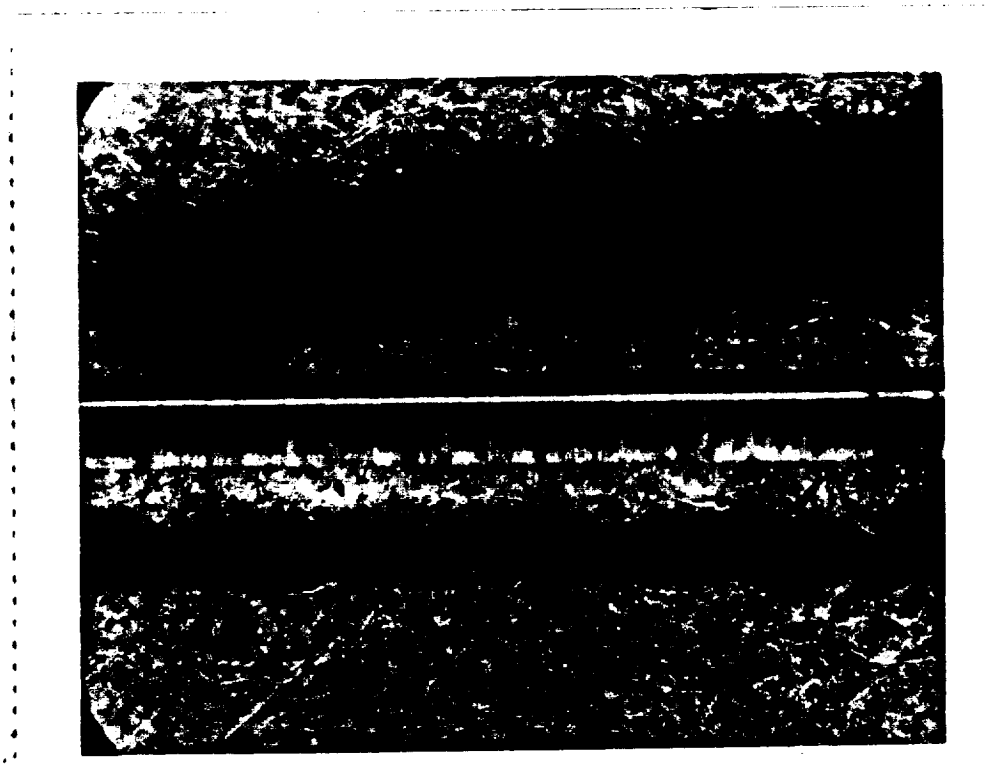

Fig. 14b. Fluoride (Iris) - 10,000 cycles

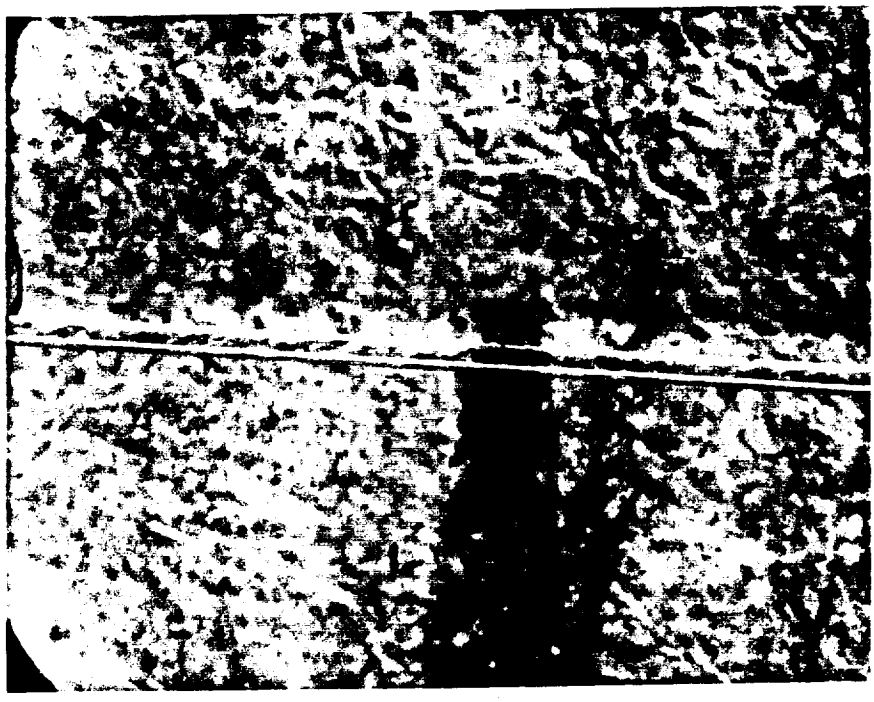

Fig. 15a. Deflectometer Fiber (MTI) - Pretest

Fig. 15b. Deflectometer Fiber (MTI) - 10,000 cycles

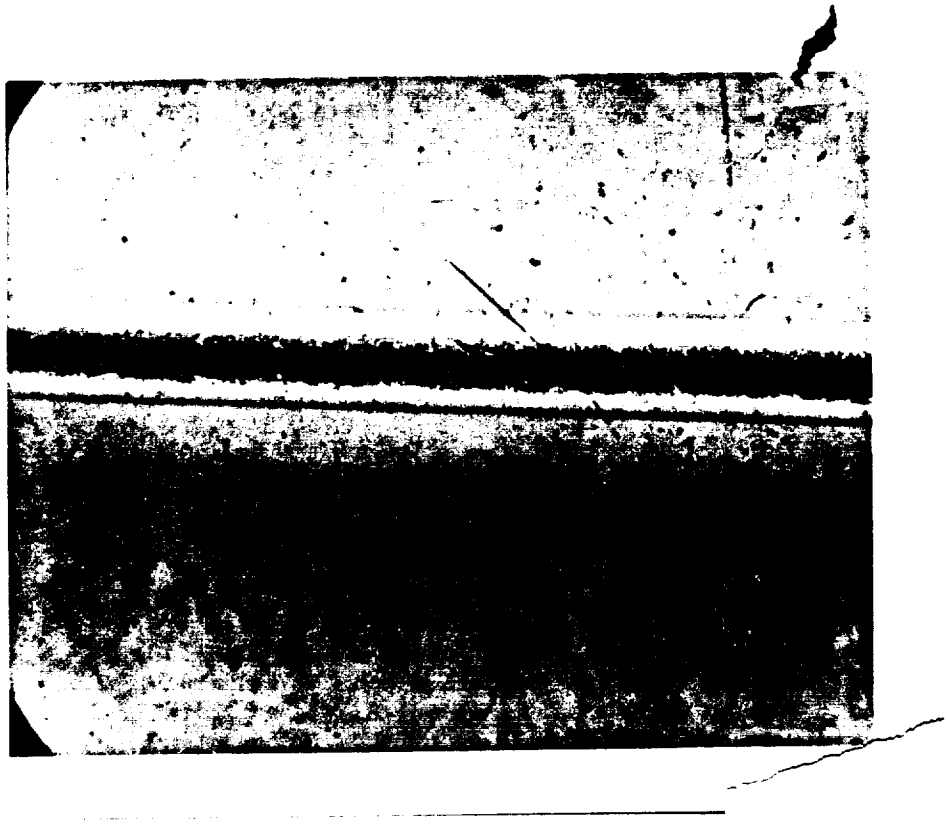

Fig. 16a. Aluminum Jacketed (Fiberguide) - Pretest

Fig. 16b. Aluminum Jacketed (Fiberguide) - 10,000 cycles

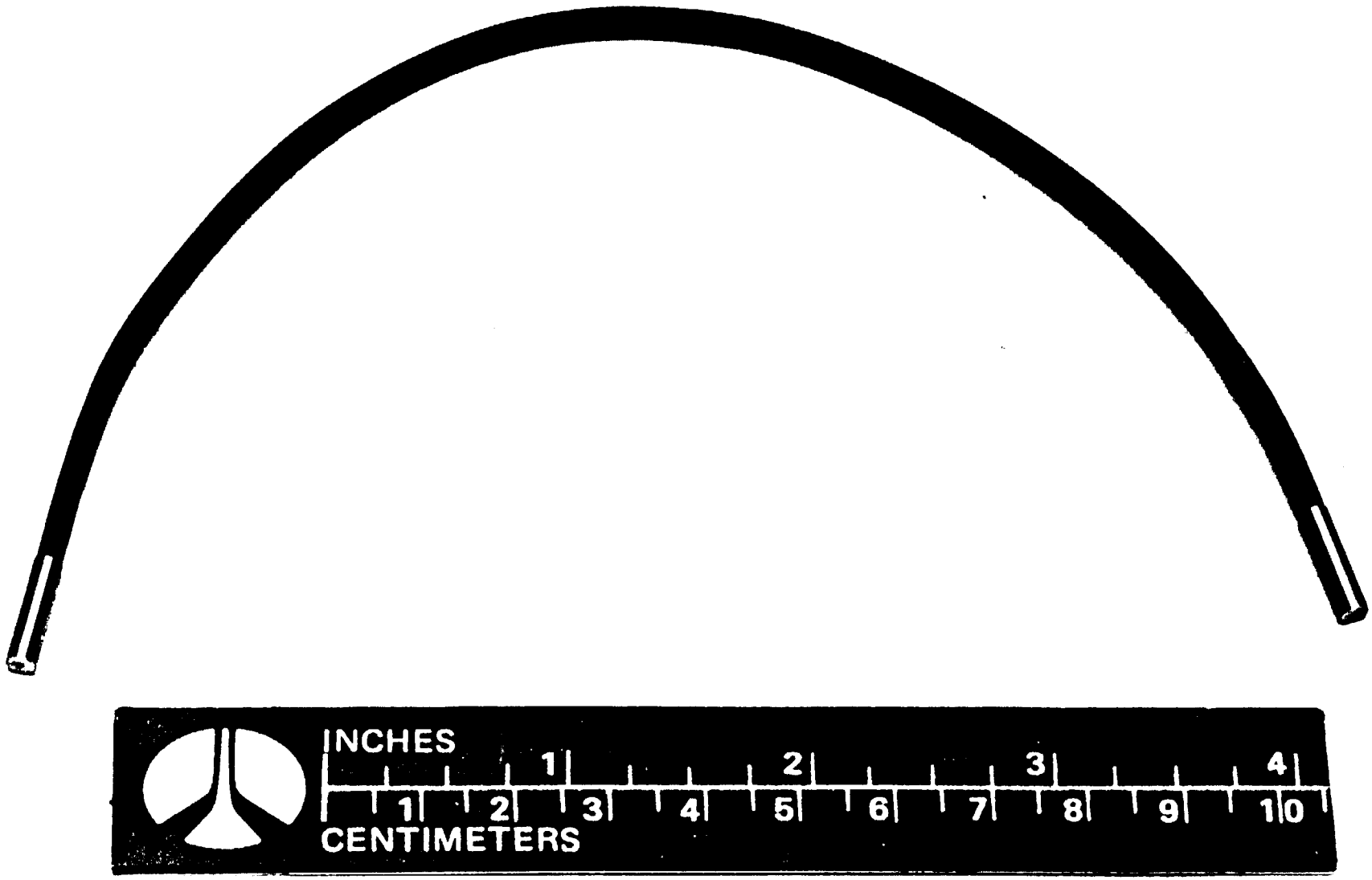

Fig. 17. Cabled 19-Fiber Bundle

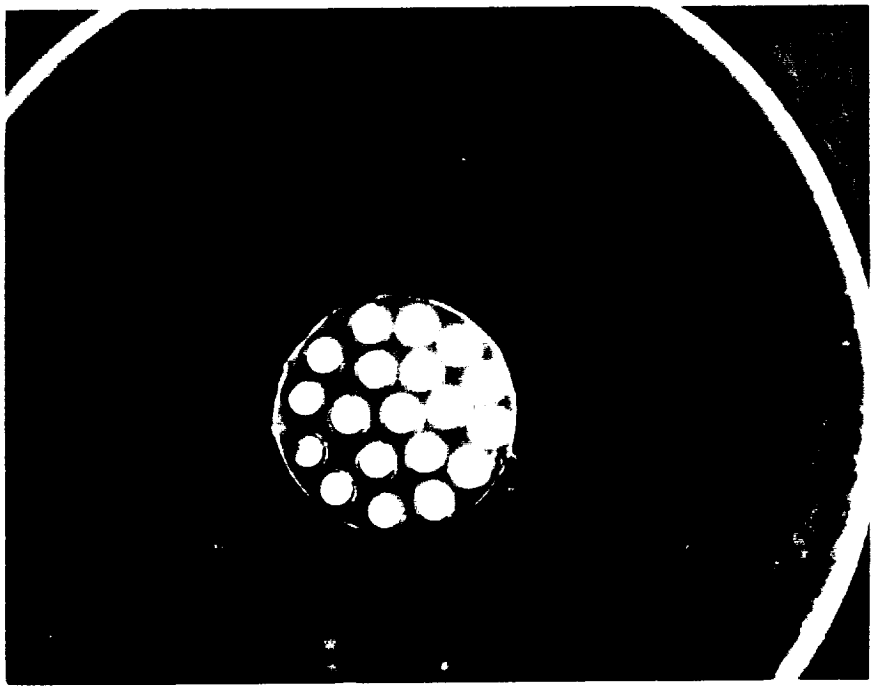

Fig. 18a. Integrity Test of Bundle Fibers Prior to Cold-Bend Test

Fig. 18b. Integrity Test of Bundle Fibers after 10,000 Flexure Cycles

Fig. 18c. Bundle Fibers After 10,000 Flex Cycles: Close Up

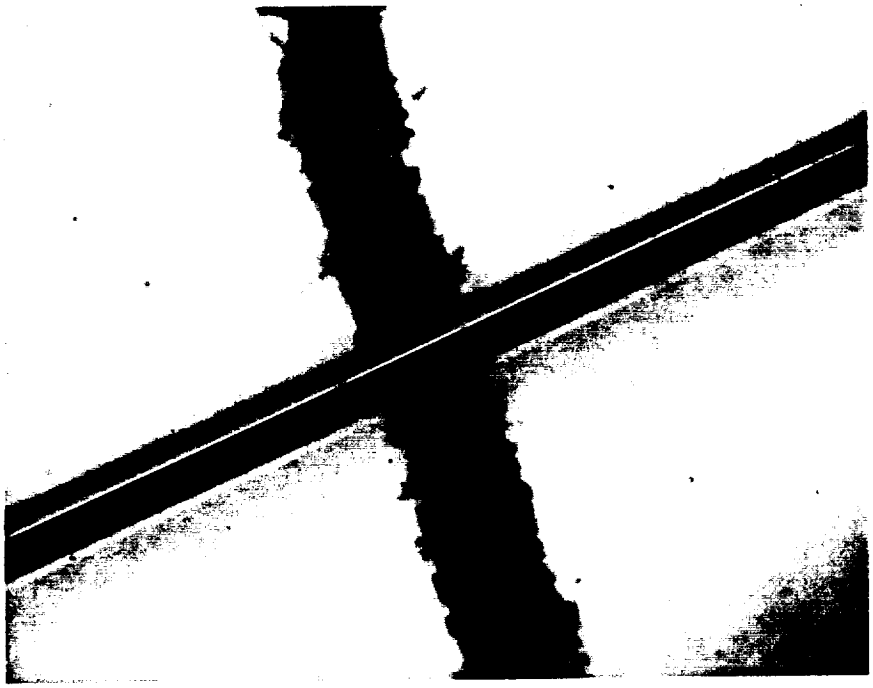

Fig. 19a. Amorphous Carbon Jacketed Fiber - Flexure Section After 10,000 Cyles

Fig. 19b. Water Intrusion into Cold Bend Test Amorphous Carbon Jacketed Fiber

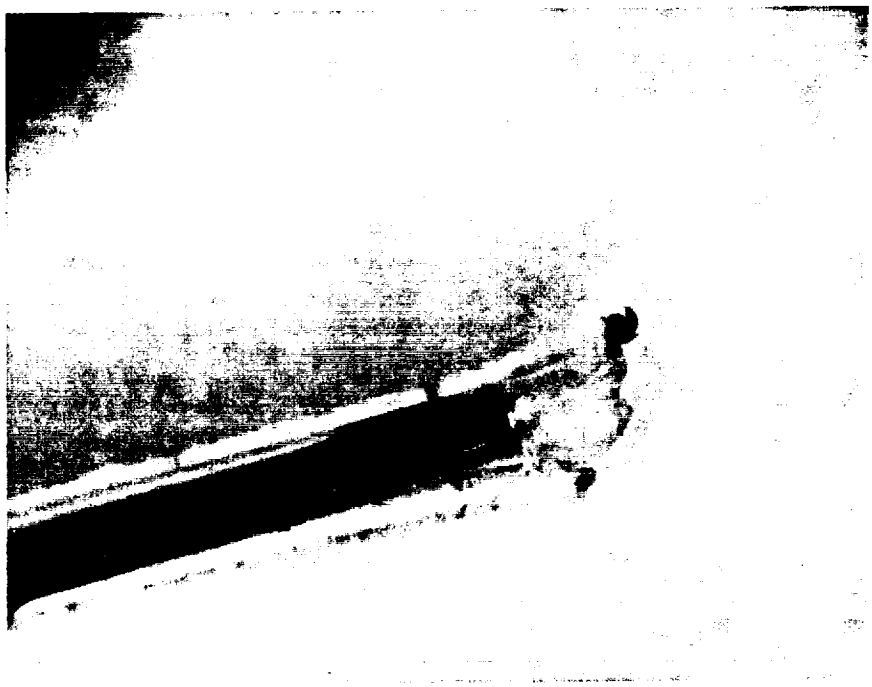

Fig. 19c. End of Amorphous Carbon Cold-Bend Specimen (Post-Test)

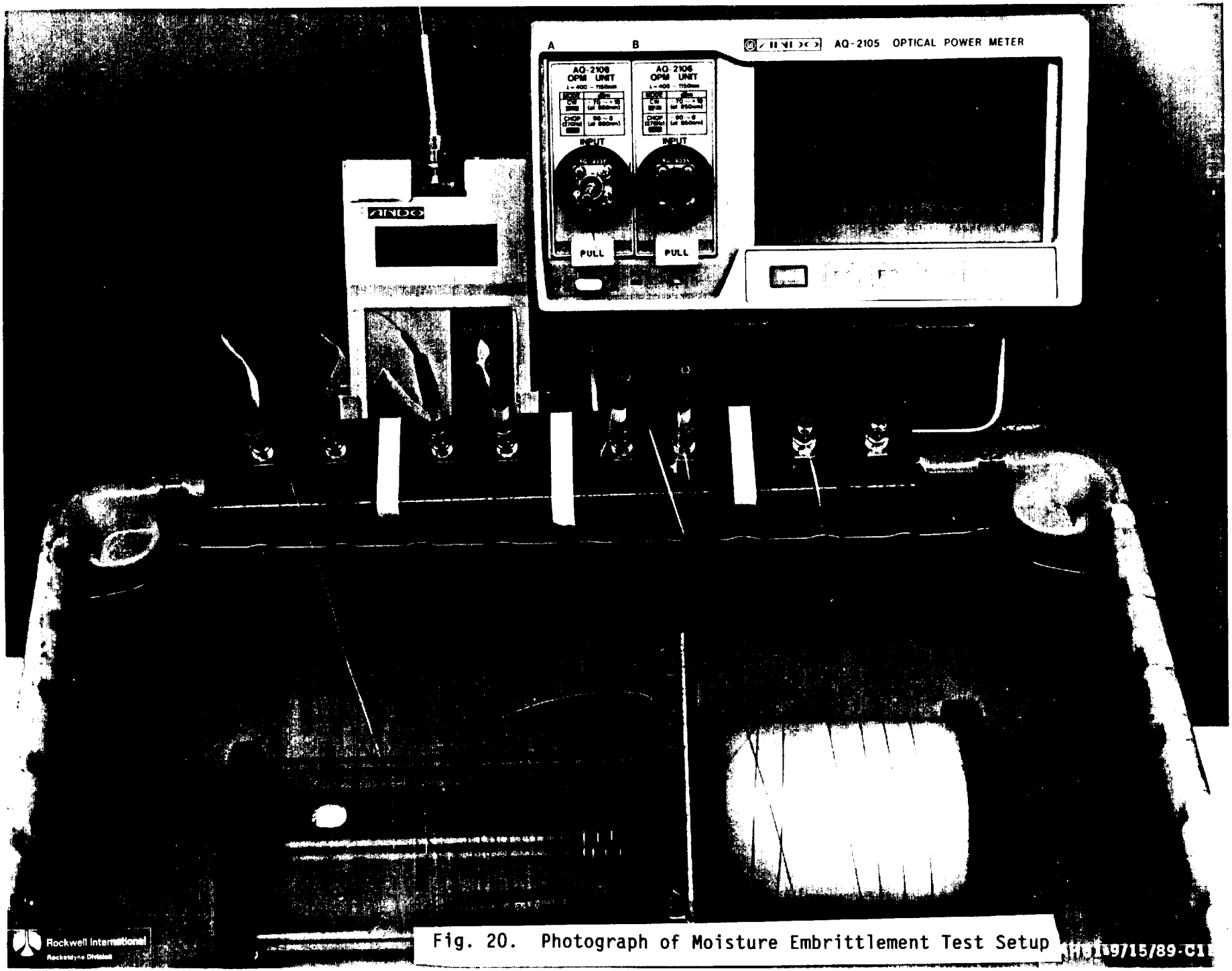

Fig. 20. Photograph of Moisture Embrittlement Test Setup

Fig. 21. Fiberguide Gold Jacketed Fiber After M.E. Test

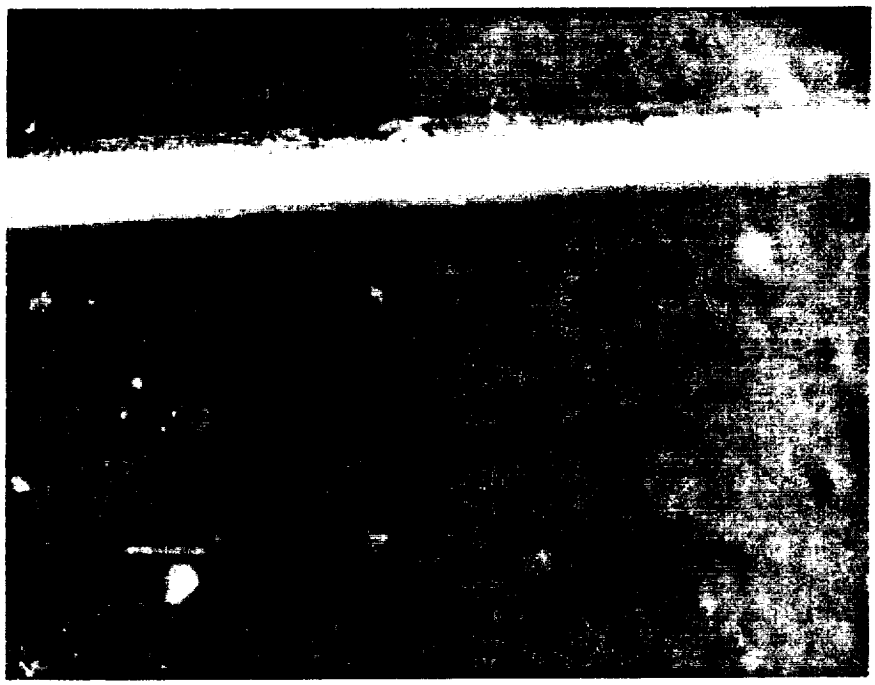

Fig. 22. Hughes Aluminum Jacketed Fiber After M.E. Test

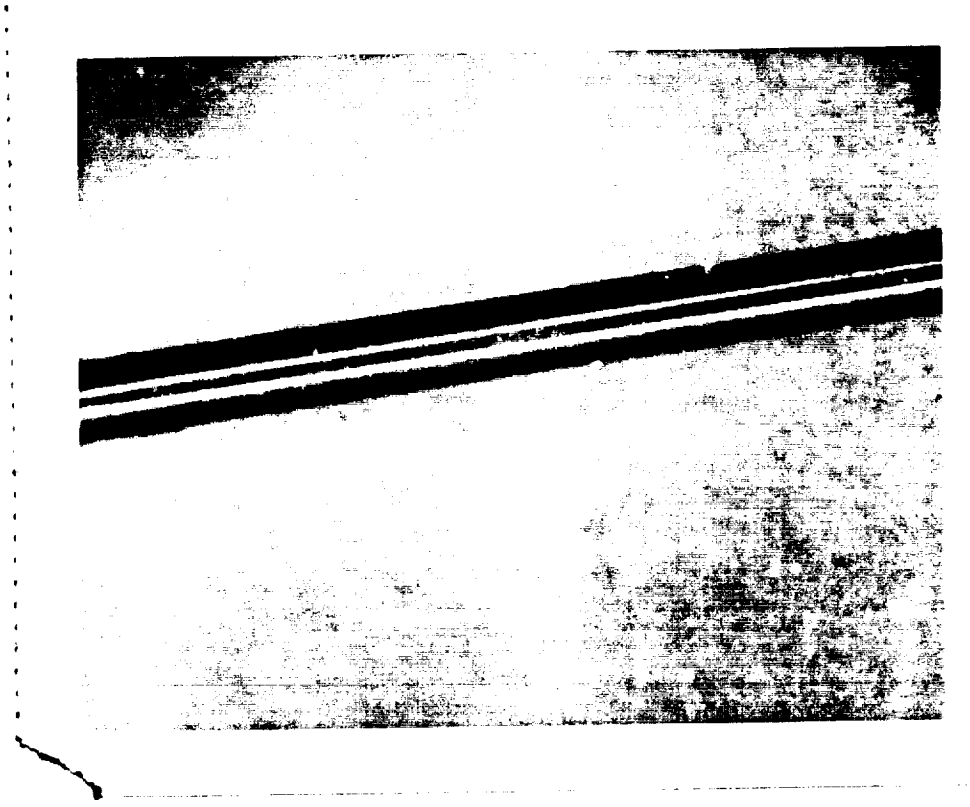

Fig. 23. Spectran Titanium carbide Jacketed Fiber After M.E. Test

Fig. 24a. Iris Fluoride Fiber Before M.E. Test

Fig. 24b. Iris Fluoride Fiber (Showing Degradation) After M.E. Test

C-2

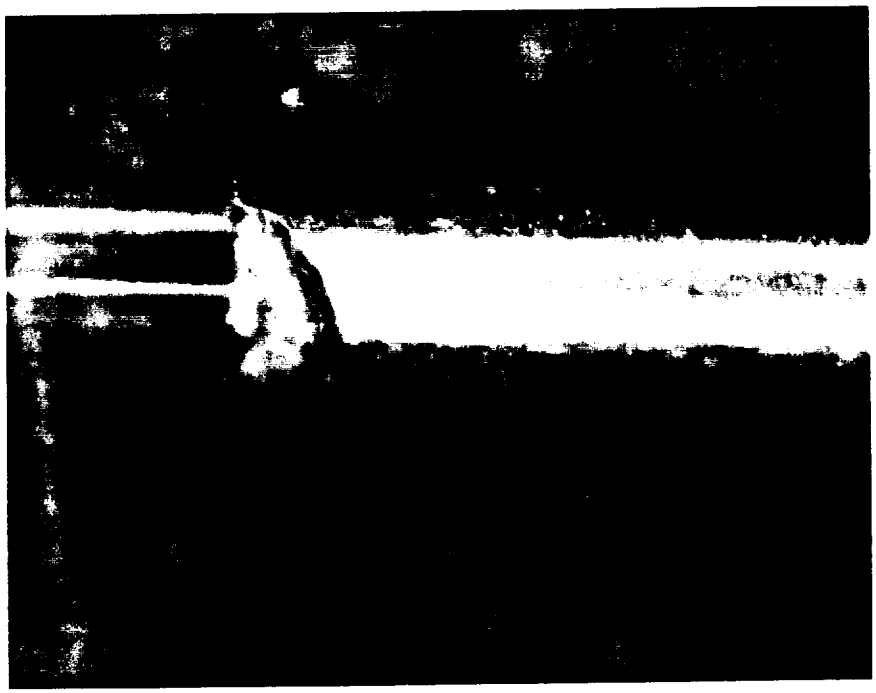

Fig. 25. Iris Fluoride Fiber Inside .010"/.018" Stainless Tubing

Fig. 26a. AT&T Amorphous Carbon Fiber Before M.E. Test

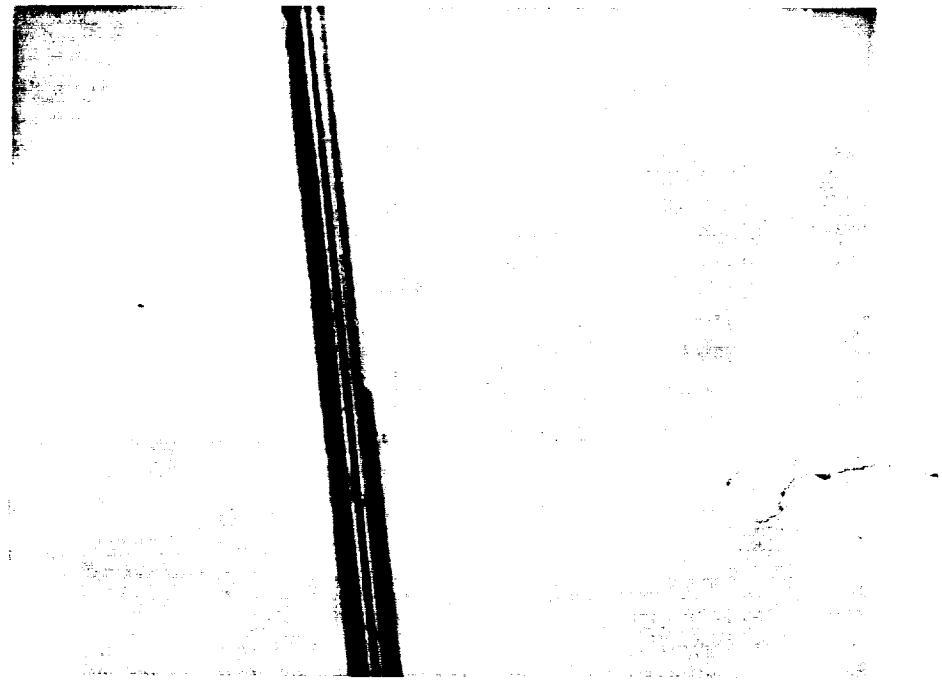

Fig. 26b. AT&T Amorphous Carbon Fiber After M.E. Test

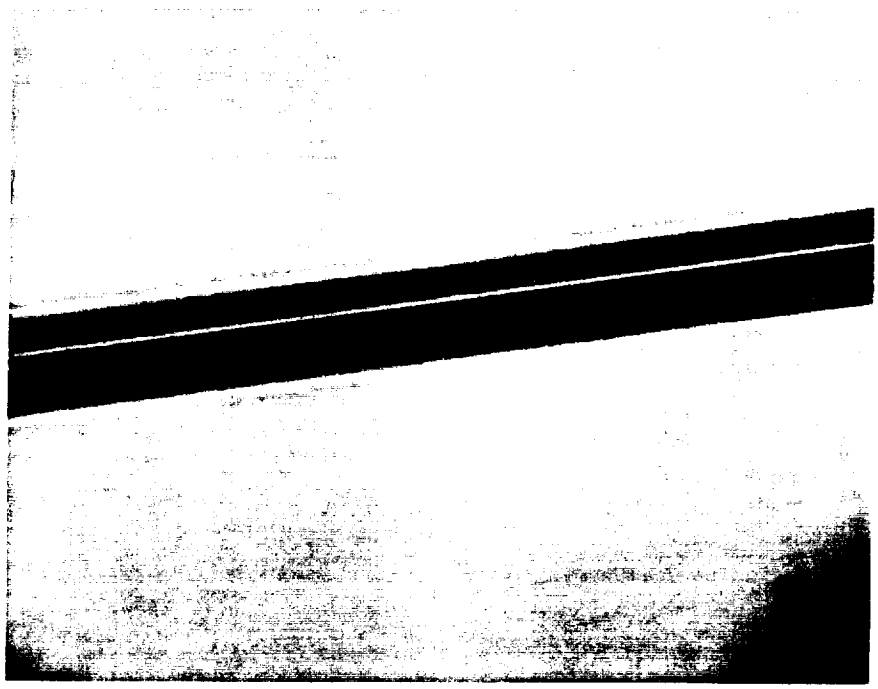

Fig. 26c. AT&T Amorphous Carbon Fiber,
Second Sample After M.E. Test

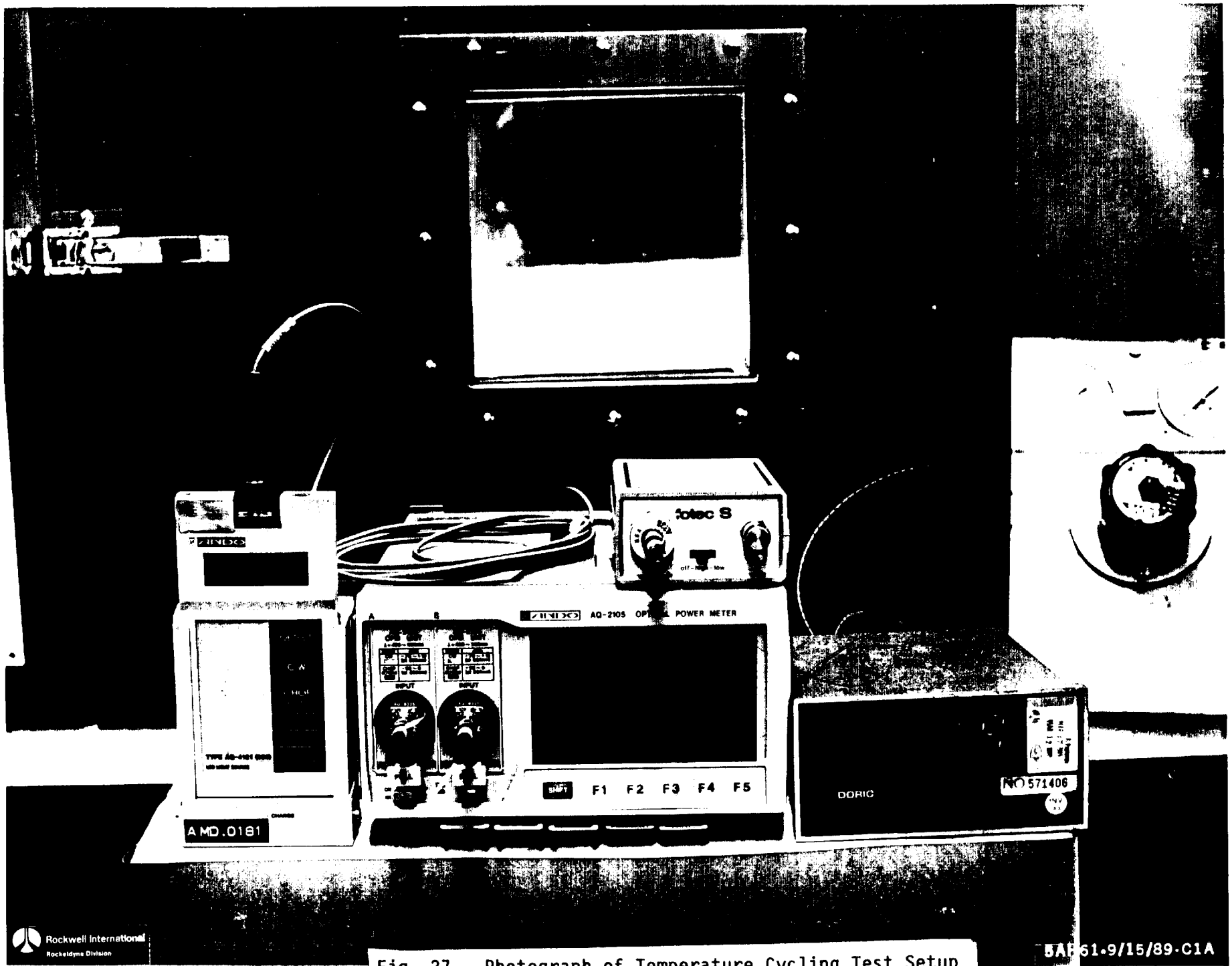

Fig. 27. Photograph of Temperature Cycling Test Setup

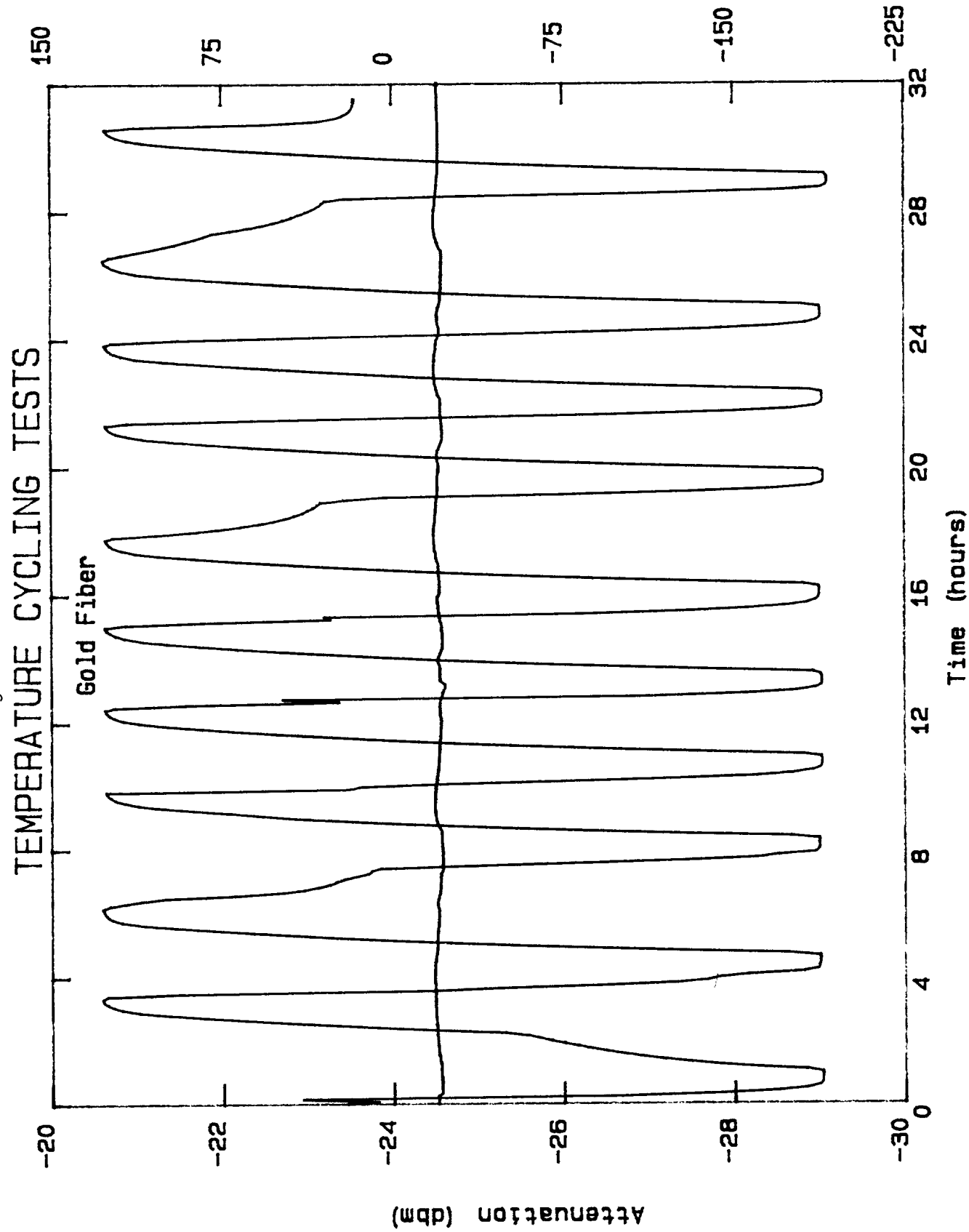
Temperature [deg C]
150
75
0
-75
-150
-225
TEMPERATURE CYCLING TESTS
Gold Fiber
-20
-22
-24
-26
-28
-30
Attenuation (dbm)
0
4
8
12
16
20
24
28
32
Time (hours)

Figure 28

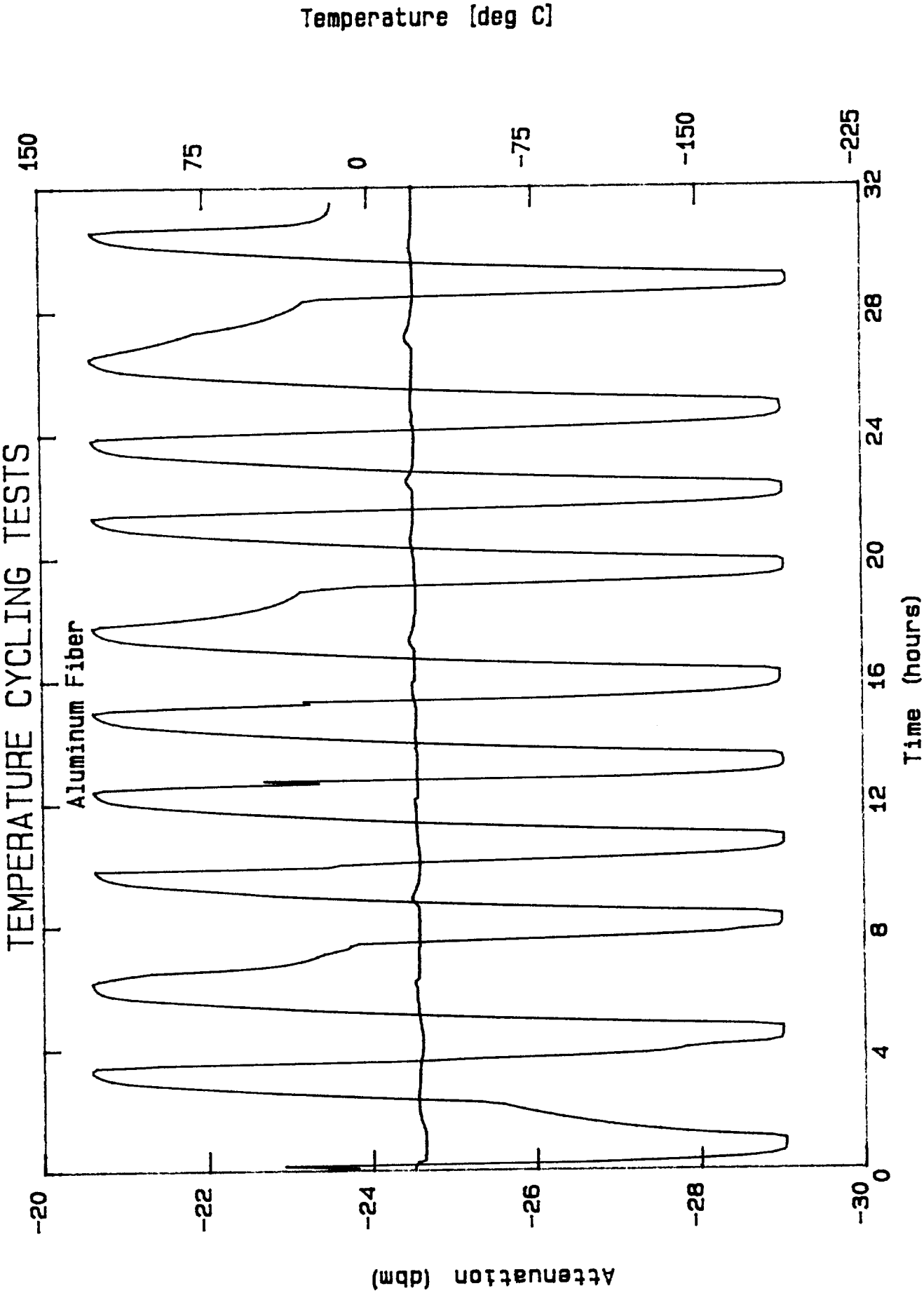
Temperature [deg C]
150
75
0
-75
-150
-225
TEMPERATURE CYCLING TESTS
Aluminum Fiber
-20
-22
-24
-26
-28
-30
Attenuation (dbm)
0
4
8
12
16
20
24
28
32
Time (hours)

Figure

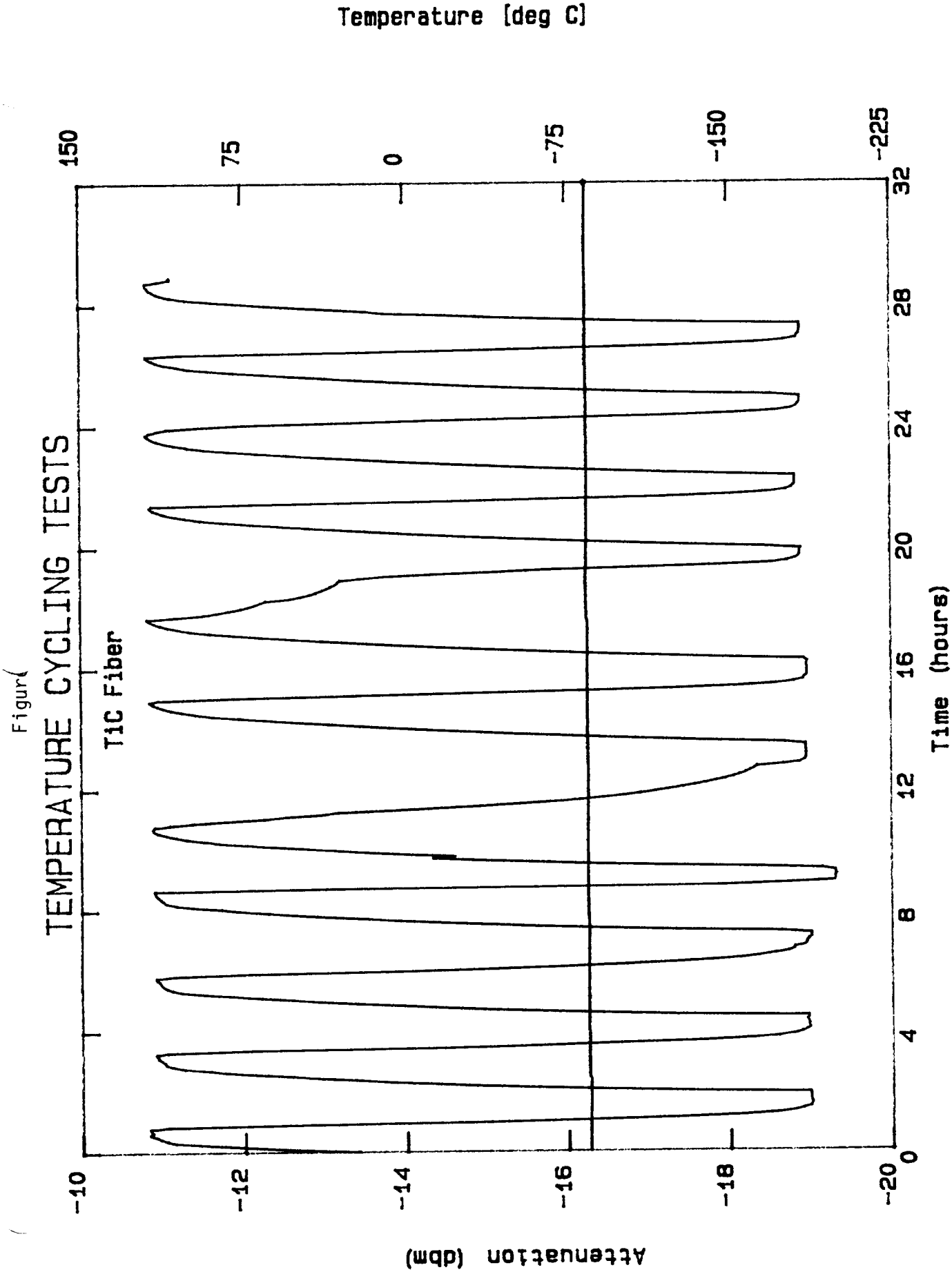
Temperature [deg C]
150
75
0
-75
-150
-225
TEMPERATURE CYCLING TESTS
TiC Fiber
Time (hours)
0
4
8
12
16
20
24
28
32
-10
-12
-14
-16
-18
-20
Attenuation (dbm)

Figur(

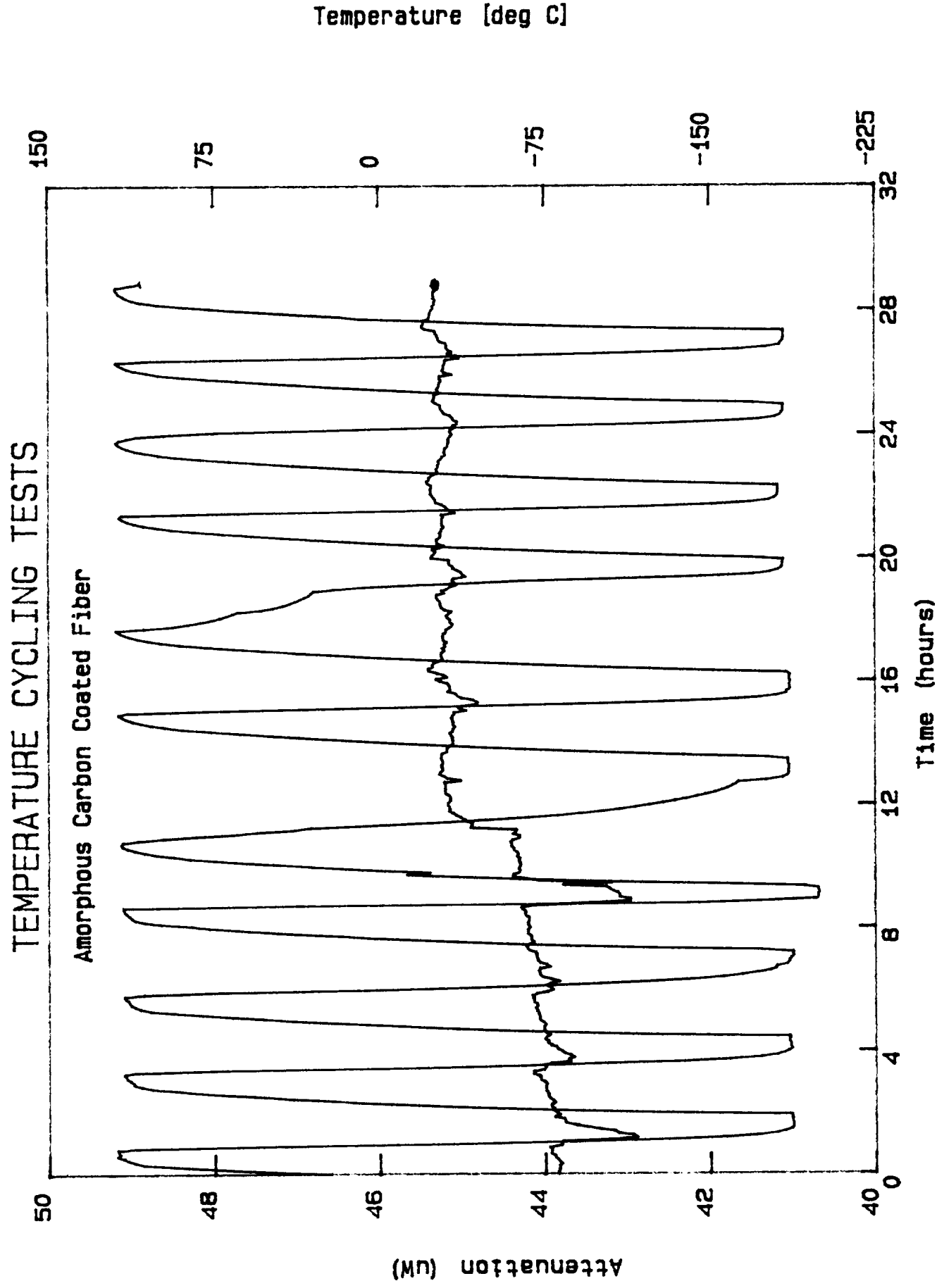
TEMPERATURE CYCLING TESTS
Amorphous Carbon Coated Fiber
Temperature [deg C]
150
75
0
-75
-150
-225
Attenuation (uW)
50
48
46
44
42
40
Time (hours)
0
4
8
12
16
20
24
28
32

Figure

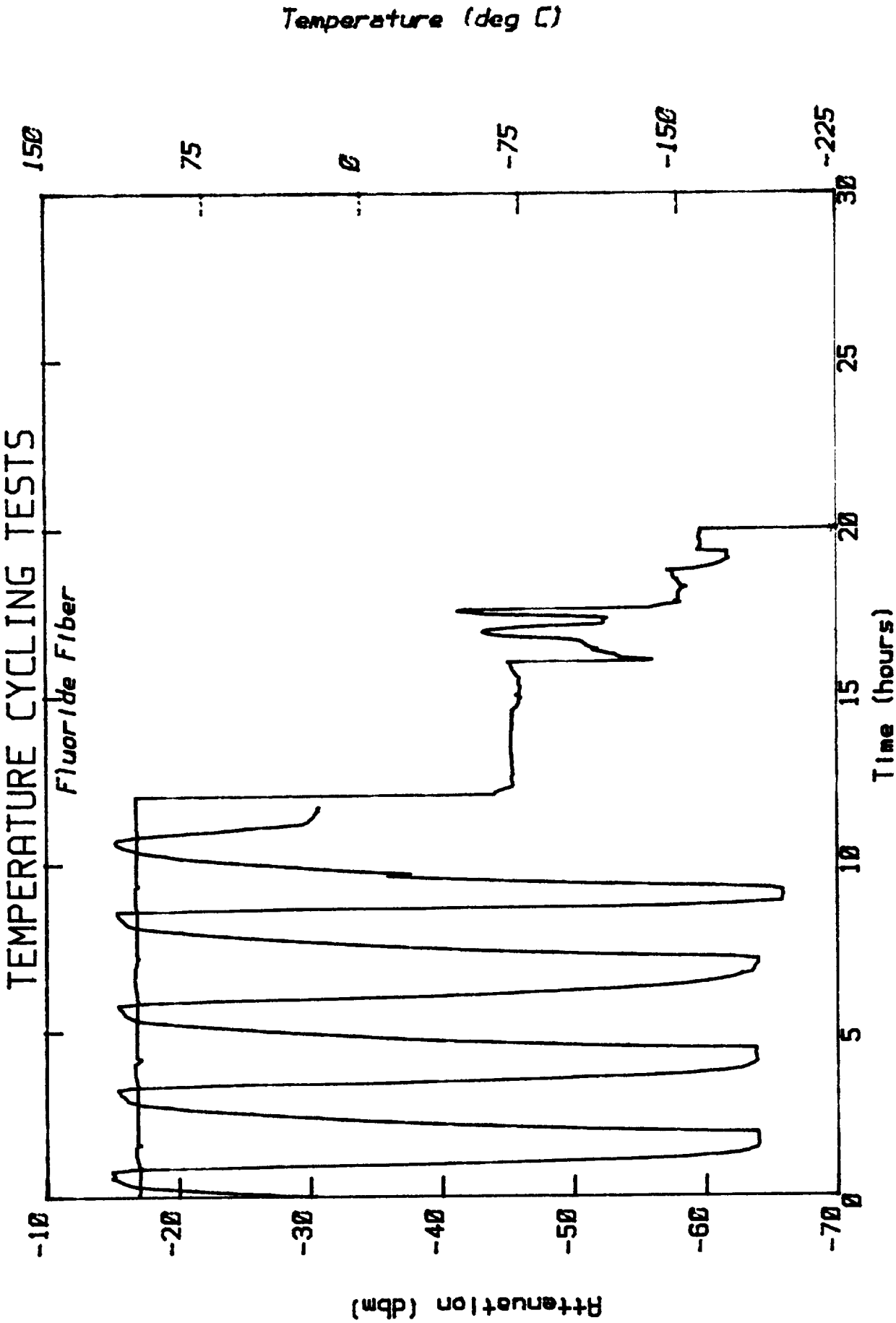

Fig. 32. Temperature Cycling Tests: Fluoride Fiber

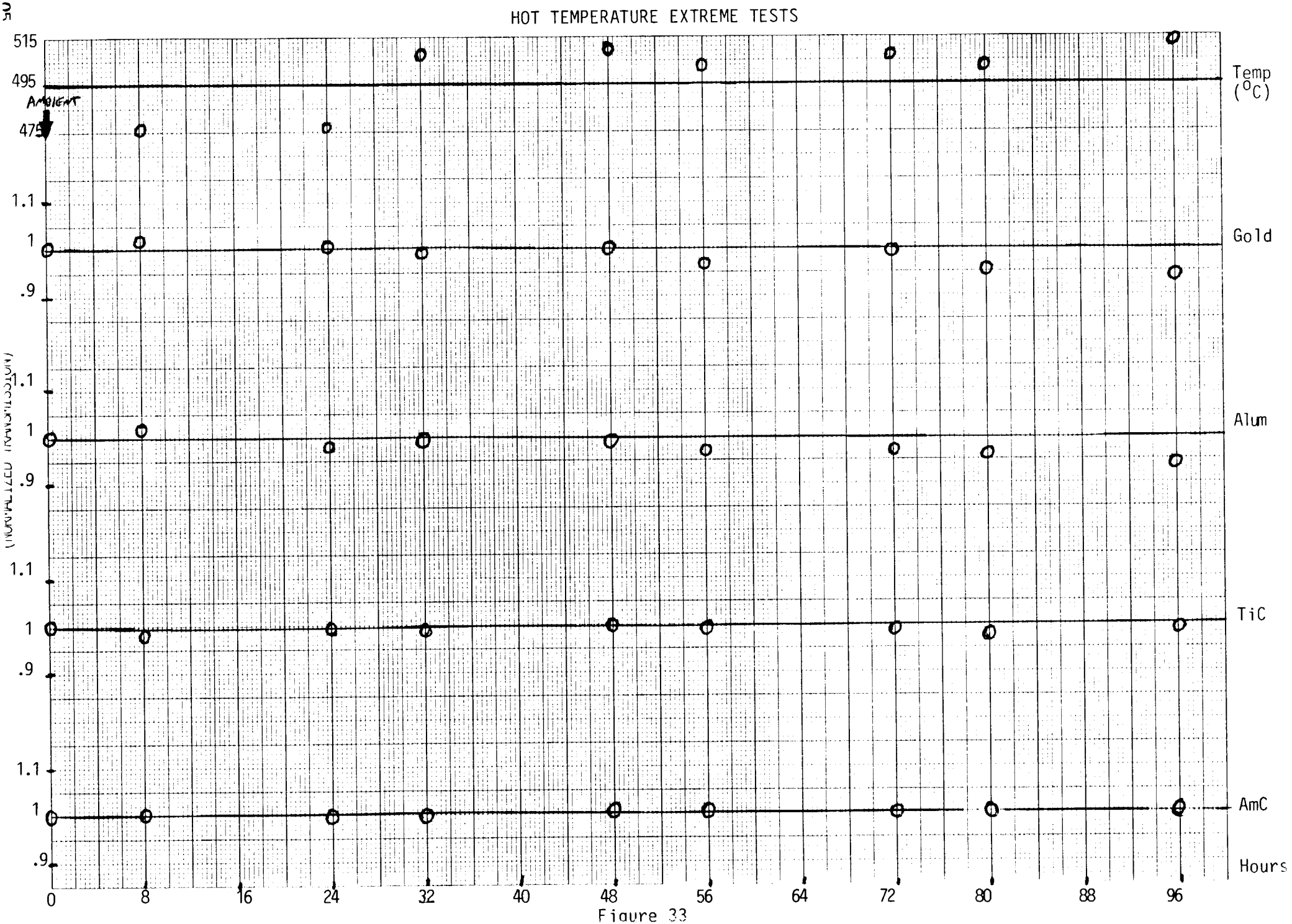

Figure 33

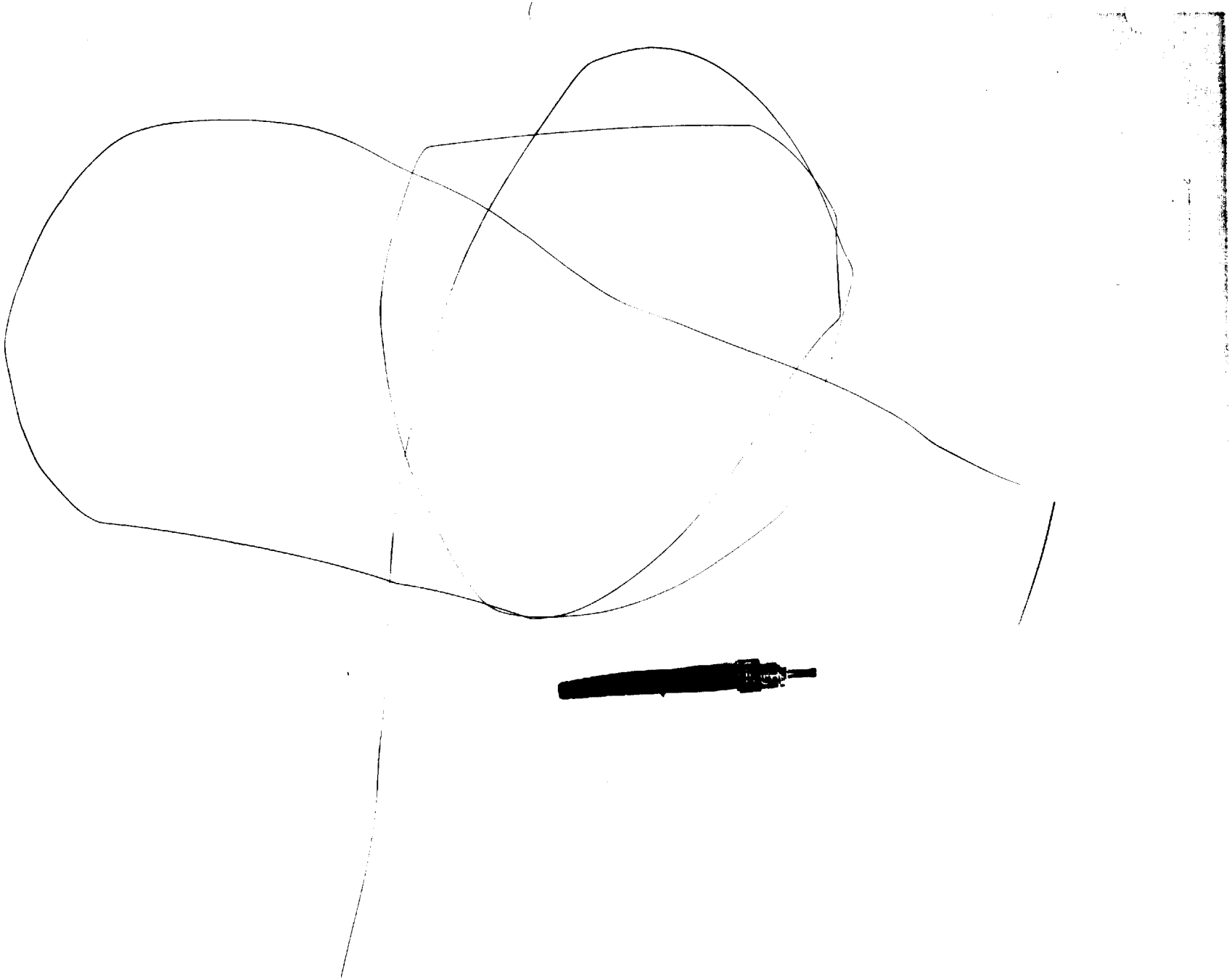

Fig. 34 Fluoride Fiber after Hot Temperature Extreme Test

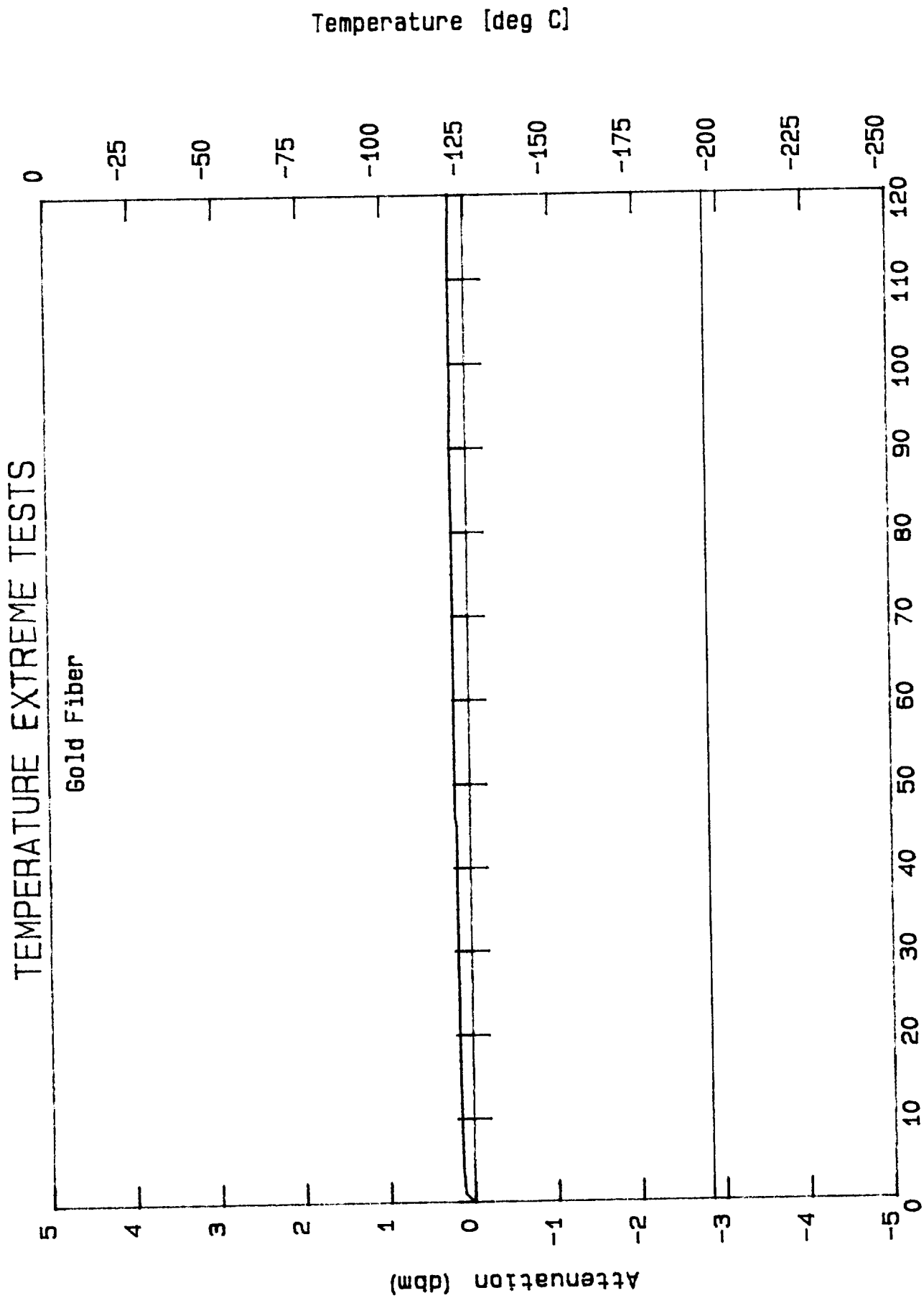

Figure 35.Cold Temperature Extreme Tests: Gold Fiber

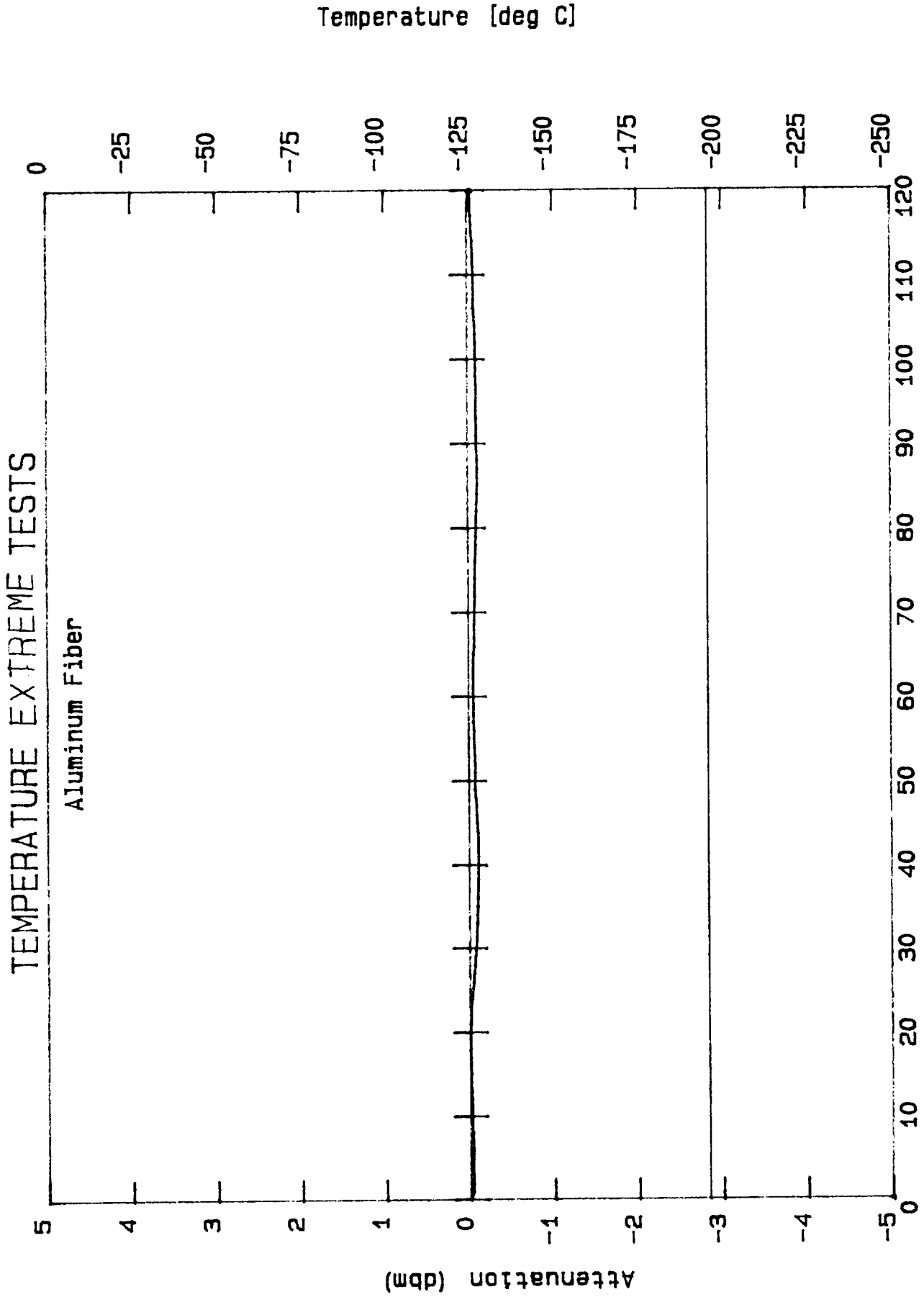

Figure 36. Cold Temperature Extreme Tests: Aluminum Fiber

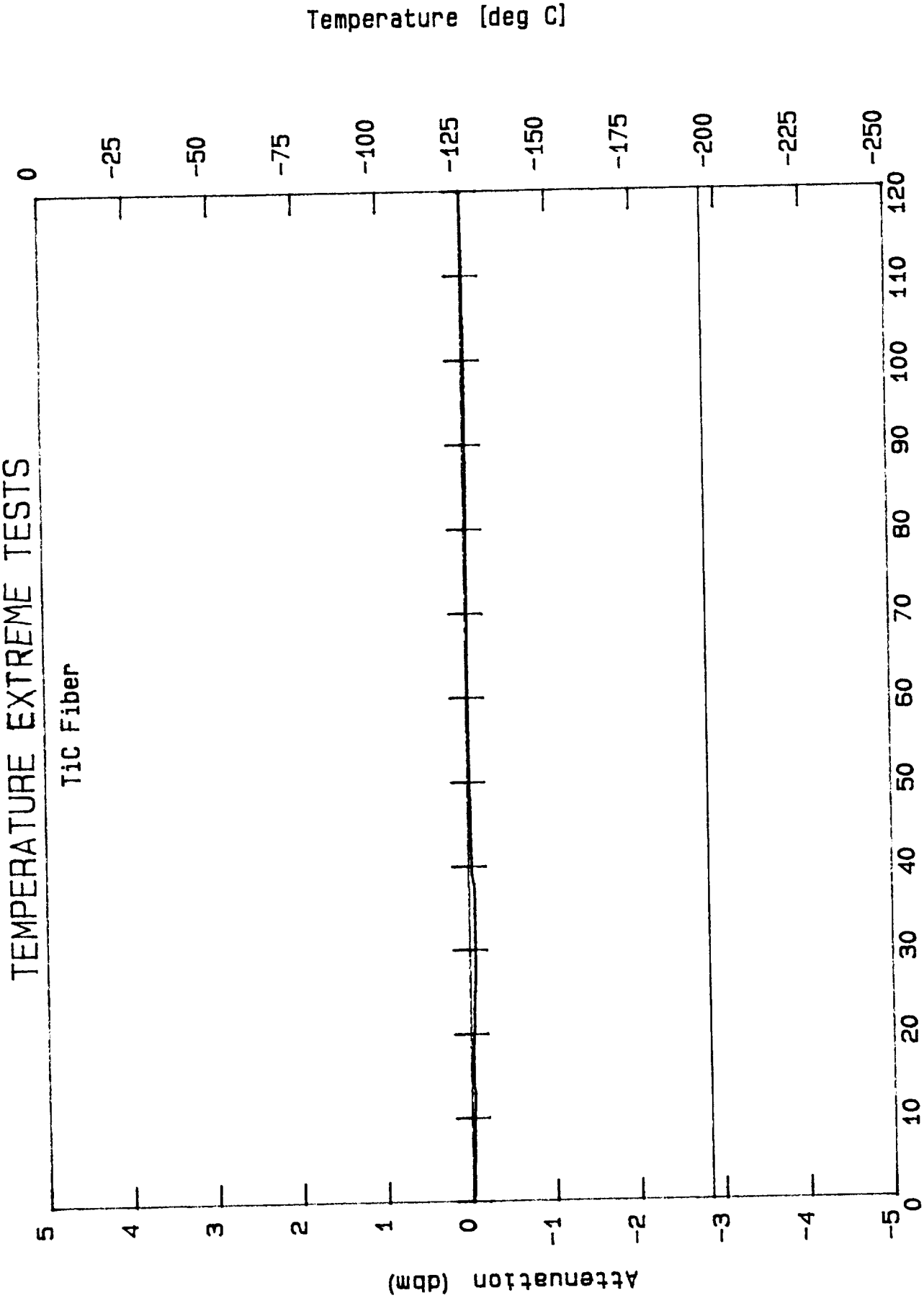

Figure 37. Cold Temperature Extreme Tests; Titanium Carbide Fiber

Fig. 38. Photograph of Smashed Amorphous Carbon Fiber

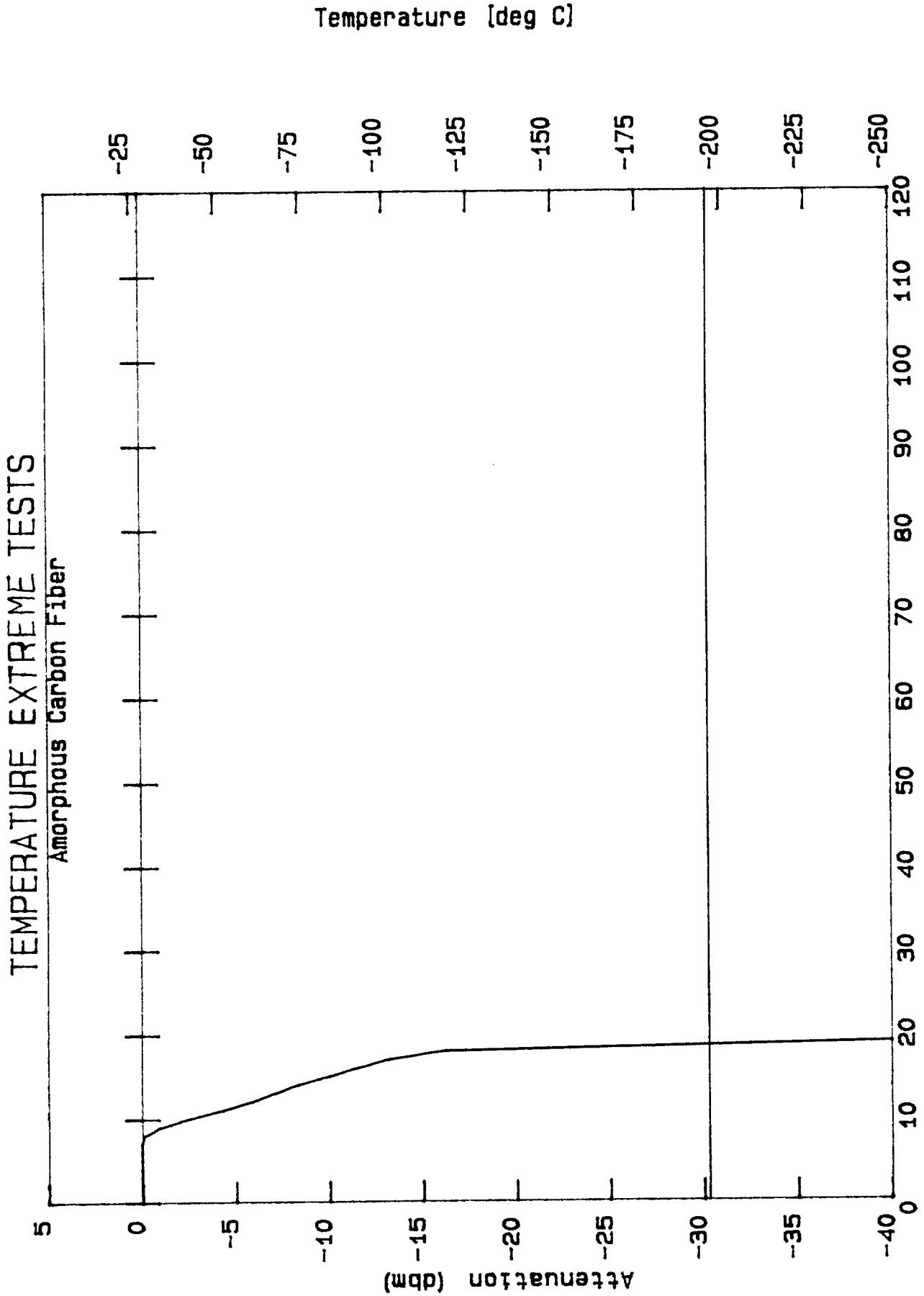

Figure 39. Cold Temperature Extreme Tests: Amorphous Carbon Fiber

Fig. 40. 30,000 Force-Pound Shaker

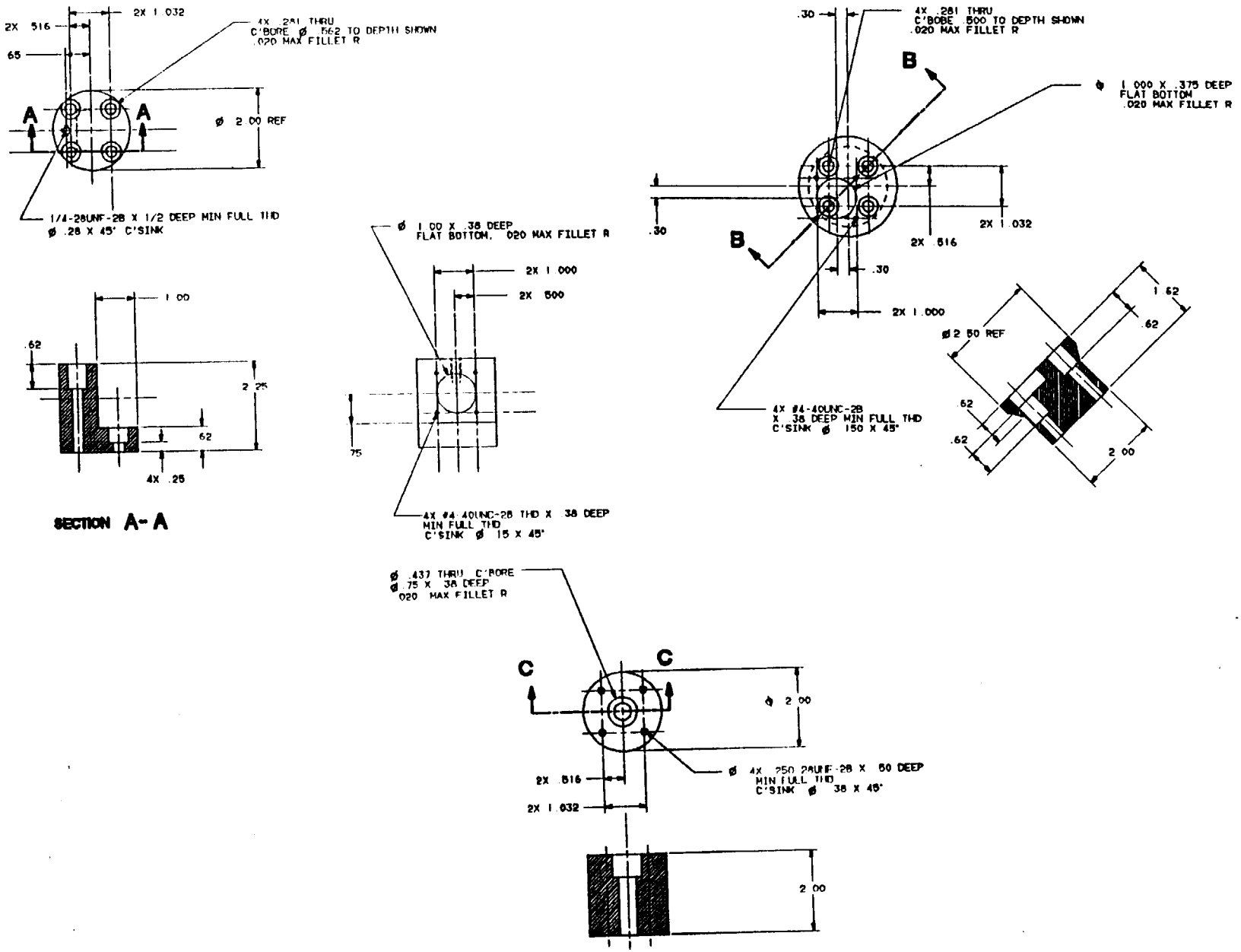

FIGURE 41 VIBRATION AND SHOCK TEST MULTIPLE FIBER CONNECTOR HOLDER ASSEMBLY

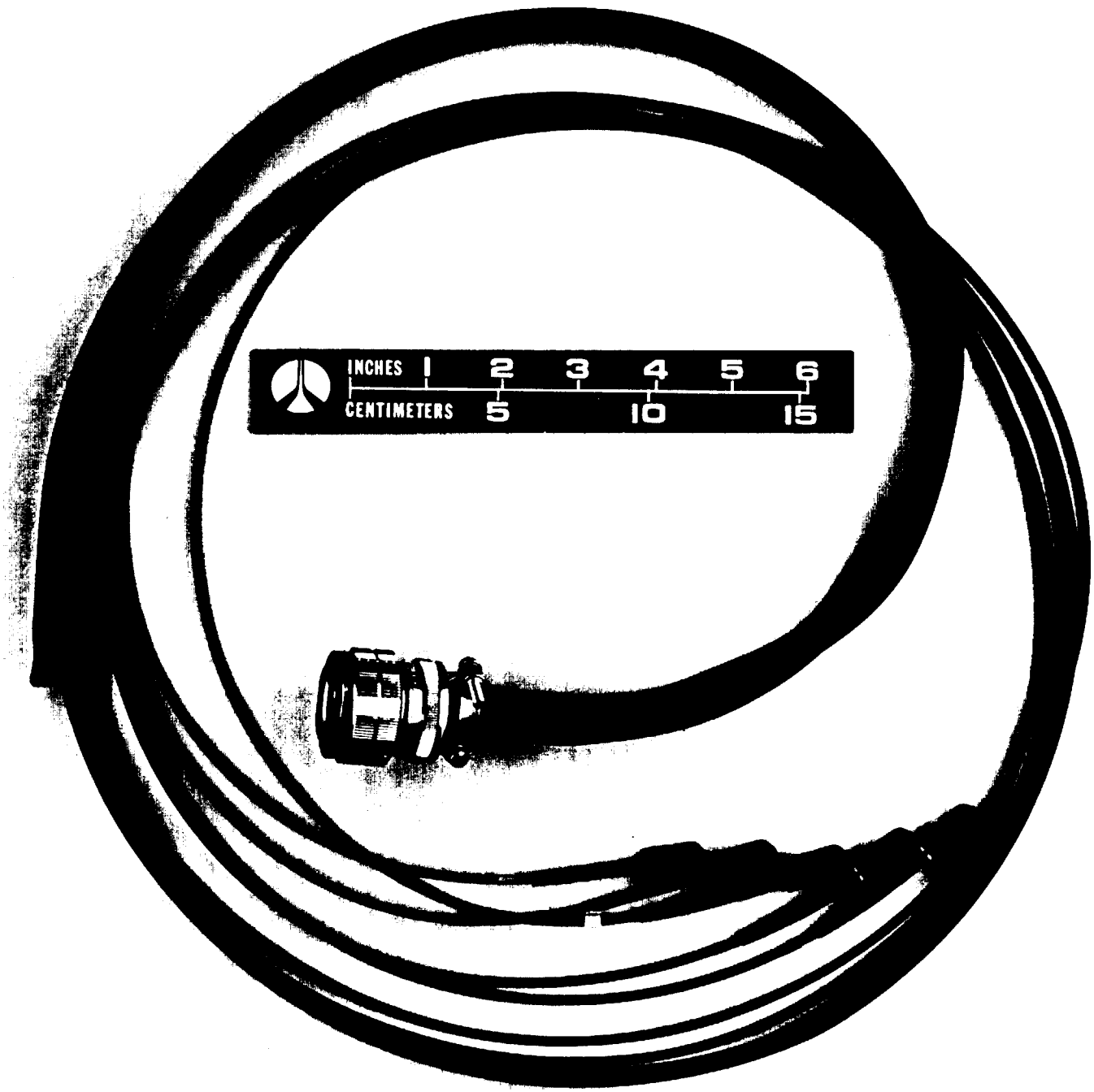

Fig. 42. Fiberoptic Harness for Vibration Testing

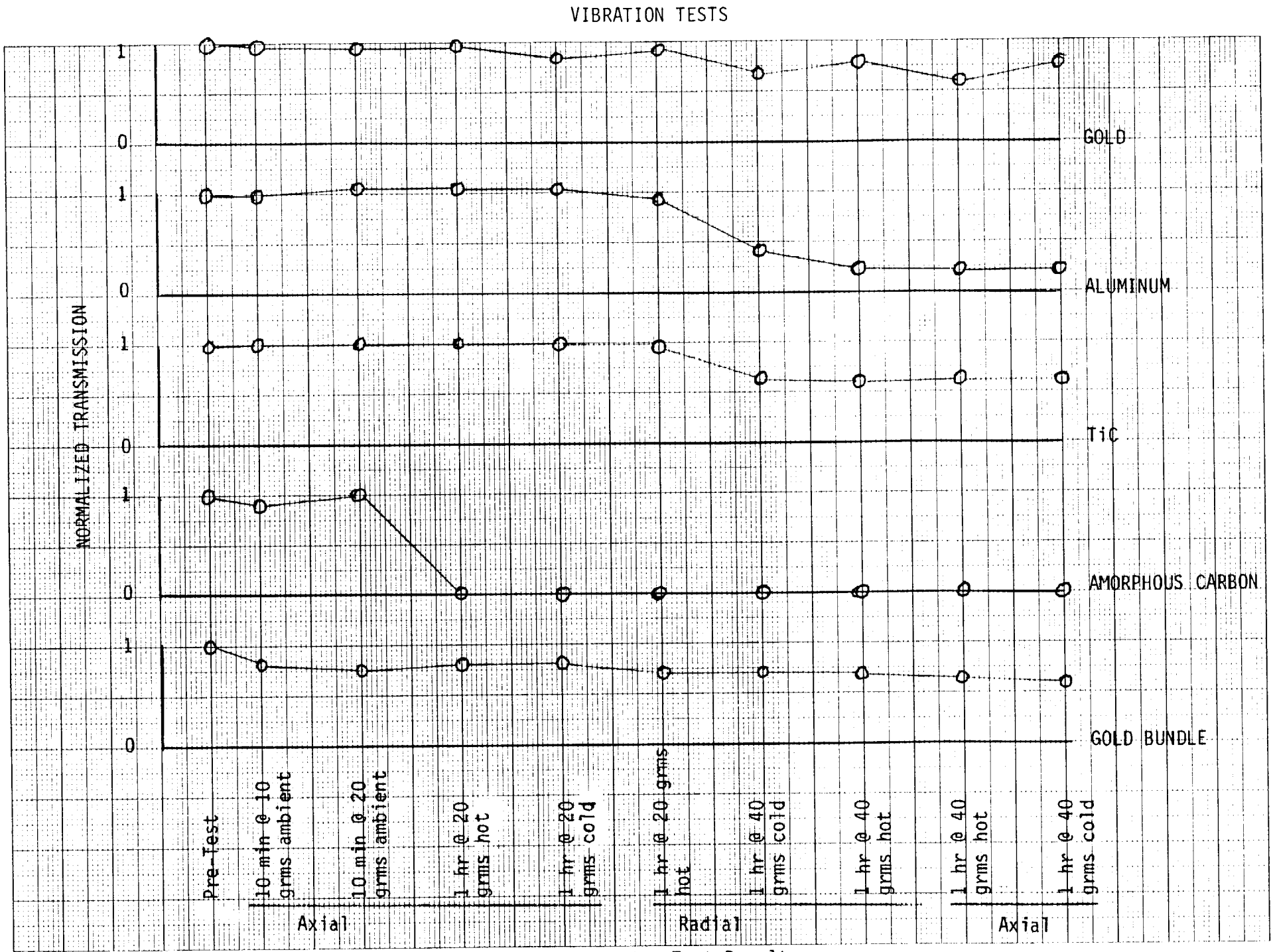

Figure 43. Vibration Test Results

SHOCK TESTS

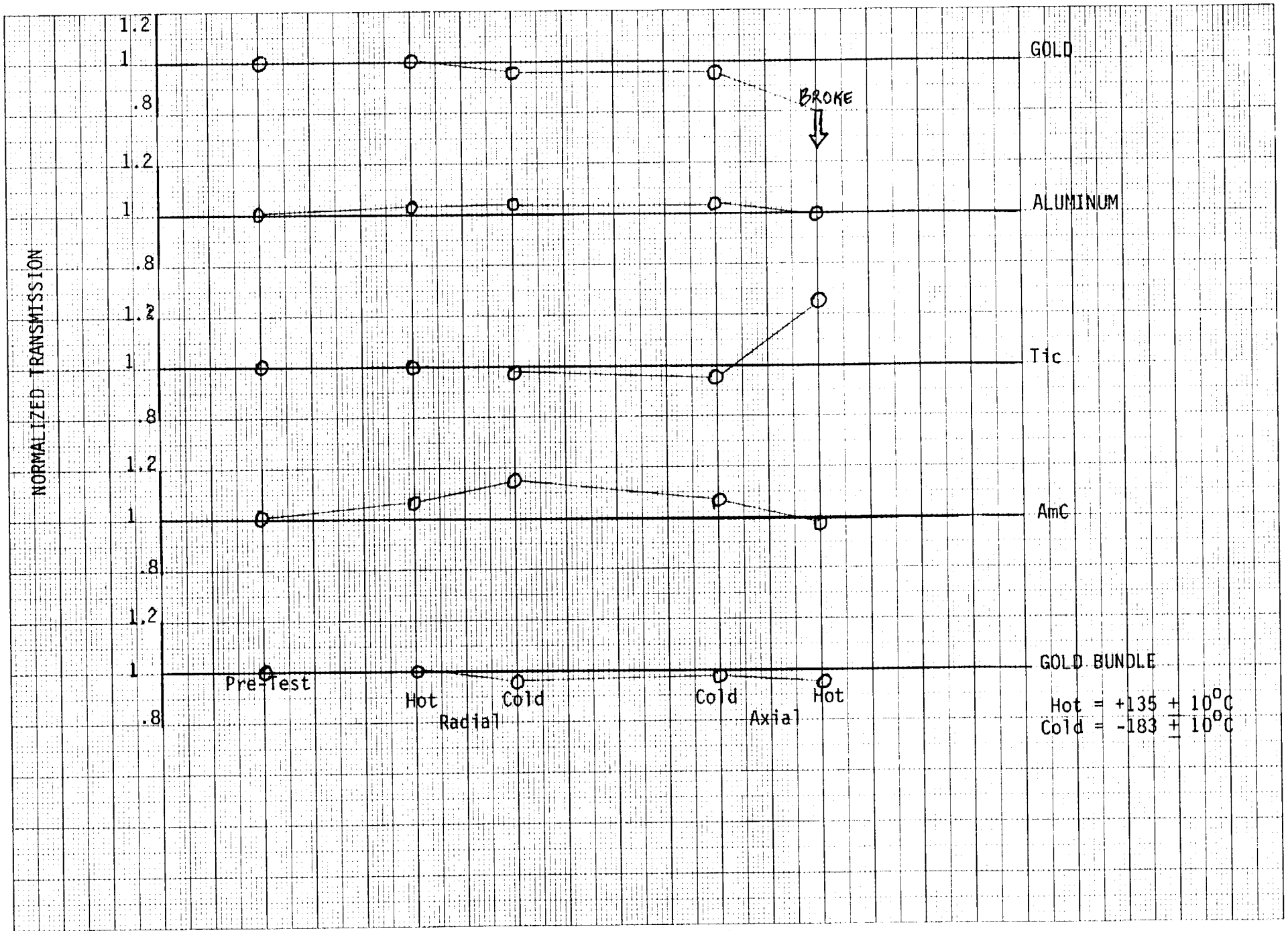

Figure 44. Shock Test Results

VIBRATION-INDUCED LOSS TEST

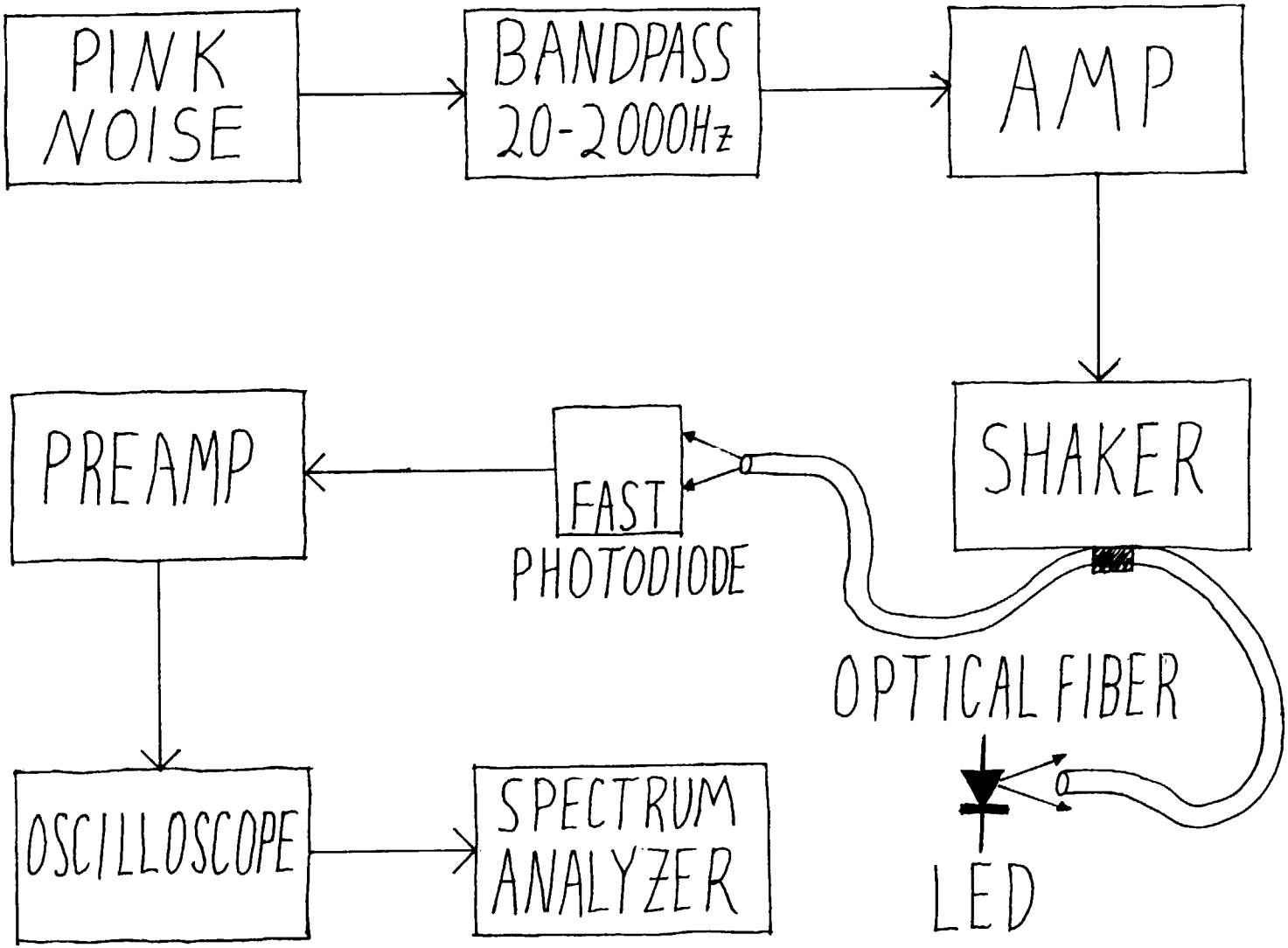

Figure 45 Vibration-Induced Loss Test Schematic

Figure 46. Vibration-Induced Loss Test Setup

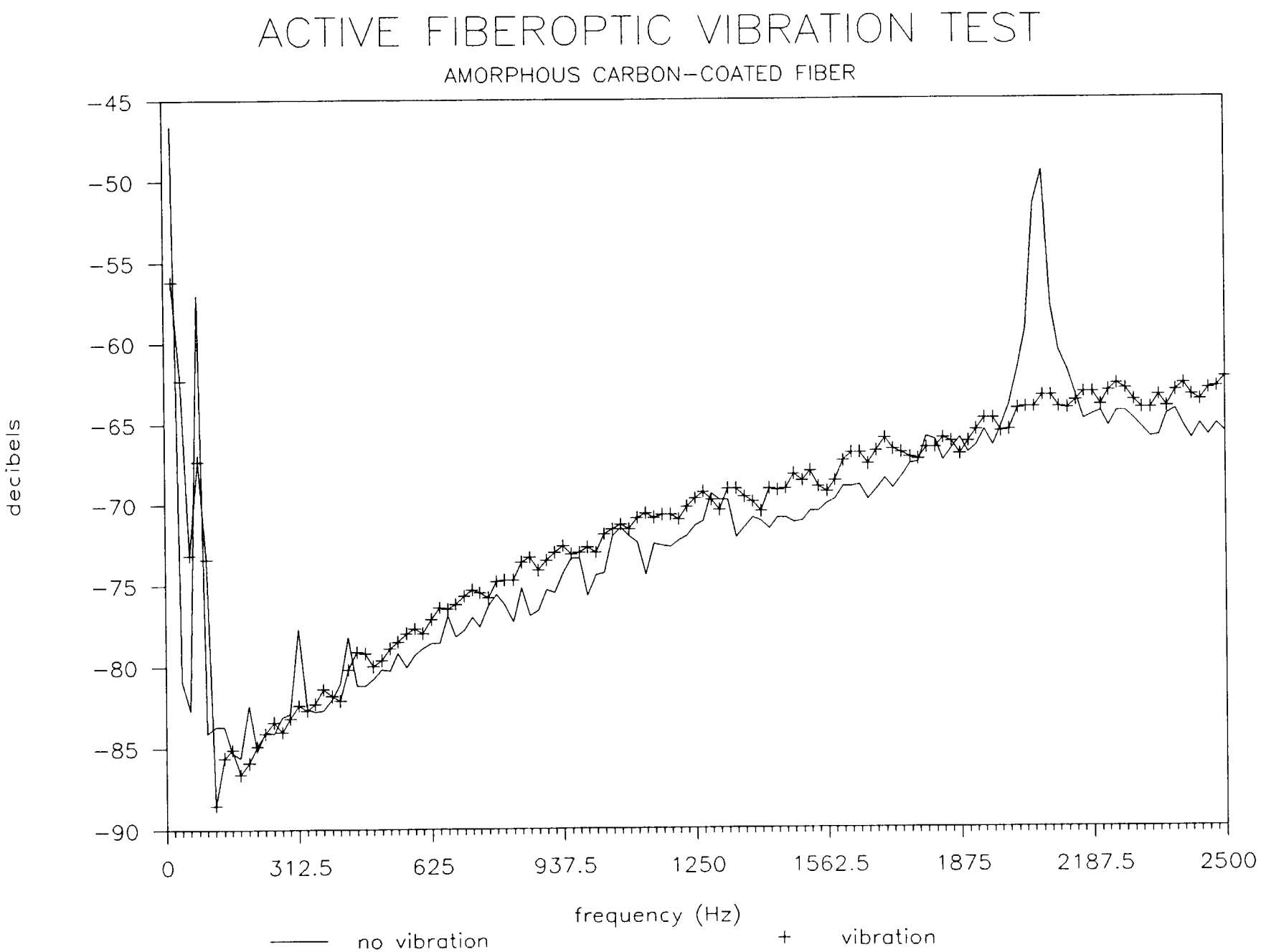

Figure 47. Vibration-Induced Loss Test Results

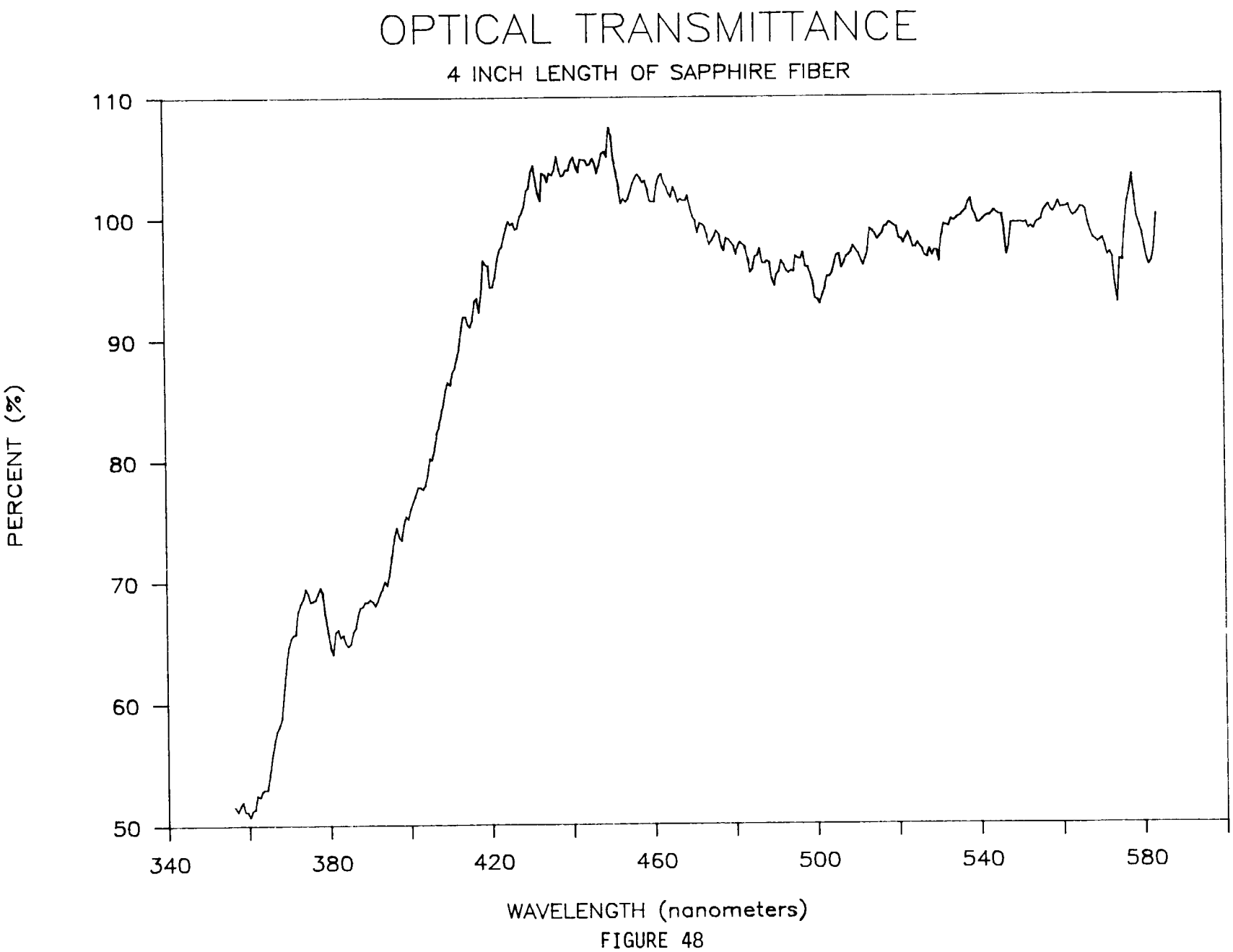
OPTICAL TRANSMITTANCE
4 INCH LENGTH OF SAPPHIRE FIBER
110
100
90
80
70
60
50
PERCENT (%)
340
380
420
460
500
540
580
WAVELENGTH (nanometers)

FIGURE 48

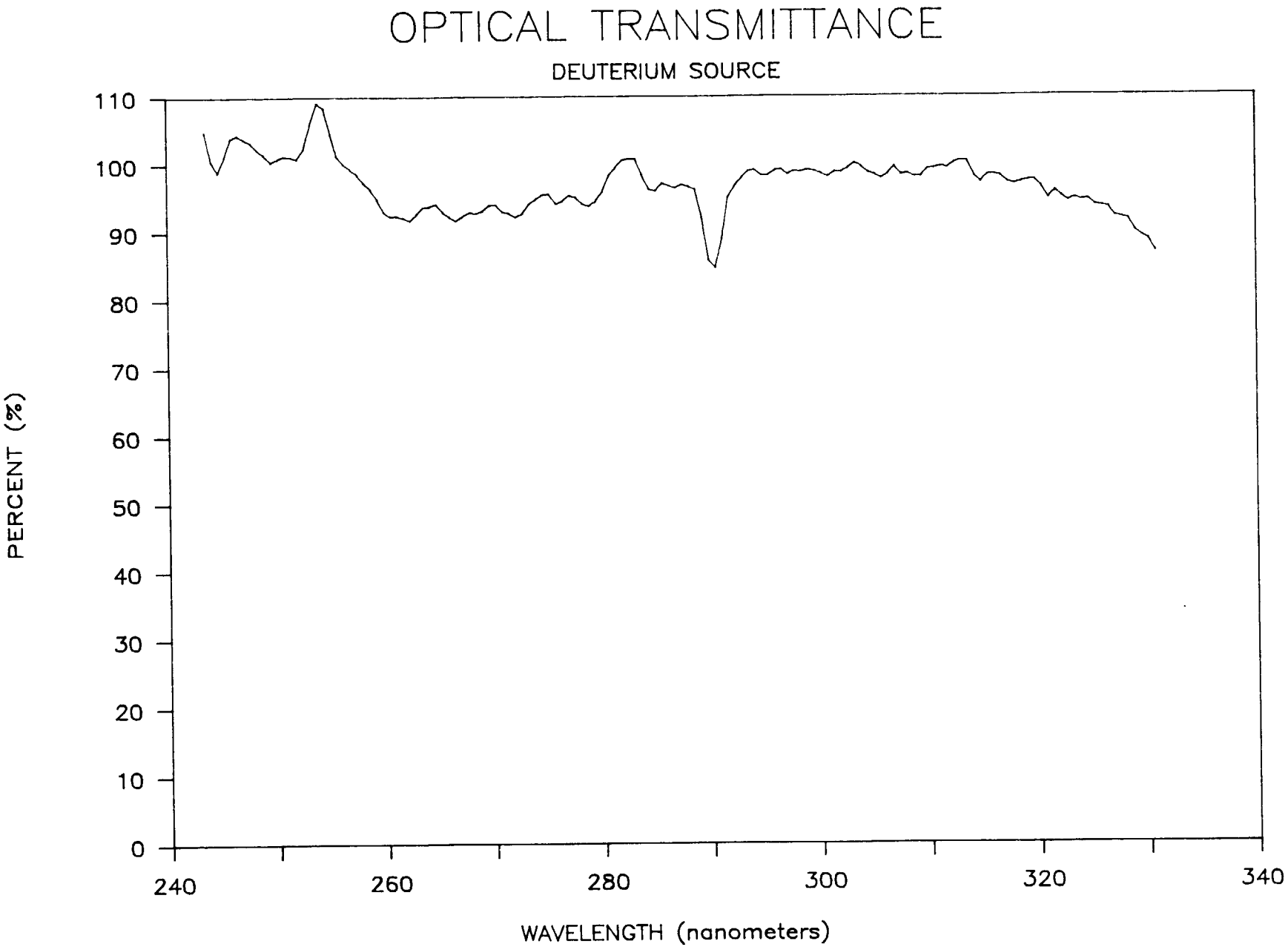
OPTICAL TRANSMITTANCE
DEUTERIUM SOURCE
PERCENT (%)
110
100
90
80
70
60
50
40
30
20
10
0
240
260
280
300
320
340
WAVELENGTH (nanometers)

FIGURE 49

TABLE 1

Requirement Definition

NUMBER	NAME	PERFORMANCE	OPERATING TEMPERATURE RANGE	CHEMICAL ENVIRONMENT	VIBRATION	SIZE	WEIGHT	PRESSURE
7001	Pressure Transducer	3±.3MV at full pressure 0±.3MV at 0 pressure Variable ranges from	-65°F to 165°F	GHe,GN2 LOX,GOx LH_2, GH_2	Random 39.5 Grms Total 40.9 Grms	3.4" x 1.62" x 1.62"	11.5 oz	0 to 10,000 psia
7002	Temperature Transducer	-300°F to 700°F Callender-Van Dusen eq.	-423°F to 500°F	LOX LH_2	Random 35.1 Grms Total 36.6 Grms		8.20 oz	10,200 psia
7004	Temperature Transducer Resistance Type	Type-X1 within - .6°F over full temperature range type X2 same	-300°F to 2200°F -320°F to 700°F	GHe, GN_2 LOX, GOx LH_2, GH_2 H_2O	Random 31 Grms Total 34.3 Grms	5.4" x 1.62" x 1.62"	6.2 oz	4000 psia 5500 psia
7005	Speed and Flow Sensor	Less than 5 DMV peak noise 3V ac for flow output 1V ac for speed output up to 50,000 Hz	-423°F to 165°F	GH_e, GN_a LOX, GOx LH_2, GH_2 driving 10,000 OHMS	Random 31.4 Grms Total 34.5 Grms	5.1" x 3.2" x-2.5"	6 oz flow 24 oz	1000 psia
7007	Hydraulic Pressure Sensor	3- .3MV at full pressure 0- .3MV at 0 pressure Variable range to 4000 psia	10°F to 250°F	Hydraulic fluid	Random 13.5 Grms Total 13.8 Grms	3.4" x 1.65" x 1.65"	11.5 oz	6000 psia
7010	Accelerometer	2.5 MV rms/grms 3000g peak sinosoidal 10,000g peak shock	-420°F to -295°F	Ambient	23 Grms	1.5" x .625 x .625	N/A	Ambient
BRE1712	Optical Probe Deflectometer Cable	1.2 min/MV 3 to 6 mil 70KHz 70Khz M/N bend Radius .75"	-297°F -100°F to Ambient	LO_x Air	Transient Same	N/A N/A	N/A N/A	600 psia Ambient
BRE1713	Optical Probe Pyrometer Cable	5.0MV/°C 160KHz	-210°F to 70°F (Pressure Seal) 0°F to 120°F	LH_2, GH_2 ALR	Transient Same	N/A N/A	N/A N/A	5000 psi (Tip) Ambient
1493	Controller	-	-55°F to 95°F	Open Air to 1x10-10 cm Hg 100% humidity	Random 31.3 Grms Total 33.06 Grms Transient <480 Grms	-	193 lb	15 psia to 10 Torr Vacuum
40M38277	Connectors	-	-250°F to 392°F	Vacuum salt spray ambient air 100% humidity	Random 20 to 100Hz 686/active 100 to 2000 Hz $1g^2$/Hz	-	-	Ambient to vacuum
RB0150-044	Cable	-	-195°F to 500°F	Ambient air, salt spray, 100% humidity vacuum	See Mating Sensor	-	- 10 oz/ft	Ambient

TABLE 2

JACKET DATA

MATERIAL	MELTING POINT	MODULUS OF RUPTURE	THERMAL SHOCK RESISTANCE
NYLON	≈260C*	100-350KPSI	POOR BELOW -73C
TEFZEL	≈260C	175-200KPSI	GOOD
ACRYLATE	**	UNDER 500KPSI	POOR BELOW -54C
TIC	≈2940C	41-97KPSI	GOOD
POLYIMIDE	**	470-750KPSI	GOOD
ALUMINUM	660C	13KPSI ***	GOOD
INDIUM	156C	0.38KPSI ***	GOOD
GOLD	1063C	19KPSI ***	GOOD

* APPROXIMATE MOLDING TEMPERATURE
** ACTUAL COMPOSITION OF THE COMPOUND IS NOT AVAILABLE FROM MANUFACTURERS
*** TENSILE STRENGTH

(1106C)

TABLE 3

Fiber Material Characteristics

FIBER MATERIAL CHARACTERISTICS

MATERIAL	COATING	MANUFACTURER MODEL	TYPE	MAX T (°C) *	MIN T (°C) *	RADIATION RESISTANCE	CHEMICAL RESIST	WAVELENGTH RANGE	ATTENUATION	TENSILE STRENGTH	REFRACTION INDEX	BEND RADIUS	PRICE ($/M)
SILICA	NYLON, TEFZEL ACRYLATE POLYIMIDE, AU	FIBERGUIDE SUPERGUIDE-G	MMSI BUNDLE	100, 150 85, 385, 750	40, -40 -40, -190 -190	GAMMA (NA)	HERMETIC	~180-1100NM	<3DB/KM @ 180NM <25DB/KM @ 800NM	50-70 KPSI	~1 5	~ 300XDIA	~4, 4 4, 4, 38, 3-5K
	ACRYLATE	CORNING, 850 PRSM	PM, SM	85	-60	GAMMA (NA)	MOST CHEMICALS	850NM	≤ 6 0DB/KM	50 KPSI	~1 5	NA	13
	ACRYLATE, TEFLON, CARBON	CORNING, SMF-28CPC3, TEFLON, CARBON	SM	85, 200 85	-60, -60, -60	GAMMA (NA)	HERMETIC	1300NM, 1550NM	≤ 0 5DB/KM	50 KPSI	~1 5	NA	20, 1 20, 1 20
	ACRYLATE, TEFLON, CARBON	CORNING, 62 5 /125 LNF CPC3 TEFLON, CARBON	MMGI	85, 200 85	-60	GAMMA (NA)	HERMETIC	800-1600NM	≤3 2DB/KM @ 850NM ≤0 9DB/KM @ 1300NM	50 KPSI	~1 5	NA	25, 1 25, 1 25
	ACRYLATE, POLYIMIDE, CARBON	AT&T RADIATION HARDENED **	RH	85, 200 85	-60, -40 -60	MIL-SPEC CR-CS-0051-001	HERMETIC	NA	NA	50-100 KPSI	~1 5	NA	~79, 3.2
	ACRYLATE, POLYIMIDE, TIC	SPEC TRAN, 420, 420P, 420H	MMSI	85, 375 85	-55, -55 -55	YES ***	HERMETIC	~800-1600NM	≤ 5DB/KM @ 850NM	50 KPSI MIN	~1 5	NA	75, 1 75, 2 25
	NYLON, TEFLON	MITSUBISHI, SI-R SERIES	MMSI	80, 150	-20	10^4 RAD GAMMA	NA	~700-1100NM	≤100B/KM	NA	~1 5	50MM	2 76, 3
	ACRYLATE	YORK, 18800	PM, SM	70	-30	NO	NA	800NM	< 5DB/KM	50 KPSI	~1 5	20MM	14
	ACRYLATE	GALILEO,	BUNDLE FUSED SI	NA	NA	NA	NA	250-1000NM	~ 10DB/KM	20 KPSI	~1 5	NA	1400
	TEFZEL	3M, FT-200-LKT	MMSI	125	-65	NA	NA	850	6DB/KM	100 KPSI	1 5	~ 10MM	80
	ALUMINUM	HUGHES	MM, SM PM	~450	~ -190	GAMMA (NA)	HERMETIC	NA	NA	100 KPSI	NA	NA	5, 8, 10
	INDIUM	ANDREW, 48280	SM, PM	~140	NA	NA	HERMETIC	633-1550NM	≤9DB/KM @ 850NM ≤3DB/KM @ 1300NM	50 KPSI	~1 5	50 MM	~10
FLUORIDE	ACRYLATE	IRIS IRISENSOR 140/200	MMSI	~150	~-200	NA	NA	300NM-4 5μM	<20DB/KM @ LOWEST LOSS	85 KPSI	1 45-1 5	6MM	100
	ACRYLATE	I F S, LASERGRADE	MMSI	250	~-180	GAMMA (NA)	HUMIDITY DEGRADES IN WATER	1-5μM	<0 1DB/M @ LOWEST LOSS	61 KPSI	~1 5	~4MM	75
	EPOXY	RADIANT, FF14	MMSI	85	-40	NA	NA	2-5μM	0 5-2DB/M	35 KPSI	~1 5	30 X DIA	100
	POLYMER	SPECTRAN, SFI	MMSI	200	NA	NA	NA	0 2-7 5μM	~DB/M	35 KPSI	~1 5	NA	30
CHAL-COGENIDE	NONE	I F S, PLASTIC CLAD	MMSI	300	~-180	NA	H^2O, ACID & BASES	~2-10μM	<0 7DB/M MIN <90B/M MAX	45 KPSI	CORE = 2 55 CLAD = 1 33	~10MM	200
	ACRYLATE	GALILEO	EXPT'L	200	NA	UNDERSTUDY	NA	1 5-10μM	10dB/M	25 KPSI	~ 2 6	NA	EXPT'L
	ACRYLATE	RADIANT, CF24	MMSI	65	-20	NA	NA	5-11μM	5-7dB/M	NA	NA	50 X DIA	250
SAPPHIRE	NA	SAPHIKON,	EXPT'L	2000	-260	10^8 RAD GAMMA 10^{12}/CM² PROTONS	ACID WEATHER SALT H^2O	190 5000NM	RANDOM AS HIGH AS 10dB/M	2 6 KPSI @ 25°C 61 KPSI @ 1000°C	~1 8	~8MM	EXPT'L

*TEMPERATURES CORRESPOND TO COATING TYPES ** RADIATION HARDENING NOT AVAILABLE ON 100/140 MICRON MULTIMODE FIBER *** QUALIFIED FOR AEGIS FEMA AND TIE GROUND LAUNCH CRUISE MISSILE PROGRAMS
NA = INFORMATION NOT AVAILABLE SM = SINGLE MODE MMSI = MULTIMODE STEP-INDEX MMGI = MULTIMODE GRADED-INDEX PM = POLARIZATION MAINTAINING RH = RADIATION HARDENED

TABLE 4

CORE & CLADDING DATA

MATERIAL	MELTING POINT*	MODULUS OF RUPTURE	THERMAL SHOCK RESISTANCE
SILICA **	≈1000-1725 C	≈9.7KPSI	EXCELLENT
FLUORIDE	≈ 350c	***	FAIR
CHACOGENIDE	≈>250c	***	FAIR
SAPPHIRE ****	≈2050c	67-95KPSI	EXCELLENT

* ALL FIBERS EXCEPT SAPPHIRE WILL BE AMORPHOUS, NOT CRYSTALLINE. THEREFORE, THEY WILL HAVE A "SOFTENING RANGE" RATHER THAN A SHARP MELTING POINT.

** VALUES GIVEN ARE FOR BULK FUSED SILICA.

*** NOT AVAILABLE FROM MANUFACTURERS OR MATERIAL TABLES (SEARCH CONTINUING)

**** IN FIBER FORM (SAPHIKON)

TABLE 5

FIBER SPECIMEN SCREENING

MANUFACTURER	MODEL	JACKET	CAPABILITIES (UV,IR,INTER.)	SCREEN <-180 (C)?	SCREEN >200 (C)?	SCREEN <0.5DB/M?	SCREEN HERMETIC?	SELECTED?
FIBERGUIDE	SUPERGUIDE	POLYIMIDE	UV	YES	YES	YES	NO	NO
FIBERGUIDE	SUPERGUIDE	GOLD	UV	YES	YES	YES	YES	YES
FIBERGUIDE	SUPERGUIDE,BUNDLE	GOLD	BUNDLE,UV	YES	YES	YES	YES	YES
CORNING	850PRSM	ACRYLATE	UV,INTERFEROM	NO	NO	YES	NO	NO
CORNING	SMF-28	POLY. +CARBON	UV	?	YES	YES	YES	YES?
CORNING	62.5/125	POLY. +CARBON	UV	?	YES	YES	YES	YES?
AT&T	RADIATION HARD	ACRYLATE	UV	NO	YES	YES	NO	NO
SPECTRAN	420	POLY.+TIC	UV	?	YES	YES	YES	YES?
MITSUBISHI	ST-R SERIES	NYLON,TEFLON	UV	NO	NO	YES	NO	NO
YORK	HB800	ACRYLATE	INTERFEROM	NO	NO	YES	NO	NO
GALILEO	BUNDLE	ACRYLATE	UV,BUNDLE	NO	NO	YES	NO	NO
3M	FT-200-LKT	TEFZEL	UV	NO	NO	YES	NO	NO
HUGHES	AL COATED	ALUMINUM	UV,SM	YES	YES	YES	YES	YES?
HUGHES	AL COATED	ALUMINUM	UV,INTERFEROM	YES	YES	YES	YES	YES?
HUGHES	AL COATED	ALUMINUM	UV,MULTIMODE	YES	YES	YES	YES	YES
IRIS	140/200	ACRYLATE	UV-IR	YES	NO	YES	NO	YES*
I.F.S.	LASERGRADE	ACRYLATE	IR	YES	YES	YES	NO	YES*
RADIANT	FF14	EPOXY	IR	NO	NO	NO	NO	NO
SPECTRAN	SF1	POLYNER	IR	?	YES	NO	NO	NO
I.F.S.	PLASTIC CLAD	NONE	FAR IR	YES	YES	NO	NO	NO
GALILEO	CHALCOGENIDE	ACRYLATE	FAR IR	?	YES	NO	NO	NO
RADIANT	CF24	ACRYLATE	FAR IR	NO	NO	NO	NO	NO
SAPHIKON	SAPPHIRE	NA	UV - FAR IR	YES	YES	NO	NO	NO
ANDREW	48420	INDIUM	UV,INTERFEROM.	?	NO	YES	YES	YES?

* THE BEND RADIUS TEST WILL DETERMINE WHICH FLOURIDE FIBER IS CHOSEN.

TABLE 6 COLD BEND TEST RESULTS

FIBER MATERIAL	JACKET	CYCLES	CONDITION
SILICA	ALUMINUM	10,000	WRINKLING OF JACKET
	ALUMINUM*	10,000	MINOR WEAR SPOTS
	GOLD	10,000	SMALL CRACKS IN JACKET (FATIGUE)
	GOLD (BUNDLE)	10,000	NO OPTICAL DEGRADATION
	TITANIUM CARBIDE	10,000	MINOR SCRATCHES ON COATING JACKET
	AMORPHOUS CARBON	10,000	NO VISIBLE SIGN OF DAMAGE
GLASS	PLASTIC	10,000	NO VISIBLE SIGN OF DAMAGE
ZIRCONIUM-BASED FLUORIDE**	ACRYLATE	10,000	MINOR SURFACE WEAR
	ACRYLATE*	~ 500	FIBER BROKE

* SECOND MANUFACTURER
** ZBLAN (ZIRCONIUM, BARIUM, LANTHANUM, ALUMINUM, SODIUM FLUORIDE)

(1111D)

TABLE 7 FIBER SELECTION RESULTS

- GOLD-COATED SILICA 200/240/275 (FIBERGUIDE)
- ALUMINUM-COATED SILICA 100/140/190 (HUGHES)
- TITANIUM CARBIDE-COATED SILICA 100/140/162.5 (SPECTRAN)
- AMORPHOUS CARBON-COATED SILICA 50/125/187 (ATT)
  (CARBON-COAT = 3-500A)
- FLUORIDE 100/140/230 (IRIS)
- 19-FIBER BUNDLE, GOLD-COATED SILICA 100/110/140 (FIBERGUIDE)

TABLE 8 ENVIRONMENT TESTING

- "COLD BEND" TEST --- 10,000 CYCLES OF ±45° @ -300°F
- MOISTURE EMBRITTLEMENT TESTING -- 30 DAYS OF WATER EMERSION
- TEMPERATURE CYCLING -- 10 CYCLES OF -300° TO +257°F
- TEMPERATURE EXTREMES -- 96 HOURS @ -300° AND +500°F
- VIBRATION -- 1 HOUR @ 40 G IN R.T., -280°F, AND +275°F
- SHOCK -- 48 SHOCKS @ -280 TO +275°F

TABLE 9

MOISTURE EMBRITTLEMENT ATTENTUATION MEASUREMENTS

DAY	FLUORIDE	TIC	AMC	ALUMINUM	GOLD
Initial	1.000	1.000	1.000	1.000	1.000
END 1 ST DAY	0.810	1.055	0.974	1.257 0.600 Average 0.926	1.016
3RD DAY	Broken	0.980	0.849	0.996	1.000
7TH DAY	----	0.993	0.880	1.029 1.005 0.998 Average 1.011	1.008
14TH DAY	----	1.022 0.915 0.936 Average 0.958	0.878	0.958 1.031 0.990 Average 0.993	1.039 1.039 1.008 Average 1.029
30TH DAY	----	0.862 0.912 0.843 0.949 Average 0.892	0.998	0.982 1.076 0.978 Average 1.012	

TABLE 10
SHOCK TESTING SPECTRUM

FREQUENCY (Hz)	PEAK LEVEL (g)
10	6
30	28
60	53
220	104
320	100
950	157
1250	245
2000	340

TABLE 1
CANDIDATE CLADDING MATERIALS

MATERIAL	N	T-MELT	(C) COEFF-EXP.	SOLUBILITY g/100g H20	WAVEBAND MICRONS	FIBER/CLADDING MATERIAL?
SAPPHIRE	1.76	2040	7.7	Insol.		yes
BeO	1.72	2520	9	Insol.		yes
MgO	1.73	2800	13.6	Insol.*		yes
SiO2	1.458	1710	0.55	Insol.		yes
MgAl2O4	1.7	2135	8.41	Insol.		yes
Al6Si2O13	1.56	1810	5.13	?		yes
Mg2SiO4	1.61	1910	8.8	----------		yes
MgSiO3	1.6	1557	8.1	Insol.		yes
Al2O3-x F2x	1.66	2040?	7.7?	Insol.		yes
SiOxNy	1.46-1.76	?	?	?		yes
TixSiyO2	1.46-1.76	?	?	?		yes
CdF2	1.63	1100	?	0.0017***		no
"	1.53	1100	?	0.0017***		no
"	1.45	1100	?	0.0017***		no
Cer-Vit C-101	1.54	?	?	?		
RbBr	1.53	693	?	205.2	1-8	no
RbCl	1.48	718	?	138.9	1-8	no
RbI	1.62	647	?	163	1-8	no
T-12	1.41	?	?	?	near ir	?
AlN	?	>2200 in N2	?	Dissolves	?	no
MgF2	1.41-1.37	1261	?	Insol.	0.21-7.5	
Intran 1	1.38-1.22	?	?	Insol.	1.0-9.0	
Intran 3	1.43-1.27	?	?	Insol.	1.0-11	
Intran 5	1.73-1.41	?	?	Insol.	1.0-9.0	
InP	0.79-1.74	1070	?	----------		
InAs	1.14-1.76	943	?	Insol.		
InSb	1.15-1.66	535	?	Insol.	>6.0	
GaP	1.03-1.7	?	?	----------		
CaF2	1.48-1.3	1435	?	0.0017*	0.23-9.73	
Quartz (ord)	1.06-1.17	?	?	Insol.	0.185-7.0	
Quartz (extr)	1.69-1.17	"	"	Insol.	0.185-2.053	
CaTiO3	1.61-1.58	1975	?	----------	0.434-0.668	
BaF2	1.51-1.39	1355	?	0.17	0.265-10.35	

REFERENCES

1) Hamilton, S. C. & Haffner, J. W., "Natural Nuclear Radiation Analysis of Six Earth Observation Orbits", SSD80-0133, IR&DA No. 242, Rockwell International, Space Operations and Satellite Systems Division, Downey, CA., (September 1980).

2) Friebele, E. J., Askins, C. G., Gingerich, M. E., and Long, K. J., "Optical Fiber Waveguides in Radiation Environments, II", Nuclear Instruments and Methods in Physics in Physics Research B1 (1984) 355-369.

3) Wilkenfeld, Jason M., Leadon, Roland E., and Mallon, Charles E., "Radiation Effects in Satellite Cables", HDL-CR-78-089-1, U.S. Army Electronics Research and Development Command, Adelphi, MD, April 1978.

4) Grattan, K. T. V., Manwell, J. D., Sim, S. M. L., and Willson, C. A., "Fibre-optic Temperature Sensor with Wide Temperature Range Characteristics", IEEE Proceedings, Vol. 124, Pt. J, No. 5, October 1987.

5) Moynihan, C. T., Loehr, S. R., Chemical Durability of Fluoride Glasses; Material Science Forum, 1988, Vol 32-33.

6) Krause, J. T., Kurkjian, C. R., DIMarcello, F. V., Huff, R. G., Technical Memorandum to be presented at 6th EFOC/LAN, Amsterdam, June 29 - July 1, 1988 (Stated on paper obtained from Author)

7) Drexhage, M. G., Moynihan, C. T., Scientific American, Vol. 259, No. 5, 1988.